Control of DAPK-1 Degradation

Yao Lin

Thesis submitted to the University of Edinburgh for the degree of Doctor of Philosophy

October 2009

海纳百川　有容乃大

壁立千仞　无欲则刚

林则徐

Contents

Declaration

I declare that this thesis has been composed by myself the undersigned Yao Lin and the work herein is entirely my own unless otherwise clearly acknowledged. This work has been submitted for the degree of Doctor of Philosophy and has not been submitted for any other qualification or otherwise.

Acknowledgements

I would like to give my heartfelt thanks to my supervisor Professor Ted Hupp for giving me this opportunity and for his great patience and enthusiasm in my work. Besides, I owe an incalculable debt of gratitude to Dr. Craig Stevens for the proofreading of my thesis. Thanks also go to Suresh Pathuri for his assistance in the s-DAPK-1 project, Dr. Craig Stevens for helping me with the Annexin V and TUNEL assays and the collaborations in TSC2 projects, Dr. Argyro Fourtouna for helping me with immunofluorescent microscopy, Dr. Jennifer Fraser for making radioactive protein and Dr. Ben Harrison for membrane blebbing assays. I would also like to thank everyone in the lab for daily support and making my time in the lab very enjoyable. Finally I would like to thank my parents, Benchun Lin and Muzhu Lin, who have always provided me with the support I need to complete this thesis.

Abstract

DAPK-1 is calcium-calmodulin regulated protein kinase involved in multiple cellular pathways including apoptosis, autophagy, cell survival and motility. The cytokine TNF-α has been reported to induce the degradation of DAPK-1. Here I identified the protease cathepsin B as a novel binding partner of DAPK-1 that protects DAPK-1 from TNF-α induced degradation. Using deletion mutants of DAPK-1, I mapped the cathepsin B binding domain on DAPK-1 to amino acids 836-947. Overexpression of this mini-protein DAPK-1(836-947) facilitated degradation of full-length DAPK-1 and apoptosis induced by TNFR-1. Moreover, siRNA mediated knock-down of DAPK-1 enhanced TNF-α induced apoptosis, confirming the role of DAPK-1 as a survival factor in the TNF-α signalling pathway.

In addition, a splice variant of DAPK-1, which I have called s-DAPK-1, was discovered. s-DAPK-1 shares part of DAPK-1's ankyrin repeats region and cytoskeletal binding domain, and possesses an unique tail region, which contains a cleavage site at its first two amino acids. Unlike DAPK-1, s-DAPK-1 does not contribute to apoptosis induced by high level of MEK/ERK signalling, but it does mimic DAPK-1's function to induce membrane blebbing. The proteolytically processed form of s-DAPK-1 is more active in the induction of membrane blebbing, which may be due to its higher stability compared to that of full-length s-DAPK-1, suggesting that the tail region can control s-DAPK-1 stability and activity.

Co-transfection of s-DAPK-1 and DAPK-1 leads to reduction in DAPK-1 expression level, suggesting a role for s-DAPK-1 to regulate DAPK-1 stability. The kinase domain of DAPK-1 is the region required for s-DAPK-1 to promote DAPK-1 degradation. Surprisingly, s-DAPK-1 does not bind directly to DAPK-1, suggesting that the interaction is indirect and mediated by as yet unidentified accessory proteins. Finally, the experiments with proteasome and lysosome inhibitors indicated that s-DAPK-1 induces DAPK-1 degradation via both lysosome and proteasome pathways.

Abbreviation

17-AAG	17-allyalamino-17demethoxy-geldanamycin
3-MA	3-methyladenine
4EBP1	Eukaryotic initiation factor 4E binding protein-1
A	Adenine in DNA sequence
A	Alanine in protein sequence
aa	Amino Acid
AMPK	5'AMP-activated protein kinase
Apaf-1	Apoptotic protease activating factor 1
APS	Ammonium Persulfate
ATG	Autophagy-related genes
ATP	Adenosine-5'-triphosphate
Bcl-2	B-cell CLL/Lymphoma 2
BSA	Bovine Serum Albumin
C	Cytosine in DNA sequence
C	Cysteine in protein sequence
CaMK	CaM kinase
CaMKK	CaM kinase kinase
cFLIP	Cellular caspase-8 (FLICE)-like inhibitory protein
CHK	Checkpoint Kinase
CHX	Cycloheximide
CLL	Chronic lymphocytic leukaemia
D	Aspartic acid in protein sequence

DAPK	Death Associated Protein Kinase
DISC	Death-inducing signalling complex
DMEM	Dulbecco's Modified Eagle's Medium
DMSO	Demethyl Sulfoxide
DNA	Deoxyribonucleic Acid
DRP-1	DAPK-1 interacting protein 1
DTT	Dithiothreitol
E	Glutamic acid in protein sequence
ECL	Electrochemiluminescence
ECM	Extracellular matrix
EDTA	Ethylenediamine Tetraacetic Acid
ERK	Extracellular Signal-regulated Kinase
F	Phenylalanine in protein sequence
FADD	Fas-associated protein with death domain
FBS	Foetal Bovine Serum
FKBP12	FK506-binding protein 12
G	Guanine in DNA sequence
G	Glycine in protein sequence
GA	Geldanamycin
G6PD	Glucose-6-phosphate dehydrogenase
H	Histidine in protein sequence
HECT	Homologous to E6-AP C-Terminus
HRP	Horse Radish Peroxidase
Hsp90	Heat shock protein 90

I	Isoleucine in protein sequence
IAP	Inhibitor of apoptosis protein
IFN	Interferon
IKK	I-κB kinase
IL	Interleukin
IP	Immunoprecipitation
K	Lysine in protein sequence
L	Litre
L	Leucine in protein sequence
LAR	Leukocyte common antigen-related phosphatase
LC3	Microtubule-associated protein 1 light chain 3
M	Methionine in protein sequence
MAP1B	Microtubule-associated protein 1B
MEF	Mouse embryonic fibroblast
MEK	Mitogen-activated protein kinase
MIB	Mind bomb
MLC	Myosin Light Chain
MOPS	3-(N-morpholino)propanesulfonic acid
MUNC-18	Mammalian homologue of the unc-18 gene
N	Asparagine in protein sequence
NP40	Nonidet-P 40
ODC	ornithine decarboxylase
P	Proline in protein sequence
p70S6K	Ribosomal p70S6 kinase

PARP	Poly (ADP-ribose) polymerase
PCD	Programmed cell death
PCR	Polymerase Chain Reaction
PE	Phosphatidylethanolamine
PI3 kinase	Phosphatidyl-inositol 3-kinase
pIpC	Polyinosinic:polycytidylic acid
PKD	Protein kinase D
PMA	Phorbol-12-myristate-13-acetate
PRAS40	Praline-rich Akt substrate 40KDa
Q	Glutamine in protein sequence
R	Arginine in protein sequence
Raptor	Regulatory associated protein of mTOR
Rictor	Rapamycin-insensitive companion of mTOR
RNA	Ribonucleic Acid
RT	Reverse Transcription
S	Serine in protein sequence
SDS	Sodium Dodecyl Sulfate
Sin1	Stress-activated protein kinase-interacting protein
Smac	Second mitochondria-derived activator of caspases
T	Thymine in DNA sequence
T	Threonine in protein sequence
TBE	Tris/Borate/EDTA
TEMED	Tetramethylethylenediamine
TGF	Tumour growth factor

TLR	Toll-like receptor
TNF	Tumour Necrosis Factor
TNFR	Tumour necrosis factor receptor
V	Valine in protein sequence
W	Tryptophan in protein sequence
Y	Tyrosine in protein sequence
ZIP kinase	Zipper interacting protein kinase

Chapter One Introduction

1.1 Cancer, cell cycle and cell death

Cancer kills several million people every year. It is caused by disorders of cell growth or cell death pathways, which give rise to uncontrolled cell proliferation resulting in tumours[1]. In normal cells, the cell cycle is the process by which cells grow, replicate their DNA and then divide into two daughter cells[2]. It consists of cell growth phase G1, DNA replication phase S, division preparation phase G2, mitosis phase M and a post-mitosis quiescent phase G0 (Figure 1.1)[2]. At the boundary of G1/S and G2/M phases, there are cell cycle checkpoints that ensure the fidelity of cell division. Therefore when mistakes like DNA damage are detected, cells are arrested at these checkpoints to allow for DNA damage to be repaired. If the damage can not be repaired, the cells are targeted for destruction by programmed cell death (PCD), which is an intrinsic cell suicide process that is regulated by a variety of cellular signalling pathways[3].

Mutation of genes involved in the regulation of cell proliferation or death are common molecular mechanisms underlying formation of tumours. The genes that facilitate the growth of tumours are called oncogenes, while those that inhibit tumour growth are called tumour suppressor genes. Many oncogenes and tumour suppressor genes have been identified. Discovery of these genes allows the study of cancer at the molecular level and provides many potential drug targets for more tailored cancer treatment compared to surgery, chemotherapy or radiotherapy. For example, the tumour suppressor gene p53 can induce cell cycle arrest and apoptosis in response to

DNA damage[4] and is mutated in more than 50% of human cancers[5]. Naturally p53 is an important drug target and more than 40,000 papers have been published concerning this gene.

Gene mutation is the major mechanism for tumourigenesis, however tumour cell survival is also regulated *in vivo* by cytokines, which are small proteins secreted by cells that mediate cell-cell communications via cytokine receptors at the surface of neighbouring cells to induce a variety of signalling pathways[6]. Cytokines that are secreted in response to infection, inflammation and immunity can function to inhibit tumour development and progression. On the other hand, cancer cells can respond to host-derived cytokines that promote growth, attenuate apoptosis and facilitate invasion and metastasis. Many cytokines have been discovered, including Interleukins (IL), lymphokins, Tumour Necrosis Factors (TNF), Tumour Growth Factors (TGF) and Interferons (IFN). Because of their potent effects to induce cell death, cytokines like TNF-α and IFN-γ have been widely used in cancer research to study the signalling pathways regulating cell death[6].

1.2 Discovery and structure of DAPK-1

In 1995, a functional screen based on random knockdown of gene expression was carried out in order to search for new genes involved in cell death[7]. In this screen, Hela cells were transfected with an antisense cDNA library, and then clones that could survive the continuous exposure to cytotoxic signals induced by IFN-γ were selected. Isolation and characterization of cell death-protective antisense cDNA

fragments within the selected clones led to the discovery of a group of cell death related genes. One of the genes isolated is transcribed into a single 6.3kb mRNA, that is translated into a 160kDa protein kinase, named Death Associated Protein Kinase 1 (DAPK-1).

In 1997, DAPK-1 was identified as a calcium/calmodulin (Ca2+/CaM)-dependent serine/threonine kinase with cell death inducing functions. DAPK is a multi-domain protein. In addition to its kinase domain and CaM regulatory domain, DAPK-1 contains an ankyrin repeats region consisting of 8 repeats, two P-loops (Phosphate binding loop), a cytoskeletal binding domain, a C-terminal death domain and a 17 amino acids (aa) tail rich in serine residues (Figure 1.2)[8]. The ankyrin repeat is a 33aa motif in proteins that mediates protein-protein interactions[9]. The P-loop is a nucleotide ATP/GTP binding motif found in many proteins[10]. The cytoskeletal binding domain, as its name indicates, mediates the interaction between proteins and the cytoskeleton[11]. The death domain is a conserved stretch of around 80aa, which is a commonly found in death receptor proteins, and acts as a protein interaction domain and a platform for death-inducing signalling complex (DISC) formation[12]. The serine-rich tail is a common feature for death domain containing proteins and possesses an inhibitory effect towards DAPK-1 activity[13, 14].

DAPK-1 plays a role in multiple cellular signalling pathways including apoptosis, autophagy, membrane blebbing and cell movement (see Section 1.8 for details). A lot of work has focussed on identifying novel interactive partners of DAPK-1. By examining DAPK-1 functional domains in isolation a number of DAPK-1 interactive

proteins have been identified (see Section 1.7 for details). Regulation of DAPK-1 activity and expression has also been intensively studied and has revealed that DAPK-1 is regulated at the transcriptional level as well as post-translationally by phosphorylation and ubiquitin-mediated degradation (see Section 1.9 for details).

1.3 DAPK-1 family members

DAPK-1 shows significant homology in its catalytic domain to those of another 4 kinases, i.e. DRP-1 (DAPK-1 related protein 1, also named DAPK-2), ZIP kinase (Zipper interacting kinase, also named DAPK-3), DRAK1 (DAPK-1 related protein 1) and DRAK2[15]. DRP-1 and ZIP kinase share around 80% homology in the catalytic domains to that of DAPK-1, while DRAK1 and DRAK2 share approximately 50% (Figure 1.2). However, the extra-catalytic domains of these five proteins are markedly different from each other. Only DRP-1 possesses a CaM regulatory domain like DAPK-1. ZIP kinase contains a leucine zipper motif, and the C-terminal regions of DRAK1 and DRAK2 don't show any known structural homology to other proteins. Because of the high similarities in the kinase domains, DAPK-1, DRP-1 and ZIP kinase are usually grouped into one superfamily. They share similar substrate preference and overlap partially in biological functions[15]. But the difference in the extra-catalytic domains of these superfamily members also confers unique functions for each of them. For instance, the leucine zipper motif of ZIP kinase mediates its dimerization and interaction with transcription factor ATF4 and the apoptosis antagonizing transcription factor (AATF)[16]. As the prototypic member of this family,

DAPK-1 has been extensively studied and reported to be involved in various cellular signalling pathways.

Interestingly, an alternative spliced isoform of DAPK-1 named DAPK-1β, which possesses a unique 12aa extension following the ser-rich tail, was identified in both mouse and human cells[17, 18]. It has been shown that this isoform functions differently from DAPK-1 to antagonize apoptosis[17]. However this observation is controversial because independent groups of researchers demonstrated that DAPK-1β's function was identical to DAPK-1[15]. Further investigation is needed to elucidate the role of DAPK-1β. In this study, DAPK-1 only refers to the form without the 12aa extension.

1.4 Kinase activity of DAPK-1

Calcium calmodulin Kinases (CaMKs) are activated by a release-of-autoinhibition mechanism[19, 20]. The regulatory domains of CaMKs contain an autoinhibitory region and a CaM recognition region (Figure 1.3). Binding of activated CaM to the CaM recognition region induces a conformational change that releases the steric block of the active site by the autoinhibitory region. It is also common that the activity of CaMKs is regulated by phosphorylation on the CaM regulatory domains and the effects of the phosphorylations vary. For example, CaMKII contains an autophosphorylation site on its autoinhibitory region that allows a prolonging of the CaM activation[20]. Myosin light chain kinase (MLCK) contains a phosphorylation site on its CaM recognition region that decreases its affinity with CaM[20].

Like other CaMKs, the catalytic activity of DAPK-1 is greatly enhanced when Ca^{2+}-activated CaM binds to its CaM regulatory domain[8]. A deletion mutant of DAPK-1 lacking the CaM binding domain displays a constitutively active kinase activity and induces phosphorylation independent of CaM binding *in vitro*[8], confirming the effect of the autoinhibitory region on the CaM regulatory domain. In addition, a single-point mutation of Ser308 on the CaM recognition region into alanine, which mimics the dephosphorylated form of DAPK-1, displayed a significant elevation in CaM binding and kinase activity *in vitro*; while another mutation of Ser308 to aspartic acid that mimicked the phosphorylated form of DAPK-1 strongly reduced the binding to CaM and minimized the DAPK-1 kinase activity[21]. These data suggest that phosphorylation on Ser308 of DAPK-1 has an inhibitory effect towards its kinase activity. Moreover, a kinase dead mutant of DAPK-1 (K42A) lost the Ser308 phosphorylation[21], indicating that the kinase activity of DAPK-1 is regulated by an autoinhibitory mechanism via autophosphorylation of Ser308 on the CaM recognition region[21]. Phosphorylation on Ser308 is Ca^{2+}/CaM independent and is inhibited by the addition of Ca^{2+}/CaM[21]. This suggests that the autophosphorylation on Ser308 favours the conformation required for binding to the autoinhibitory region, thus creating a two-step mechanism for activation of DAPK-1. In summary, in order to fully activate DAPK-1 in cells, the dephosphorylation of Ser308 and the addition of Ca^{2+}/CaM are both required.

1.5 Localization of DAPK-1

The intracellular localization of DAPK-1 is an important aspect for understanding its function. It was published in 1997 that DAPK-1 localized to the cytoskeleton via its cytoskeletal binding domain[8]. It was subsequently discovered that DAPK-1 localized to actin stress fibers of the cytoskeleton and that this localization requires its ankyrin repeats region in addition to the cytoskeletal binding domain[22, 23]. It has been shown that proteins containing ankyrin repeats are able to prevent microtubule-dependent vesicular transport[24], suggesting a possible interaction between ankyrin repeats and microtubules. Indeed, a recent study demonstrated that DAPK-1 can interact with tubulin and colocalize with mibrotubules[25]. However, it has to be noted that although DAPK-1 demonstrates a strong colocalization with the cytoskeleton, a diffused DAPK-1 staining in the cytoplasm is also observed in all the published works together with the cytoskeletal co-staining[22, 23, 25]. This suggests that *in vivo* there may be several pools of DAPK-1, which differ from each other in their binding partners and localization.

1.6 Expression of DAPK-1

1.6.1 Tissue specific expression of DAPK-1

Tissue distribution and developmental changes in mRNA expression can in part reflect the physiological role of a gene. Several groups investigated the mRNA expression of DAPK-1 by Northern blot and *in situ* hybridization analyses, and found that DAPK-1 was expressed predominantly in brain and lung, and with relatively

high levels in heart, spleen, eye ball and kidney[26, 27]. In brain, DAPK-1 mRNA appeared at embryonic day 13 and was detected thereafter throughout the embryonic period. At postnatal stage, the expression of DAPK-1 is restricted to the hippocampus[26, 27]. These data suggest that DAPK-1 mRNA is under strict regulation during development. Although it has been reported that DAPK-1 null mice have no significant developmental defects[15], mutation of a negative regulator of DAPK-1 activity could lead to overactive DAPK-1 during development and cause defects or lethality.

1.6.2 DNA methylation of DAPK-1 gene

DNA methylation is an enzyme-mediated chemical modification that adds methyl (CH_3) groups at selected sites on DNA (Figure 1.4)[28]. In humans, DNA methylation is the only known natural modification of DNA, and only affects the Cytosine base (C) when it is followed by a Guanosine (G)[28]. Thus the DNA methylation sites on human genes are called CpG islands. Gene silencing by DNA methylation is a well-known mechanism in tumourigenesis and promoter methylation mediated expression loss of a number of tumour suppressor genes like p16 or Rb has been demonstrated in various cancers[28].

In 1997, a survey of DAPK-1 mRNA and protein expression in cell lines derived from human B cell neoplasms, bladder, breast and renal cell carcinomas discovered loss of DAPK-1 expression in these cell lines and this loss was not due to a deletion or rearrangement of the DAPK-1 gene, but due to the epigenetic silencing of the gene by DNA methylation[29]. The follow-on work by the same group in 2001 revealed that

the DAPK-1 gene was methylated in 26% of the primary tumour samples from patients with colon cancer[30]. From then on, a massive amount of research by different laboratories investigated DAPK-1 gene methylation and expression in various human tumours. In many cases, the detection of methylation in a certain region of DAPK-1 gene by methylation specific PCR correlated well with the loss of DAPK-1 mRNA expression. Today, DNA methylation-mediated DAPK-1 expression loss has been observed in various cancers originating from different tissues, including lymhomas and leukemias, lung, breast, colon, cervix, prostate and brain[31-42]. Therefore, loss of DAPK-1 expression by DNA methylation in cancers seems to be a general phenomenon and strongly suggests a tumour suppressor role of DAPK-1. The strongest support for this assumption came from a recent study showing that loss or reduced expression of DAPK-1 underlies cases of heritable predisposition to chronic lymphocytic leukaemia (CLL) and the majority of sporadic CLL, in which epigenetic silencing of DAPK-1 by DNA methylation on its promoter region occurs in almost all cases[43].

In some cases, however, DAPK-1 gene methylation status does not correlate with its expression. For example, it has been reported that for some B cell and lung cancer cell lines, treatment of the DNA methylation inhibitor 5'-azadeoxycytidine (5-aza-dC) did not restore the expression of DAPK-1[29, 44]. Loss of DAPK-1 expression in the absence of DNA methylation has also been observed[45-47]. The mechanisms underlying this DNA methylation independent expression loss of DAPK-1 is still unclear. One study demonstrated that loss of heterozygosity was responsible for loss of DAPK-1 expression in around 15% of human colon and breast cancer samples[30].

Another two studies showed that homozygous deletion of DAPK-1 gene in pituitary tumours and soft tissue leiomyosarcomas led to loss of DAPK-1 expression[48, 49]. These studies showed the complexity in tumour genesis and provided more clues in understanding the role of DAPK-1 in cancer at genetic level.

1.6.3 General degradation pathway

In addition to transcriptional regulation, the expression of intracellular proteins are also regulated by post-translational degradation pathways at rates spanning from a few minutes to many days. For example, the protein half life of ornithine decarboxylase (ODC) is around 10 minutes, while that of glucose-6-phosphate dehydrogenase (G6PD) is 15 hours[50]. Two major pathways for protein degradation have been identified in eukaryotic cells, i.e. the lysosomal pathway and the ubiquitin-proteasome pathway.

Lysosomes are organelles containing acidic hydrolases that predominantly degrade long-lived protein and organelles. Lysosomal degradation is utilised in digestion processes such as pinocytosis and phagocytosis, which ingest other dying cells or exogenous proteins and particles, endocytosis to recycle the membrane bound receptor proteins, and microautophagy and macroautophagy to digest unneeded proteins and organelles to produce energy (Figure 1.5)[50]. Proteases of the cathepsin family are the best studied lysosomal hydrolases[51]. The term "cathepsin" stands for "lysosomal proteolytic enzyme" regardless of the enzyme class[52]. Therefore, cathepsins can be divided into three subgroups according to their active-site amino acid, i.e. cysteine, aspartate and serine cathepsins[53]. They are synthesized as inactive

preproenzymes, post-translationally glycosylated and directed to the lysosomal compartment by cellular mannose-6-phosphate receptors[52]. Cathepsins are optimally active in the acidic pH of lysosome (pH4-5), but can also function in more neutral pH outside of the lysosome but with lower efficacies[51].

The 26S proteasome in eukaryotic cells is a barrel-shaped multiprotein complex that predominantly degrades short-lived proteins[54]. It is composed of two sub-complexes, a 20S subunit containing the catalytic activity and a 19S regulatory subunit[55]. Degradation of a protein via the ubiquitin-proteasome pathway involves two successive steps; conjugation of ubiquitin, followed by degradation of the ubiquitin tagged protein by the downstream 26S proteasome complex[50]. Ubiquitin is an evolutionarily conserved 76-residue globular protein present in all eukaryotes and is usually attached to lysine side chains of target proteins, resulting in branched and isopeptide-linked ubiquitin-protein conjugates (ubiquitination)[56]. Ubiquitination is a very complicated process and can act as a signal for protein to be targeted for proteasomal degradation. The conjugation of ubiquitin with the substrate proceeds through a three-step cascade mechanism (Figure 1.6). Three classes of enzymes known as E1, E2 and E3 are involved in this process. Initially E1 activates ubiquitin for conjugation by using the energy of ATP to form a high-energy thiolester linkage with the C-terminus of ubiquitin. Then, one of several E2 enzymes, which also bind ubiquitin covalently through a thiolester bond, transfers the activated ubiquitin moiety to the substrate protein either directly or via an E3 ligase[56]. In many cases, E3s play a key role in ubiquitination since they mediate the highly specific recognition of the target proteins that are to be degraded. However, the mechanisms

through which E3s select substrates remains the poorest understood part of the ubiquitination process. To date, the known E3s can be classified into two major families: the HECT (Homologous to E6-AP C-Terminus) domain containing E3s and the structurally related RING-Finger/U-box domain containing E3s[56].The HECT domain can directly bind to ubiquitin via a thioester bond and then transfer ubiquitin to the substrate, while the RING/U-box domain usually acts as a docking station for the substrate and the E2 enzyme[57]. The RING domain is stabilized by Zn^{2+} ions mediated by the cystine and a histidine on it, whereas the U-box is stabilized by a system of salt-bridges and hydrogen bonds[58]. Interestingly, all mammalian U-box containing proteins have been reported to interact with molecular chaperones or co-chaperones, suggesting an important role of these proteins in mediating the degradation of unfolded or misfolded proteins[59].

Although the best-studied function of ubiquitination is targeting substrates towards proteasomal degradation, there are other functions for ubiquitination and there exist several distinct types of ubiquitination. Substrates can be monoubiquitinated or polyubiquitinated, and polyubiquitin chains can be linked through any of the seven lysine residues in ubiquitin[60]. In cells, monoubiquitination primarily regulates subcellular relocalization of substrates[61]. In humans cells, polyubiquitin chains are usually linked by Lys-48 or Lys-63 residues[61]. Lys-48-linked ubiquitin chains often target substrates for proteasomal degradation and in order to accomplish this function must contain at least four ubiquitins[61]. Lys-63-linked ubiquitin chains generally don't promote degradation, but are involved in regulating protein activity and localization[61].

1.6.4 Degradation of DAPK-1

Not much is known about the degradation mechanisms regulating DAPK-1. It was reported that DAPK-1 can be degraded via the ubiquitin-proteasome pathway and two ubiquitin E3s have been identified that target DAPK-1 towards the proteasome. The first is DIP-1 (MIB-1), which was a RING domain E3 and reported to interact with the ankyrin repeats region on DAPK-1 and is able to actively ubiquitinate and degrade DAPK-1[62]. The other is the carboxyl terminus of HSC70-interacting protein (CHIP), which is a U-box-containing E3 ubiquitin ligase that can bind to Hsp90 and Hsp70[63]. CHIP facilitates the ubiquitination of some Hsp90 client proteins[63] and as a Hsp90 interacting protein, DAPK-1 is targeted for degradation by CHIP[64].

Little is known about lysosomal degradation of DAPK-1. however it was demonstrated that DAPK-1 is associated with the cysteine protease cathepsin B in the lysosome[65, 66]. Previous reports also demonstrated that DAPK-1 can be cleaved to yield a 60KDa product[65, 66] and that the accumulation of the 60KDa cleavage product of DAPK-1 protein is specifically blocked by a cathepsin B inhibitor[66], suggesting that DAPK-1 can be cleaved by cathepsin B. Moreover, the observation that DAPK-1 is involved in regulating autophagy strongly suggests that DAPK-1 can be regulated via an alternative lysosomal degradation pathway.

1.7 Interactive partners of DAPK-1

Protein-protein interaction refers to the association of protein molecules and forms the basis of signalling pathways and foundation of all biological activities in cells. As

DAPK-1 is reported to be involved in multiple signalling pathways, it is important to understand its interactive partners in order to comprehensively understand the molecular mechanisms underlying the biological functions of DAPK-1. This section will introduce all the known and predicted proteins that can directly interact with DAPK-1. The roles of these interactions in signalling pathways involving DAPK-1 will be discussed together with the biological functions of DAPK-1 in section 1.7.

1.7.1 Substrates of DAPK-1

Being a Ca^{2+}/CaM dependent serine/threonine kinase, the substrates of DAPK-1 are naturally the first interesting interactive partners to study. Due to lack of DAPK-1 substrates at the early stage in the field, the search for a DAPK-1 phosphorylation consensus motif was carried out in 2001 using positional scanning substrate library synthesis and activity screens[67]. A peptide analogue of the myosin light chain (MLC) phosphorylation site was used as a starting point because MLC is the first identified substrate for DAPK-1 and not much was known about other substrates at that time[67]. The result showed that DAPK-1 has a preference for basic residues in the core P-2, P-1 and P1, although a variety of amino acids are tolerated at these positions. For example, peptides with D or N at P1 and R or K at P-2 are more effectively phosphorylated by DAPK-1. Moreover, DAPK-1 has a loose preference for positive charged amino acids R or K further upstream[67]. In conclusion, the consensus for the DAPK-1 phosphorylation site based on the study of MLC is KRxxxxxKRxxS/T (Table 1.1).

More recently, a new method using biochemical fractionation and mass spectrometric analysis to purify and identify potential substrates from HeLa cell lysate was developed[68]. Total Hela cell lysate was subjected to consecutive fractionation using phenyl-HP hydrophobic column and then incubated *in vitro* with a recombinant protein consisting of the catalytic domain of DAPK-1. The corresponding phosphorylated substrates were then cut out of the gels and sent for mass spectrometric analysis[68]. Minichromosome maintenance complex component 3 (MCM3), which is a DNA replication licensing factor, was pulled out by this method and proved to be phosphorylated by DAPK-1 not only *in vitro*, but also *in vivo* at Ser160[68]. This success indicates the usefulness of this approach in identifying new physiological substrates of DAPK-1 and may greatly shorten the time spent on searching for new substrates of DAPK-1 in the future.

The DAPK-1 substrates identified to date include CaM-regulated protein kinase kinase (CaMKK), DAPK-1 itself, MCM3, MLC, cell cycle regulator p21, p53, ribosomal protein S6, neural protein Syntaxin-1A, tropomyosin-1 and the DAPK-1 family member ZIP kinase (Table 1.1). Not all these substrates match the identified consensus motif (Table 1.1). However, the consensus does provide a clue for predicting the potential substrates of DAPK-1 and will be helpful in identifying new substrates for DAPK-1.

Table 1.1 Known substrates of DAPK-. The amino acids and numbers in red signify the phosphorylation site. Proteins are listed in alphabetical order.

Substrate	Phosphorylation Site
CaMKK[69]	GSRREERSLS[511]APG

DAPK-1[21]	ARKKWKQS[308]VRLI
MCM3[68]	TKKTIERRYS[160]DLTTL
MLC[22]	TTKKRPQRATS[19]NVF
p21[70]	RKRRQT[145]SMTDFYHSK
p53[70]	PPLSQET[18]FS[20]DLWKLL
S6[71]	QIAKRRRLS[235]SLRAS
Syntaxin-1A[72]	IIMDSSIS[188]KQALSEIE
Tropomyosin-1[73]	HALNDMTS[283]I
ZIP kinase[74]	KT[299]TRLKEYTIKS[309]HS[311]S[312]LPPNNS[318]YADFERFS[326]
Consensus	KRxxxxxKRxxS/T

Although the sites of phosphorylation on these substrates by DAPK-1 have been defined, the functions of some phosphorylations are still not clear. For example, the effect of phosphorylation of p53, p21 and MCM3 have not been clearly demonstrated. Moreover, phosphorylation on Ser235 of ribosome protein S6 was suggested to inhibit its activity *in vitro*[71]. However, the same phosphorylation on Ser235/Ser236 was reported by other groups to promote its activity[75]. This contradiction highlights the lack of understanding of the function of these phosphorylation events, thus more experiments are required to clarify the functional effects of the phosphorylations.

1.7.2 Binding partners of DAPK-1

All the DAPK-1 substrates are binding partners of DAPK-1. Moreover, as a protein containing multi-functional domains, DAPK-1 has other binding partners in addition

to its substrates that can interact with its other functional domains. So far, the known non-substrate binding partners of DAPK-1 include 14-3-3, CaM, extracellular signal-regulated kinase (ERK), Fas-associated protein with death domain (FADD), heat shock protein 90 (Hsp90), Leukocyte common antigen-related phosphatase (LAR), microtubule-associated protein 1B (MAP1B), mind bomb 1 (MIB1), protein kinase D (PKD), Tyrosine kinase Src, tumour necrosis factor receptor 1 (TNFR-1) and netrin-1 recepter UNC5H2 (Table 1.2).

Table 1.2 Known binding partners of DAPK-1. The proteins are listed in the alphabetical order.

Binding protein	Binding region on DAPK-1
14-3-3[76]	Not yet identified
CaM[8]	Ca^{2+}/CaM regulatory domain
ERK[77]	Death domain
FADD[76]	Not yet identified
Hsp90[78]	Kinase domain
LAR[79]	Ankyrin repeat region
MAP1B[25]	Kinase domain
MIB1[62]	Ankyrin repeat region
PKD[80]	Not yet identified
Src[79]	Not yet identified
TNFR-1[76]	Not yet identified
UNC5H2[81]	Death domain

As shown on Table 1.2, the region on DAPK-1 important for binding to some partners has not been defined. For example, 14-3-3, TNFR-1 and FADD are shown

to interact with DAPK-1 in rat neuron cells after brain seizure[76]. Presumably, as death domain containing proteins, they should all be able to interact with DAPK-1 via their death domains. However, no experiments have been performed to confirm this assumption. Moreover, the functional significance of these interactions is not clear.

1.7.3 Predicted DAPK-1 interactive proteins

In addition to all the known interactive partners, there are still many DAPK-1 interactive proteins awaiting for discovery. For example, DAPK-1 can induce cell death through the p19ARF-p53 pathway or by inhibiting integrins and extracellular matrix (ECM) signalling[15]. However, DAPK-1 doesn't seem to directly interact with p19ARF or integrins. Moreover, DAPK-1 was also reported to induce autophagy, while no interactions between DAPK-1 and any autophagy related genes have been found. Therefore, there must be some unknown proteins that link DAPK-1 and the reported downstream signalling pathways. It is a great challenge to find these unknown DAPK-1 interactive partners in order to further elucidate the functional role of DAPK-1.

1.8 Cellular functions of DAPK-1

1.8.1 Cell death pathways

Although the term "apoptosis" is often used to describe cell death, there exist some other morphologically and biochemically different forms of cell death (Figure

1.7)[82].Cell death falls into several categories and the difference between them are not very clear. In general, cell death can be divided as non-physiological (necrotic) cell death and physiological cell death, which consists of autophagic cell death and apoptosis (Figure 1.8)[83]. Therefore, it is very important to distinguish the unique characteristics of these cell death pathways and find out which type of cell death DAPK-1 participates in.

As the most typical PCD, apoptosis is characterized by morphological changes such as cell shrinkage and rounding, cytoplasm condensation, chromatin condensation and fragmentation, packaging of the decreased cell into apoptotic bodies without plasma membrane breakdown and finally removal of apoptotic bodies by phagocytes like macrophages (Figure 1.7c)[3, 82, 84, 85]. These morphological features of apoptosis can occur dependent or independent of the cysteine protease caspase cascade, which plays an essential role in the execution of apoptosis[83]. Caspases are activated by either death receptor ligation (Extrinsic pathway)[86] or disruption of mitochondrial membrane potential ($\Delta\psi_m$) (Intrinsic pathway)[87] (Figure 1.8,1.9), and requires energy in the form of ATP[83]. In the intrinsic pathway, when its potential is disrupted, mitochondria release into the cytosol a small protein cytochrome c, which first binds with Apaf-1 (apoptosis protease activating factor 1) and ATP, and then binds to pro-caspase 9 to create a protein complex known as an apoptosome. The apoptosome cleaves pro-caspase 9 to its active form of caspase-9, which in turn activates caspase 3 and caspase 7 that execute apoptosis (Figure1.9)[61]. In the extrinsic pathway, the execution of apoptosis also requires caspase 3 and caspase 7 (Figure 1.9). Importantly, there is a great deal of crosstalk between the intrinsic and extrinsic cell

death pathways (Figure 1.9). For example, in response to stress, mitochondria also release proteins called Smacs (second mitochondria-derived activator of caspases), which binds to the IAPs (inhibitor of apoptosis proteins) such as XIAP (X-linked IAP), cIAP1 (cellular IAP 1) and cIAP2 to relieve their inhibition of caspase 9, caspase 3 or caspase 7, thus promoting apoptosis (Figure 1.9)[88, 89].

A large amount of proteins are involved in the regulation these distinct apoptotic pathways[61]. Of note, some death receptor pathways possess both pro- and anti-apoptotic functions in the extrinsic pathway. For example, TNF-α can activate both survival and apoptosis pathways (Figure 1.9)[61]. There are two TNF-α receptors, TNFR-1 and TNFR-2[90]. TNFR-1 is found in most cells and activated by soluble ligand[90]. TNFR-2 is primarily expressed in haemopoietic cells and mainly activated by membrane-integrated ligand[90]. Studies using TNFR-1 and TNFR-2 deficient mice suggest that TNFR-1 mediates most of the apoptosis, proliferation and pro-inflammatory pathways downstream of TNF-α, while the TNFR-2 mediated signalling is less well characterized[91]. In TNFR-1 signalling, the default effect is induction of genes involved in inflammation and cell survival[92]. When TNFR-1 is ligated to TNF-α, it starts to bind to TRADD, which recruits the secondary adaptors, RIP-1, TRAF2 or TRAF5, forming receptor complex I (Figure 1.9)[61, 92]. Receptor complex I catalyzes the phosphorylation and degradation of the NF-κB inhibitor, I-κB, which results in the translocation of transcription factor NF-kB (composed of two subunits RelA and p50) into the nucleus where it can induce the expression of pro-inflammatory genes as well as a series of negative regulators of apoptosis such as cFLIP (Cellular caspase-8 (FLICE)-like inhibitory protein) and Bcl-2 (B-cell

CLL/Lymphoma 2)[93]. If the NF-κB signal is not successful, complex I can then disassociate from the membrane bound TNFR-1 and bind to the protein FADD in the cytosol, which mediates the recruitment of caspase 8 and caspase 10 to induce apoptosis through caspase 3 and caspase 7 (Figure 1.9)[93].

There are reagents that can switch TNF-α from inflammation and survival to its apoptotic function. For example, the protein synthesis inhibitor cycloheximide (CHX) can promote TNF-α induced apoptosis. It has been suggested that CHX facilitates TNF- mediated apoptosis by suppressing the synthesis of the anti-apoptotic, NF-KB-regulated bcl-2 and cFLIP proteins[94-96], In addition, co-treatment with the pro-apoptotic protein Smac or a Smac peptide mimetic has also been found to sensitize human cancer cells to TNF-α induced apoptosis, probably due to Smac's ability to block the inhibitor of apoptosis proteins (IAPs)[89, 97]. The lysosomal protease cathepsin B can participate in TNF-α induced apoptosis in some cellular contexts. For example, it has been reported that isolated cells from cathepisn B-knocked-out mice are resistant to TNF-α induced apoptosis and the cathepsin B null mice were protected from TNF-α induced liver damage[98], suggesting an important role of cahtepsin B in the TNF-α stimulated apoptosis pathway in liver cells. However, although this model is also consistent with some experiments performed in human cells[99], the opposite results have been observed, showing cathepsin B in not involved in TNF-α induced apoptosis[100]. Therefore, the exact role of cathepsin B in TNF-α pathway may vary according to the cellular conditions.

Autophagy is a cellular catabolic response to a lack of nutrients or to stress. During autophagy, cellular proteins, organelles and bulk cytoplasm are sequestered into double-membrane vesicles called autophagosomes. Autophagosomes then fuse with lysosomes to form autophagolysosomes where the sequestered cargo is degraded and recycled to provide energy for the cells[101]. The morphological characteristics of autophagy are the formation of double-membraned autophagosomes, nuclear condensation without DNA fragmentation and an intact and functional cytoskeleton until late in the process (Figure 1.7b)[102]. As shown in section 1.6.3, autophagy is intimately linked to the lysosomal degradation pathway (Figure 1.5).

The core molecular machinery of autophagy is highly conserved in yeast, C.elegans, Drosphila and mammals[103]. , In the mammalian system 31 autophagy-related genes (ATGs) have been identified[104]. The core machinery of autophagy is based on two systems similar to the ubiquitin cascade, which deliver small ubiquitin-like proteins to its binding partners with the help of some E1 and E2-like proteins (Figure 1.10). In one system, Atg12 was first activated by Atg7, and then transferred to Atg5 by Atg10, to form a complex. The Atg5-Atg12 complex then interacts with tetramer Atg16 to form a multimer complex that localizes to membranes of early autophagosomes[105, 106]. The assembly of this system is independent of autophagy activation and therefore may provide a platform for autophagy activation. In the other system, Atg8, the mammalian ortholog of which is microtubule-associated protein 1 light chain 3 (LC3), is first cleaved by Atg4 to expose its C-terminal conserved Gly[120]. Atg8/LC3 is then transferred to phosphatidylethanolamine (PE) by Atg7 and Atg3[107]. Unbound Atg8/LC3 (named LC3-I) is in the cytosol, whilst the

conjugated form (named LC3-II) is localized to the autophagosomal membrane by the Atg5-Atg12-Atg16 complex[107]. The association of Atg8/LC3-PE complex to the autophagosome is important for the autophagosome membrane extension and the closure of the membrane to form vesicles. When the autophagosomes are mature, the Atg12-Atg5 complex detaches from autophagosomes, whereas Atg8/LC3 stays trapped on the membrane until it is degraded by the lysosomes. Therefore, Atg8/LC3 is widely used as a marker for autophagy[106].

Although autophagy was initially discovered as a process that allows cells to survive times of famine, it is also found to participate in cell death. For example, loss or reduction of autophagy regulating proteins such as Atg7 and Beclin-1 attenuate apoptosis-independent cell death[108-111], suggesting a positive role for autophagy in cell death. The dual roles of autophagy in cell death and cell survival are intriguing, but make it difficult to understand how autophagy chooses between survival and death. Some genetic studies may provide some clues. In C.elegans, in response to starvation, excessive or insufficient autophagy both lead to cell death, suggesting that only a balanced level of autophagy is cytoprotective[112]. Moreover, although the beclin-1 knock-out mice died early in embryogenesis, beclin-1 heterozygous mice displayed high incidence of spontaneous tumours, suggesting overactive survival pathways in these single allele knock-out mice[113]. Taken together, it seems the level of autophagy is very important for determining the cell fate. However, the physiological level of autophagy may vary among cell lines, tissues and species. There is no morphological or biochemical difference between autophagic cell survival and autophagic cell death since autophagosomes are the main characteristics

of autophagy. In addition, autophagy was found to collaborate with or even induce apoptosis and necrosis[114-119], suggesting intense cross-talk between autophagy and other cell death pathways. Therefore, so far there is still little known about the actual "physiological" level of autophagy in cells and makes it difficult to interpret the function of autophagy when autophagic morphology is observed in cells. It is possible that autophagy is a "checkpoint" process for cells. Different from cell cycle checkpoint, autophagy is not stimulated by DNA damage, but by nutrient or energy insufficiency. Its primary function is to provide energy and nutrient to help cells survive famine. But when cells are exposed to cell death signals or the environmental conditions are too harsh, autophagy can in turn participate in and facilitate cell death processes like apoptosis and necrosis. Of note, it doesn't mean that autophagy is an indispensable step before cell death, since cell death can be stimulated independently of autophagy[82]. The exact biochemical mechanisms underlying the cross-talk between autophagy and other cell death pathways are still unclear and require a lot of work in the future. Ideally, some specific markers for autophagic cell survival or death such as poly (ADP-ribose) polymerase (PARP) cleavage for apoptosis will be discovered, and thus will greatly help identify the actual role of autophagy under different conditions.

In contrast to the physiological cell death processes, necrosis is a result of energetic catastrophe such as ATP depletion and has been characterized morphologically by vacuolation of the cytoplasm, breakdown of the plasma membrane and an induction of inflammation around the necrotic cells (Figure 1.7d)[82, 120]. Because necrosis leads to disintegration of cells, not much is known about the biochemical alterations of this

process and the only way to measure necrosis so far is to monitor morphological changes. Therefore, in some assays like Trypan blue staining, it's very difficult to distinguish apoptosis and necrosis, and the use of additional apoptosis markers are required to confirm the type of cell death being observed.

1.8.2 Cell death and autophagy induction by DAPK-1

In order to study the physiological role of DAPK-1, the most elegant and convincing tools may be knock-down of DAPK-1 expression by RNA interference or knock-out of DAPK-1 gene through gene targeting. Early experiments showing that DAPK-1 antisense cDNA attenuated IFN-γ and Fas induced cell death[7, 121] suggest that the primary function of DAPK-1 is to induce cell death. Later on, the DAPK-1 knock-out mouse was created[15]. Although no defects were observed in developmental cell death in these DAPK-1 -/- mice, some experiments with the primary cells derived from the knock-out mouse further suggest a death-promoting role of DAPK-1. For example, DAPK-1 -/- hippocampal neurons were more resistant to ceramide-induced cell death than their wild type counterparts[122]. DAPK-1 -/- mouse embryonic fibroblasts (MEFs) displayed decreased levels of apoptosis in response to forced expression of oncogenes c-myc and E2F compared to wild-type MEFs[123]. UNC5H2-mediated cell death was also partially attenuated in DAPK-1 -/- MEFs[81]. In addition, retinal ganglion cells obtained from DAPK-1 -/- mice displayed increased survival compared to control (79% vs 56%) following administration of glutamate[124]. All these data support the notion that DAPK-1 is a physiological death-promoting kinase.

Ectopic expression of DAPK-1 or its mutants can in another way provide a clue to its cellular functions. The mutants in theory should antagonize the function of endogenous DAPK-1, although the high level of ectopically expressed DAPK-1 usually bypasses the physiological level of DAPK-1. Ectopic overexpression of wild type DAPK-1 was shown to be sufficient to induce cell death in various cell lines[8, 77, 121, 123, 125-127]. It was also found to enhance cell death induced by ceramide[128], UNC5H2[81] and MEK (mitogen-activated protein kinase)/ERK[77] signalling. The kinase dead mutant of DAPK-1 (K42A) and some miniprotein of interfering fragments, such as the death domain, have also been widely used. They have been found to antagonize multiple cell death signals like Fas[121], ceramide[122, 128], TGF-β[126] and so on. However, although being enlightening, the data obtained from the mutant overexpression, especially fragment overexpression, may not necessarily reflect the role of DAPK-1. For example, DAPK-1 is a cytoplasmic protein, which is determined by its cytoskeletal binding domain and ankyrin repeats region as mentioned in section 1.4. The death domain miniprotein or the kinase domain miniprotein may move into the nucleus and, interfere with some signalling pathways that full-length DAPK-1 would never do. Extra caution is needed when interpreting data on these fragment mutants.

DAPK-1 was found to actively participate in apoptosis pathway. In addition to IFN-γ, DAPK-1 was shown to positively regulate apoptosis downstream of other stimuli including Fas ligand[121], TGF-β[126], ceramide[122, 128], TRAIL[129], brain seizure and ischemia[66, 76, 130], cell detachment from extra cellular matrix[127] and forced expression of oncogenes like c-myc and E2F[123]. Moreover, DAPK-1's binding partner ERK was

found to stimulate apoptosis through DAPK-1 when cells are exposed to active MEK signal[77, 131]. Besides, another DAPK-1 binding partner UNC5H2 was reported to induce apoptosis partially via DAPK-1[81]. However, in the UNC5H2 paper, Trypan blue was the only assay for measuring cell death. Considering Trypan blue is more sensitive for necrotic cells, it may suggest that DAPK-1 can also be involved in necrosis. Actually, one recent report demonstrated that when the cells were treated with H_2O_2, DAPK-1 can activate PKD and is required for the caspase-independent necrotic cell death induced by oxidative stress[80], which further supports the idea that DAPK-1 can be involved in necrosis.

Interestingly, DAPK-1 is not exclusively a positive regulator of cell death. Since its discovery, a lot of work has been carried out to investigate the role of DAPK-1 in the TNF-α signalling pathway. It has been shown by several groups independently that DAPK-1 was neutral[7, 126] or protective[18] in TNF-α induced apoptosis by comparing the response to TNF-α treatment in DAPK-1 knocked-down and wild type cells. One opposing report demonstrated that overexpression of the death domain fragment of DAPK-1 can block TNF-α induced apoptosis[121], suggesting that DAPK-1 is a positive regulator of cell death in TNF-α pathway. However DAPK-1 is able to bind to downstream factors in the TNF-α pathway such as TNFR-1 and FADD presumably through death domain homotypic interaction[76], therefore it is likely that the death domain miniprotein does not mimic the function of full-length DAPK-1 *in vivo*, and may interfere with the downstream functions of TNF-α via non-specific bindings. Some more recent studies further proved that DAPK-1 is not a positive regulator in TNF-α induced apoptosis; instead, it is a negative regulator. It was found

that in Hela cells, the expression of MIB1, an ubiquitin E3 ligase that degrades DAPK-1, promotes TNF-α-induced apoptosis[62]. In addition, although antisense depletion of DAPK-1 in Hela cells protects cells from IFN-γ induced apoptosis, it promotes TNF-α induced apoptosis[18]. Therefore, although it functions as a death-promoting kinase, DAPK-1 can also act as a survival factor under certain circumstances.

It has been reported that DAPK-1 is involved in the regulation of starvation induced autophagy in C.Elegans[112]. In mammalian cells, DAPK-1 was reported to be necessary for interferon-γ-induced autophagy[125], albeit it does not seem to be crucial for starvation or rapamycin-induced autophagy[31]. Moreover, ectopic expression of DAPK-1 in some cell types can induce autophagy, as defined by the formation of autophagy markers such as autophagasomes[25, 74, 125]. These data suggest that there may be multiple signalling pathways that regulate autophagy pathways in cells and that DAPK-1 is only involved in some of them.

Taken together, it is clear that DAPK-1 is involved in multiple cell death pathways. However, it has to be noted that most of the experiments showing DAPK-1 as a positive effector of apoptotic cell death were performed in the presence of other upstream signals such as IFN-γ or MEK/ERK. When DAPK-1 level was increased by ectopic transfection, the response observed in most reports is autophagy. The only experiment showing DAPK-1 overexpression per se induces apoptosis was performed in suspended cells, and thus the apoptosis induced was anoikis. As discussed above, autophagy may act as a checkpoint process. Therefore, it is possible

that the main function of DAPK-1 is to act as an autophagy regulator and its role in other cell death pathways vary according to cellular stimuli and environment. This indicates that DAPK-1 can have dual functions in cell fate, i.e. both survival and death, and may help to explain the controversial observation that DAPK-1 acts as a resistance factor in the TNF-α death-signalling pathway. It is still unclear exactly how DAPK-1 contributes to apoptosis or necrosis, however with the increasing understanding of the complicated crosstalk between autophagy, apoptosis and necrosis, extra caution is needed when interpreting the roles of DAPK-1 in these pathways.

The mechanisms through which DAPK-1 induces autophagy and cell death are still not clear, but the interactive proteins of DAPK-1 may provide some clues. For example, CaMKK is an enzyme key to maintain neuronal survival and phosphorylation by DAPK-1 attenuated its activity[69]. Phosphorylation of PKD by DAPK-1 enhances its activity to promote oxidative stress induced cell death[80]. Syntaxin-1A is a positive regulator of autophagy and its phosphorylation by DAPK-1 enhanced its interaction with MUNC-18 (mammalian homologue of the unc-18 gene) and presumably increases its role to promote autophagy[72]. Moreover, DAPK-1 induces apoptosis through p19ARF-p53 pathways. Although no direct interaction between DAPK-1 and p19ARF was observed, the discovery that DAPK-1 can phosphorylate p53 may provide a new angle for investigation[132]. Besides, interaction between ERK and DAPK-1 not only leads to phosphorylation of DAPK-1 by ERK that results in activation of DAPK-1 kinase activity, but also retain ERK in the cytoplasm that prevents its cytoprotective effect. These downstream pathways of

DAPK-1 display the complexity of this protein and clearly indicate that although the cellular outcome observed may be similar, DAPK-1 can achieve these outcomes via multiple cellular pathways in different cell types or under different stimuli. The identified interactive partners of DAPK-1 that are involved in apoptosis and autophagy are summarized in Table 1.3.

Table 1.3 Known binding partners of DAPK-1that are involved in apoptosis and autophagy.

Interactive protein	Roles of the interaction in apoptosis and autophagy
CaM[8]	Promote apoptosis
ERK[77]	Promote apoptosis
LAR[79]	Promote apoptosis
MAP1B[25]	Promote autophagy
PKD[80]	Promote cell death
Src[79]	Inhibit apoptosis
UNC5H2[81]	Promote apoptosis
ZIP kinase[74]	Prmote cell death

1.8.3 Membrane blebbing induction

In most eukaryotic cells, the plasma membrane is bound to the cell cortex, which is composed of actin, myosin and associated proteins[133]. Under certain circumstances, the plasma membrane separates from the cortex and expands into spherical protrusions called blebs (Figure 1.11) and membrane blebbing refers to the cell status when cells have blebs. Blebs differ from other cellular protrusions like lamellipodia or filopodia, because the growth of blebs is pressure-driven instead of being pushed against the membrane by polymerizing actin filaments[134]. In general, the life cycle of

membrane blebbing can be subdivided into three stages: bleb initiation, expansion and retraction (Figure 1.12)[133]. The bleb initiation can be caused by two distinct mechanisms, a local dissociation of the membrane from the cortex[135] or a local rupture of the actin cortex[136] (Figure 1.12a). After initiation, the hydrostatic pressure in the cytoplasm drives the cytosol fluid into the blebs, which leads to the size increase of the blebs (Figure 1.12b)[133]. The retraction step consists of reformation of cortex and the follow-on bleb retraction[133]. After the bleb expansion slows down, actin cortex repolymerization begins to form a new layer of cortex under the bleb membrane (Figure 1.12c)[137]. Then myosins are recruited to discrete spots on the new cortex and create a contractile force that mediates bleb retraction (Figure 1.12d)[133].

Membrane blebbing is primarily viewed as a morphological characteristic of apoptotic or necrotic cell. In addition, some studies demonstrated that membrane blebbing can be induced by the reassembly of the contractile cortex and act as part of a normal cell division process such as cytokinesis[138]. In addition, membrane blebbing has been observed in a lot of invasive cancer cells[139]. It has been shown that experimental induction of membrane blebbing in non-invasive cells promotes their ability to invade into 3D matrices[139-141], suggesting that membrane blebbing enables cells to gain directed motility.

In early studies, membrane blebbing was used as a marker to measure the apoptosis induced by DAPK-1 and overexpression of DAPK-1 significantly induced membrane blebbing in some cell types[8, 74, 121]. However, later studies suggested that membrane

blebbing induced by DAPK-1 may reflect autophagy instead of apoptosis[25, 74, 125]. It was shown that membrane blebbing induced by DAPK-1 was greatly enhanced when its binding partner MAP1B was cotransfected and could be inhibited by the treatment of autophagy inhibitor 3-methyladenine (3-MA)[25], suggesting that DAPK-1 induces autophagy and that subsequently leads to membrane blebbing.

Conversely, a recent study demonstrated that knockdown of endogenous DAPK-1 attenuates oxidative stress induced membrane blebbing, suggesting at a physiological level a negative role of DAPK-1 in inducing membrane blebbing[73]. Tropomyosin-1 is a protein reported to be phosphorylated downstream of the ERK pathway in endothelial cells activated by oxidative stress[142, 143]. The key role of tropomyosin-1 is to induce or stabilize actin stress fibres when it is phosphorylated at Ser283. DAPK-1 was found to be the kinase that directly phosphorylates tropomyosin-1 at Ser283 downstream of ERK[73] upon oxidative stress. Interestingly, when DAPK-1 was knocked down, the cells lost stress fibres formation and underwent rapid membrane blebbing upon oxidative stress, which can be rescued by transfection of constitutively active tropomyosin-1[73]. This report adds more complexity in understanding DAPK-1's role in membrane blebbing.

Membrane blebbing is initiated by increased myosin contractility, which has been reported to be induced by phosphorylation of MLC at Thr18 and Ser19, in conjunction with weakening of the structural integrity of the cortical actin network owing to proteolysis of many of its components[15, 144-146]. DAPK-1 was found to phosphorylate MLC at Thr18 and Ser19 directly[22, 23] or indirectly through ZIP

kinase[74]. ZIP kinase localizes to both the nucleus and the cytoplasm and fractionates as momeric and trimeric forms[74] and can phosphorylate MLC efficiently at both Thr18 and Ser19 in the cytoplasm. DAPK-1 phosphorylates ZIP kinase at six specific sites on its C-terminus, and these phosphorylations retain ZIP kinase in the cytoplasm as a trimer. Thus DAPK-1 greatly enhances MLC phosphorylation by ZIP kinase[74].

Moreover, phosphorylation of MLC was reported to be sufficient and necessary for the formation of stress fibres and focal adhesions[147]. However, the phosphorylation of MLC by DAPK-1 leads to formation of actin stress fibres, but not the concomitant stimulation of focal adhesion assembly[22]. Actually, in cells cultured in serum-containing medium, DAPK-1 is even capable of inducing focal adhesion disassembly without affecting stress fibres[22]. This uncoordinated regulation of stress fibres and focal adhesions may disrupt the balance in the cytoskeletal structure and explains how enforced expression of DAPK-1 results in membrane blebbing.

Of note, under oxidative stress, the MLC kinase inhibitor ML-7 was reported to cause rapid membrane blebbing similar to the effect when DAPK-1 was knocked-down with siRNA[143]. In addition to inhibition of MLC phosphorylation, ML-7 treatment also led to decrease in tropomyosin-1 phosphorylation[143] similar to the effect of DAPK-1 siRNA treatment, even though DAPK-1 is the kinase that is reported to directly phosphorylate tropomyosin-1[73]. It has been reported that DAPK-1 is insensitive to ML-7[22], which ruled out the possibility that ML-7 took effect via DAPK-1. Therefore, although the exact mechanisms are still unclear, ML-7 and

DAPK-1 siRNA both inhibit the phosphorylations of MLC and tropomyosin-1. Because both MLC and tropomyosin-1 are critical for stress fibre formation, this dual inhibition of both kinases may lead to focal adhesion misassembly and thus result in rapid membrane blebbing in cells under oxidative stress.

The disruption of the homeostasis of the endogenous cytoskeletal structure in cells underlies the basic mechanism for membrane blebbing. Although the outcome may be the same, the cellular pathways leading to the outcome may vary dramatically. Therefore, when oxidative stress was applied, the activated pathways that lead to membrane blebbing are probably very different from those in DAPK-1 overexpressed cells. For example, as mentioned previously, DAPK-1 can induce necrotic cell death by activating PKD under oxidative stress[80]. The interaction between PKD and DAPK-1 was greatly enhanced when H_2O_2 was applied[80]. Therefore, although the basic function of DAPK-1 may be promotion of stress fibre formation, the actual role of this protein in membrane blebbing depends on the specific circumstances.

Another important aspect about membrane blebbing induced by DAPK-1 is its relationship with autophagy. Although it was shown that 3-MA can inhibit the membrane blebbing induced by overexpression of DAPK-1[25], it has to be noted that 3-MA is a general inhibitor of PI3 kinase (phosphatidyl-inositol 3-kinase), and thus interferes with numerous cellular processes besides autophagy[148]. Therefore, it can not be ruled out that 3-MA inhibited the membrane blebbing induced by DAPK-1 via pathways other than autophagy. Interestingly, it has been shown that treatment on the

highly metastatic human fibrosarcoma HT1080 cells with 3-MA can inhibit membrane ruffle formation independent of autophagy inhibition, as downregulation of Beclin-1, a protein required for autophagosome formation, did not have the same effect[149]. It is possible that autophagy and membrane blebbing observed in DAPK-1 overexpressed cells are two independent pathways, or there is even the possibility that autophagy is actually the consequence of the membrane blebbing induced by DAPK-1, for the structural changes may cause stresses in cells that later lead to autophagy. So far the observation of concomitant membrane blebbing and autophagy is only observed in DAPK-1 overexpressed cells. More experiments are needed to clarify the relationship between autophagy and membrane blebbing and the role that DAPK-1 has in these processes.

1.8.4 Inhibition of cell motility

Cell migration is crucial for multiple biological processes, including embryonic development, wound healing, immune surveillance and metastasis of tumour cells. As mentioned above, membrane blebbing promoted cell motility in 3D matrices[139-141]. Therefore, in theory, the membrane blebbing caused by enforced expression of DAPK-1 should lead to enhanced cell motility. Conversely, it was found that overexpression of DAPK-1 actually inhibited random cell migration by reducing directional persistence and directed migration via blockage of cell polarization[150]. These effects are mediated by an inhibitory effect of DAPK-1 on talin head domain associated with integrin, thereby suppressing the integrin-Cdc42 polarity pathway[150].

In addition to the specific integrin pathway inhibited by DAPK-1, there may be other reasons for the motility suppression effect observed. Of note, although DAPK-1 was shown to inhibit cell mobility, the number of cell protrusions was still markedly enhanced by DAPK-1 overexpression, suggesting the membrane blebbing promotion effect was the same in this assay[150]. Moreover, the cell migration rate after DAPK-1 overexpression was not greatly reduced[150] and the dramatic decrease in migration distance was actually caused by loss of directional persistence[150]. Interestingly, the cell movement assay in this report was performed only at 2D environment[150], whereas most reports showing blebbing motility occurred in 3D matrices or living tissues[133]. Therefore, membrane blebbing caused by DAPK-1 might enable cells to migrate better in 3-dimensions, which was not able to be observed in the 2-D assay used and may instead cause a decrease in cell movement in a 2-D assay. Besides, wound healing migration was the major assay used to test DAPK-1's function in this report[150]. Considering the multiple inflammation pathways activated in response to wounds and the complicated involvement of DAPK-1 in the cytokine signalling pathways, it is possible that some unknown signalling events were activated that synergize with DAPK-1 to inhibit random cell migration. To date, this is the only piece of work that connects DAPK-1 with cell motility. However, considering DAPK-1's active role in membrane blebbing and as a tumour suppressor in multiple signalling pathways, this work may provide a new angle for investigating the actual function of DAPK-1.

1.9 Regulation of DAPK-1

1.9.1 Regulation by dephosphorylation and phosphorylation

The autoinhibition effect of the Ser308 phosphorylation provides a direct pathway for the activation of DAPK-1, i.e. dephosphorylation at Ser308 will lead to enhanced kinase activity of DAPK-1. Indeed many stresses activate DAPK-1 through dephosphorylation on this site, including TNF-α[151], ceramide[151], cerebral ischemia[66] and mitochondrial toxins[152].

Interestingly, the phosphatase utilized by different pathways may vary. For example, it was shown that calcineurin (PP2B) was the phosphatase that dephosphorylates DAPK-1 at Ser308 during ischemia[66]. However, upon mitochondrial toxins treatment, calcineurin inhibitors could not rescue DAPK-1 from dephosphorylation, suggesting the existence of other phosphatases that can dephosphorylate DAPK-1 in this pathway[152].

In addition to Ser308, there are several other phosphorylation sites on DAPK-1 that can influence its catalytic activity (Figure 1.13). Interestingly, all these phosphorylation sites were related to growth factor-stimulated pathways. At first, it was found that ERK can directly interact with and phosphorylate DAPK-1 at Ser735, which led to enhanced kinase activity of DAPK-1[77]. This Ser735 phosphorylation can be stimulated by serum or phorbol-12-myristate-13-acetate (PMA)[77], which activates the Ras-MEK-ERK pathway[153, 154]. Subsequently, it was reported that RSK1/2 can directly interact with and phosphorylate DAPK-1 at Ser289 in response

to PMA[155]. The influence of this phosphorylation on the kinase activity of DAPK-1 was not tested. However, mutation of Ser289 to alanine results in a DAPK-1 mutant with enhanced apoptotic activity, whereas the phosphomimetic mutation (Ser289Glu) attenuates its apoptotic activity[155]. To bring more complexity to the pathway, a recent report demonstrated that DAPK-1 can be phosphorylated by Src at Tyr491/492, and dephosphorylated by LAR at these two sites[79]. Phosphorylation of these sites has an inhibitory effect towards DAPK-1 kinase activity and is induced by EGF[79].

Because the Ser289Ala mutant of DAPK-1 is more apoptotic, it seems that this phosphorylation enhances the catalytic activity of DAPK-1[155]. However, considering the controversial roles of DAPK-1 in apoptosis, it is not necessarily the case. The increased apoptosis-promoting function may be caused by a decrease in the kinase activity of DAPK-1. Moreover, Ser289 locates at the autoinhibitory region of the CaM regulatory domain of DAPK-1 (Figure 1.3). Phosphorylations on this region tend to lead to activation of the CaMKs, rather than inactivation[20]. Therefore, kinase assays using the Ser289 mutants are needed to confirm the function of Ser289 phosphorylation.

The observation that serum, PMA and EGF all activate the growth factor pathways in cells creates extra difficulties in understanding the seemingly contradictory effects of DAPK-1 phosphorylations at Ser735 by ERK and that at Tyr491/492 by Src. Of note, in the Src/LAR paper, EGF was treated directly on cells growing in serum containing medium[79]. As mentioned in the previous papers of the same authors, the culture medium they used already contained a high concentration of EGF[127] and DAPK-1

catalytic activity was increased following serum stimulation[22]. Therefore, the extra treatment of EGF in the Src/LAR paper may lead to an EGF concentration beyond the tolerance of the cells and super-active endogenous DAPK-1, which can be toxic to cells. Importantly, Src kinase was reported to activate Raf, which can activate the MEK/ERK pathway upstream of DAPK-1[156]. So it is possible that Src possesses dual functions. On one hand, it can activate DAPK-1 in response to growth factors via the MEK/ERK pathway; while on the other hand, it can directly phosphorylate and suppress DAPK-1 activity when growth factor signalling is over the limit tolerable by cells.

1.9.2 Regulation of DAPK-1 transcription

DAPK-1 gene expression was also found to be regulated in response to stress. For example, in neuronal cells, both seizures and ischemia were found to regulate DAPK-1 mRNA expression[65, 66, 76]. However, opposing effects were observed in neuron cells taken from different regions of the brain[65, 66, 76] and the mechanisms which regulate DAPK-1 mRNA expression in response to stress was unclear.

TGF-β was reported to induce DAPK-1 expression[126]. TGF-β significantly enhanced the level of DAPK-1 mRNA and the promoter activity of DAPK-1[126]. This induction is mediated by the Smad pathway and requires Smad2, Smad3 and Smad4[126], providing a mechanism for regulation of DAPK-1 transcription via its promoter region.

Another transcription factor that is reported to regulate the transcription of DAPK-1 through its promoter region is p53[157]. It was found that DNA damage stresses such as UV or Doxocycline induce DAPK-1 mRNA expression through p53, and the p53 binding site on the DAPK-1 gene locates on intron 1[157]. c-Myc induced DAPK-1 expression was also reported to be p53 dependent[157], providing a mechanism for the previous observation that overexpression of oncogenes like c-Myc and E2F increase DAPK-1 expression[123]. Of note, in p53 -/- MEFs, the expression of DAPK-1 mRNA is not less than that in p53 +/+ MEFs, suggesting that p53 doesn't control the steady state level of DAPK-1 expression[157].

A recent publication identified C/EBP-β as a transcriptional regulator of DAPK-1 that binds to the promoter region of DAPK-1 and is required for DAPK-1 steady state expression and its expression in response to IFN-γ[158]. Two elements on the promoter region of DAPK-1 were identified. One is a consensus C/EBP-β site that permits constitutive binding of C/EBP-β[158]. The other shows homology to the cyclic AMP response element/activating transcription factor binding sites. C/EBP-β binds to this site in an IFN-γ dependent manner[158]. Interestingly, ERK mediated phosphorylation of C/EBP-β at Thr189 is required for the interaction of C/EBP-β with the IFN-γ-dependent element on DAPK-1 promoter region, thus ERK is required for DAPK-1 induction by IFN-γ[158].

1.9.3 Regulation of DAPK-1 degradation

Not many stresses have been shown to induce the degradation of DAPK-1. The fact that CHIP targets DAPK-1 for degradation implies that Hsp90 acts to stabilize DAPK-1. It was shown that inhibition of Hsp90 by its inhibitors geldanamycin (GA) or 17-allyalamino-17demethoxy-geldanamycin (17-AAG) leads to degradation of DAPK-1[64, 78]. This is consistent with previous findings that after Hsp90 inhibition, many of its client proteins are destabilized and subsequently degraded via the ubiquitin proteasome pathway[159]. Interestingly, knock-down of both MIB-1 and CHIP can attenuate this degradation[64], suggesting that multiple ubiquitin-proteasome related factors can control DAPK-1 degradation after Hsp90 inhibition.

The other stress that was clearly shown to degrade DAPK-1 was TNF-α[62, 64]. Although MIB-1 was shown to promote TNF-α induced apoptosis and degrade DAPK-1[151], there was no direct evidence that TNF-α degrades DAPK-1 via MIB-1. In addition, the effect of TNF-α on the stability of DAPK-1 is much weaker than Hsp90 inhibitors and has to be used in combination with the protein translation inhibitor cycloheximide, suggesting that some other slower degradation pathways such as lysosomal pathway may be involved. In addition, ceramide displayed a similar effect to TNF-α to degrade DAPK-1[151]. However, controversial observations were reported that ceramide actually induced DAPK-1 expression. Therefore, more experiments are required to elucidate the role of DAPK-1 in the ceramide/TNF-α signalling pathway.

1.10 Project aims

This chapter has highlighted the importance of DAPK-1 in multi-cellular signalling pathways and its potential role as a tumour suppressor. The DAPK-1 gene is methylated in various tumours and its expression is lost as mentioned in Section 1.6. However, the mRNA level of DAPK-1 does not always correlate with its protein level. It has been reported that DAPK-1 protein expression can be detected in the presence of significant hypermethylation[160], suggesting the existence of important post-translational mechanism regulating DAPK-1 protein level. Although two ubiquitin E3s for DAPK-1 have been identified as mentioned in Section 1.9.3, it is still unclear how the ubiquitin-proteasome pathway regulates DAPK-1 and whether DAPK-1 is regulated by alternative degradation pathways such as lysosome-mediated degradation.

It has been published that TNF-α induces degradation of DAPK-1[151] and DAPK-1 was found to be cleaved by cathepsin B[66]. Therefore, it will be the overarching aim of this project to investigate the regulation of DAPK-1 by the TNF-α signalling and cathepsin B degradation pathways. Specifically, whether cathepsin B is responsible for the TNF-α induced degradation of DAPK-1, which domain on DAPK-1 does cathepsin B interact with, and how cathepsin B and DAPK-1 regulate TNF-induced apoptosis will be addressed.

In addition, splicing is a common event for many genes and results in proteins with distinct functions[161]. A potential splice variant of DAPK-1 exists in the human cDNA database, which was indentified from the NEDO human cDNA sequencing project.

A secondary aim of this project is to to determine whether this sequence is a DAPK-1 splice variant. If so, I will determine whether the splice variant behave similarly to DAPK-1, whether it regulates the function or expression of the full-length DAPK-1 and wihether this variant is regulated as full-length DAPK-1.

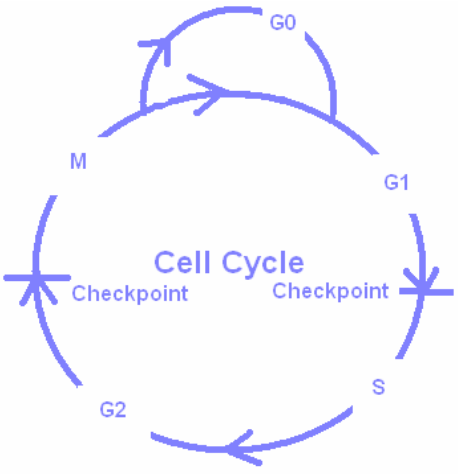

Figure 1.1 A schematic diagram of the mammalian cell cycle. Cell cycle consists of G1, S, G2 and M phases. Two major checkpoints exist between G1/S phases and G2/M phases to ensure the fidelity of cell division. G0 is a quiescent stage of cells after mitosis. The length of G0 depends on cell type and environmental conditions.

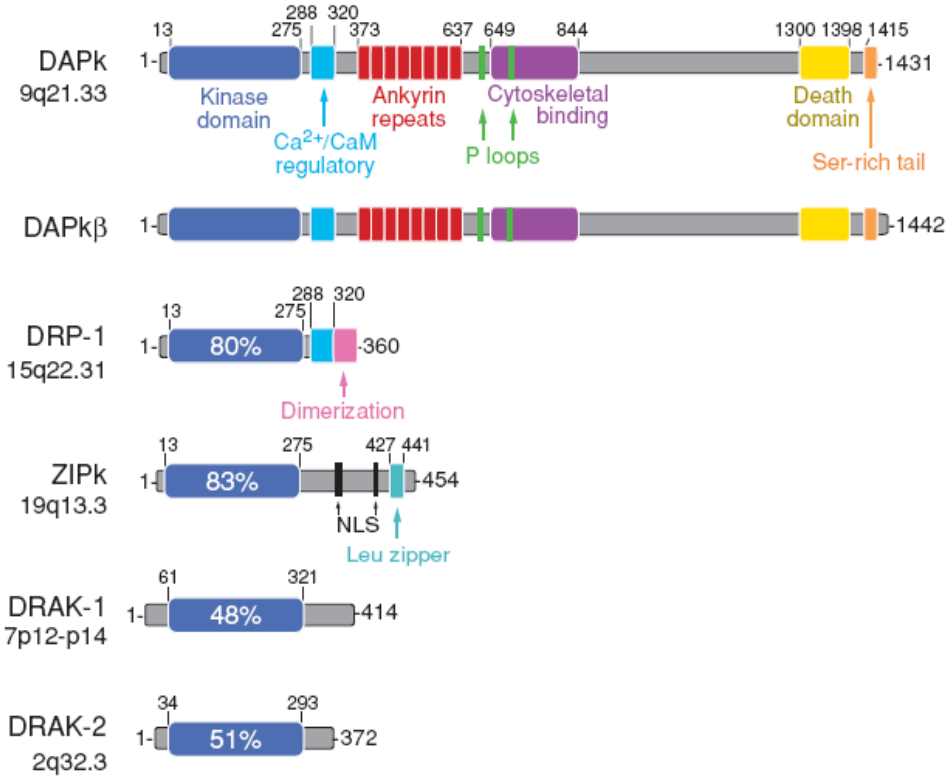

Figure 1.2 A schematic diagram of DAPK-1 structure and its family members[15]. The numbers above the proteins demarcate the amino acid position of each domain. The quantities within the kinase domains indicate the degree of amino acid identity to the kinase domain of DAPK-1. Chromosomal designations for the human orthologues are also indicated. (Taken from Reference 14)

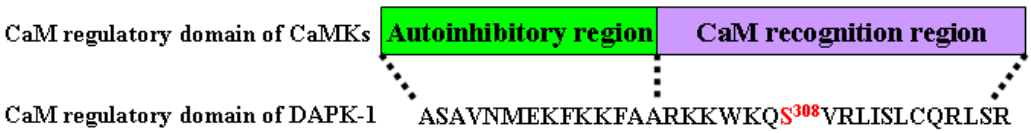

Figure 1.3 A schematic diagram of the CaM regulatory domain of CaMKs and the amino acid sequence of the CaM regulatory domain of DAPK-1. The amino acid and number in red signify the autophosphorylation site of DAPK-1.

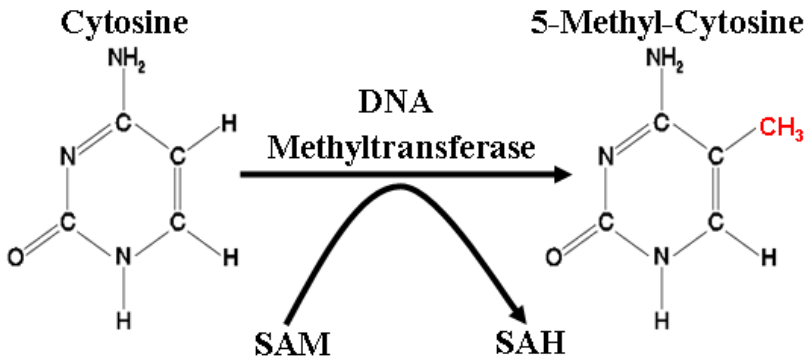

Figure 1.4 Schematic reaction of DNA methylation in humans. DNA methylation in humans refers to the transfer of a methyl (CH_3 group) to cytosine. The reaction is catalyzed by a DNA methyltransferase, and uses S-Adenosyl Methionine (SAM) as a methyl donor. During the reaction, SAM is converted to S-adenosylhomocysteine (SAH).

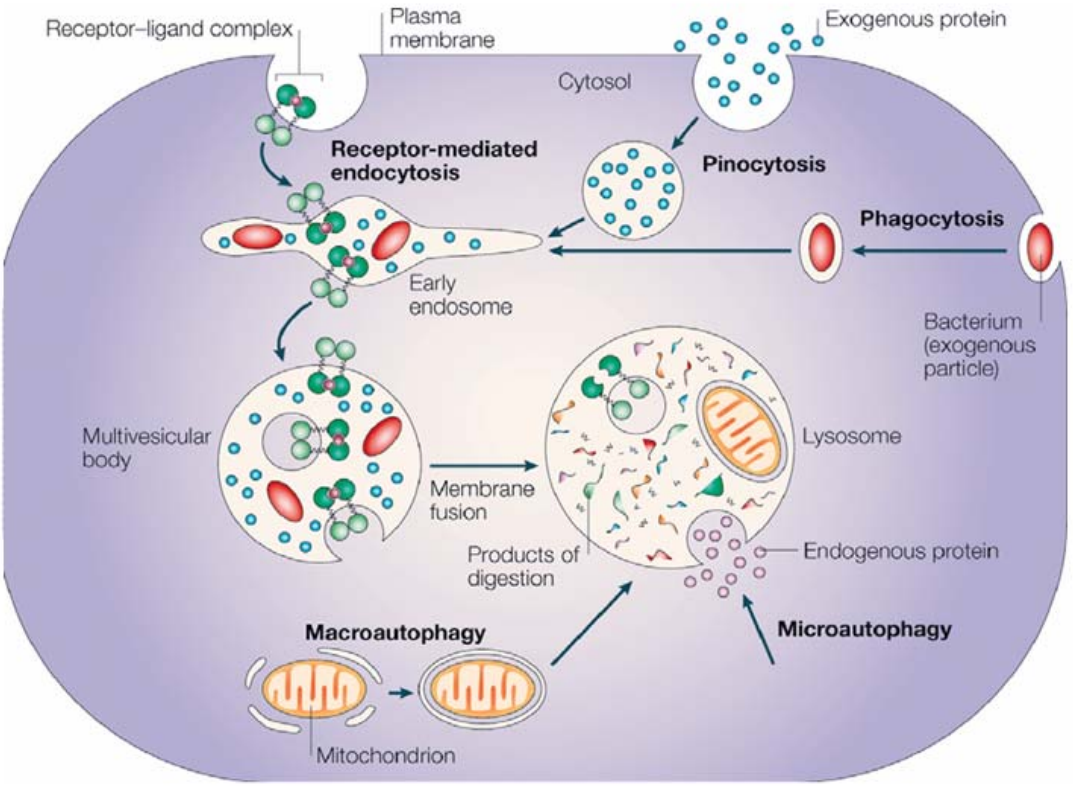

Figure 1.5 The four digestive processes mediated by the lysomsome[50], including specific receptor-mediated **endocytosis**, **pinocytosis** for non-specific engulfment of cytosolic droplets containing extracellular fluid, **phagocytosis** for bacterium and extracellular particles, **microautophagy** for endogenous proteins and **macroautophagy** for intracellular organelles. (Taken from reference 49)

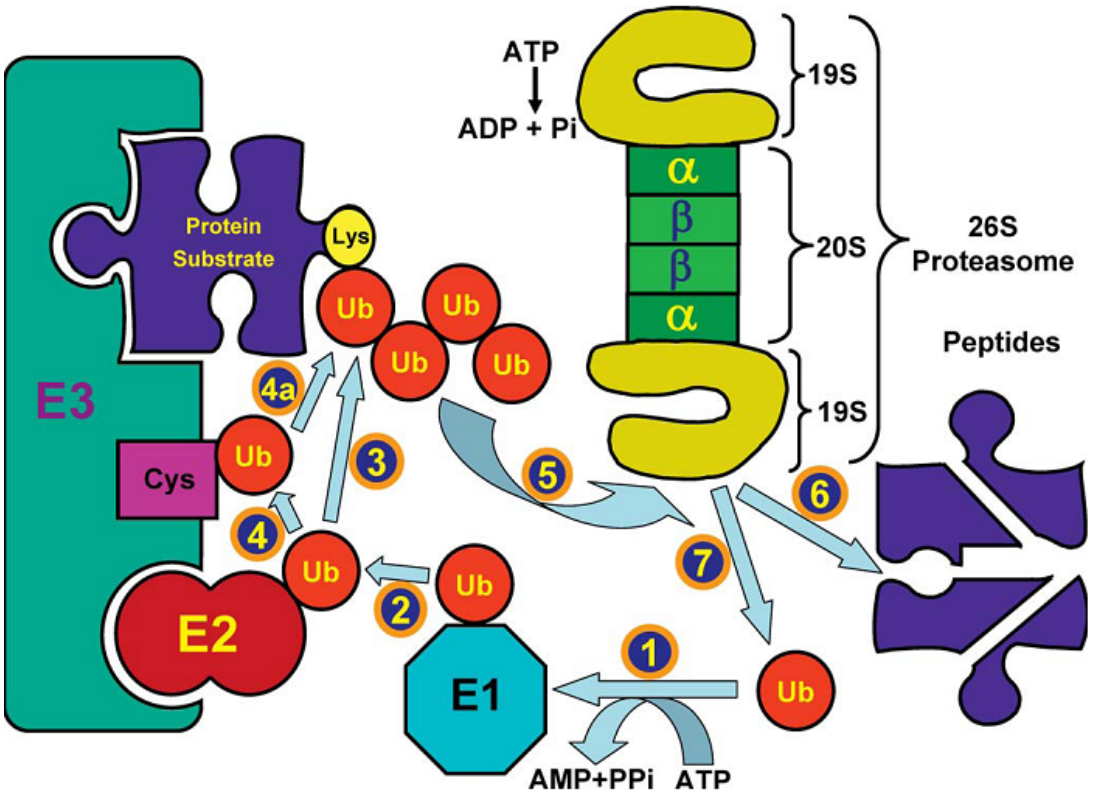

Figure 1.6 The ubiquitin-proteasome proteolytic system[50]. Ubiquitin is activated by the ubiquitin-activating enzyme, E1 **(1)** followed by its transfer to a ubiquitin-carrier protein (ubiquitin-conjugating enzyme, UBC), E2 **(2)**. E2 transfers the activated ubiquitin moieties to the protein substrate that is bound specifically to a unique ubiquitin ligase E3. The transfer is either direct (**(3)** in the case of RING finger ligases) or via an additional thiol-ester intermediate on the ligase (**(4, 4a)** in case of HECT domain ligases). Successive conjugation of ubiquitin moieties to one another generates a polyubiquitin chain that serves as the binding **(5)** and degradation signal for the downstream 26S proteasome. The substrate is degraded to short peptides **(6)**, and free and reusable ubiquitin is released by DUBs **(7)**. (Taken from reference 49)

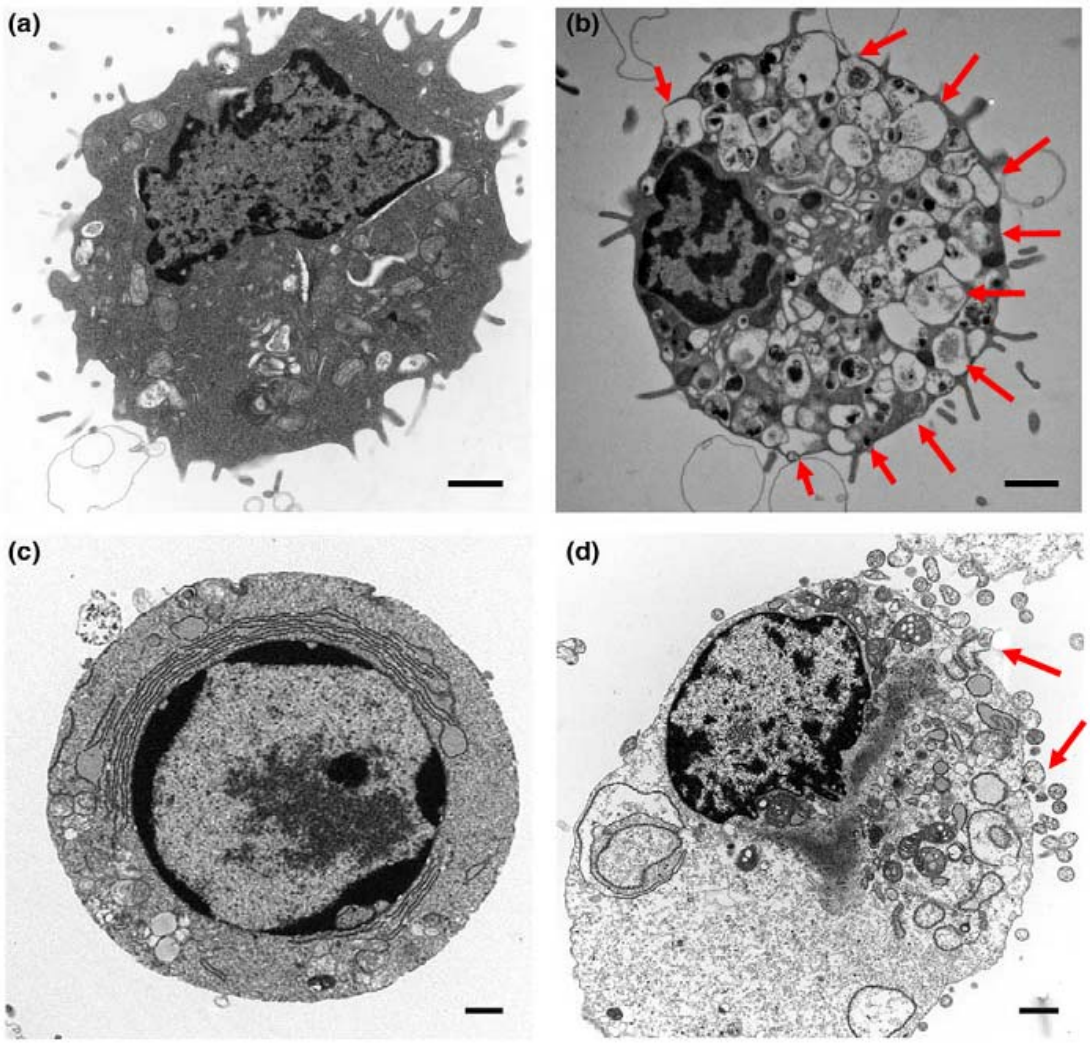

Figure 1.7 Electron microscopic pictures showing the morphological features of [82] (a) Normal, (b) Autophagic, (the most obvious charateristics of which is the accumulation of a lot of visible autophagosome bodies as pointed out by red arrows) (c) Apoptotic (the charateristics of which are cell shrinkage,and rounding, cytoplasm condensation, chromatin condensation and fragmentation, and importantly a intact plasma membrane) and (d) Necrotic (the most obvrous characteristics of which are the breakdown of plasma membrane and vacuolation of the cytoplasm as pointed out by red arrows) cells. The scale bar represents 1μm. (Taken from reference 78)

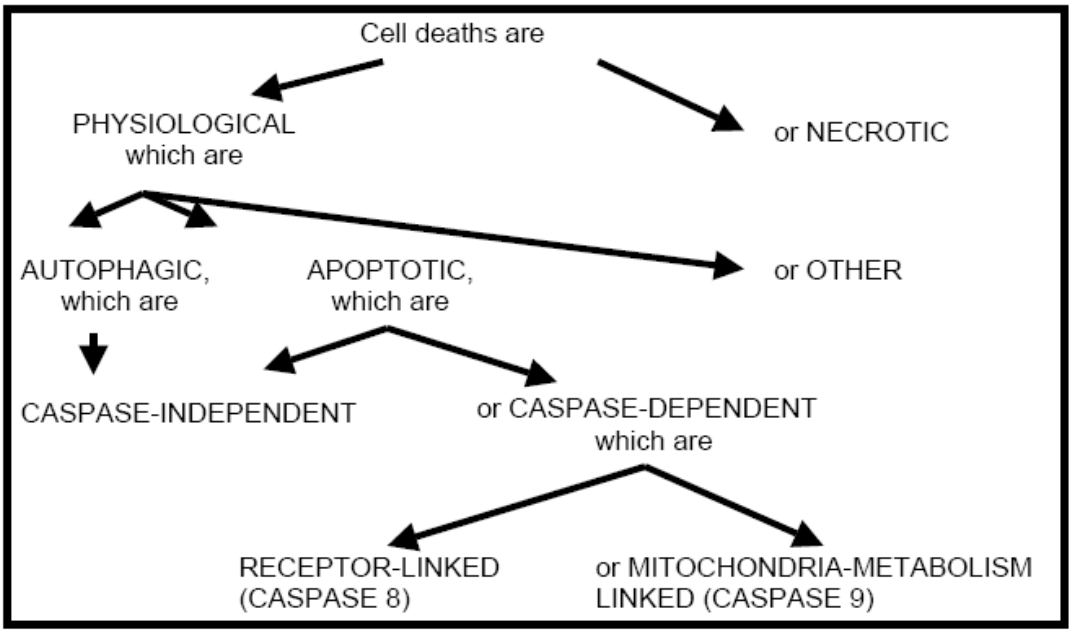

Figure 1.8 Categories of cell death[83]. (Taken from reference 79)

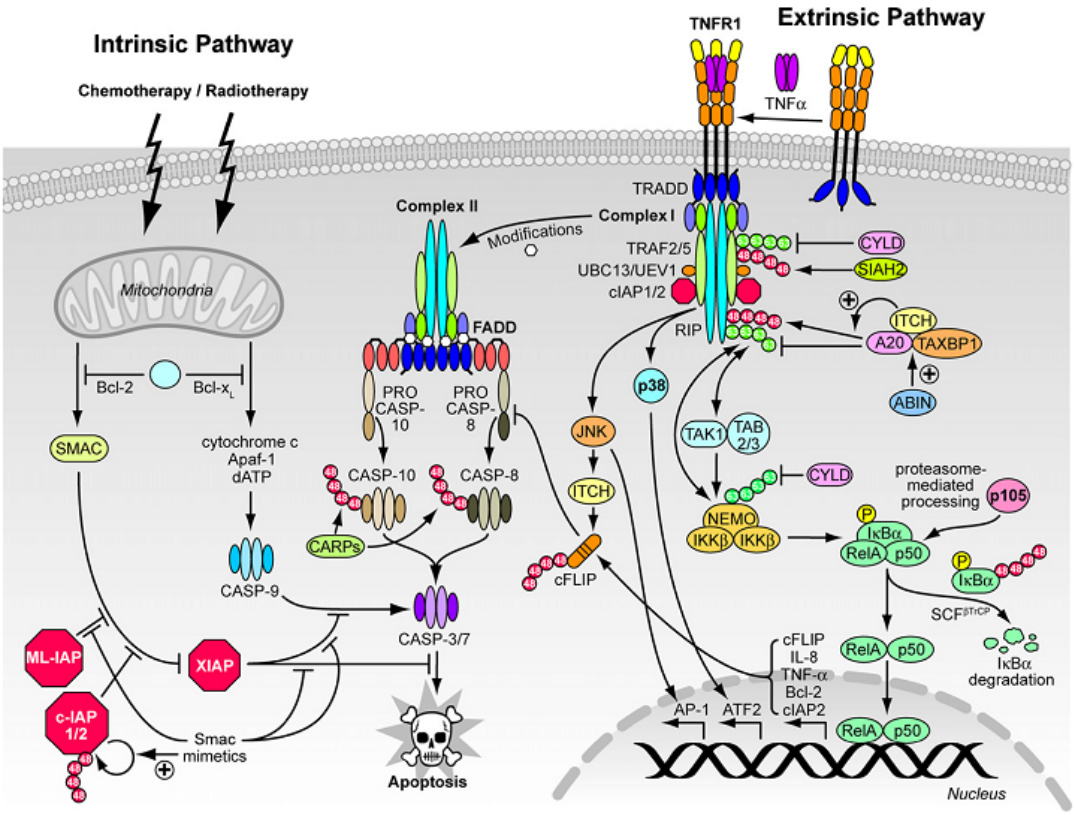

Figure 1.9 TNF-α induced signalling pathways[61]. The intrinsic pathway disrupts mitochondrial membrane potential, leading to the release of cytochrome c, and induction of cell death via caspase 9. The extrinsic pathway works through death receptors. Upon TNF-α treatment, TNF-α binds to TNFR-1 and promotes recruitment of the complex I composed of TRADD, TRAF2/5, cIAP1/2 and RIP. Complex I subsequently activates NF-kB, JNK and p38 pathways to induce the transcription of a series of pro-survival factors, which antagonize the apoptosis pathway. When released from TNFR-1, complex I can recruit FADD via TRADD and forms complex II, which induces apoptosis through caspase 8 and caspase 10. (Taken from reference 57)

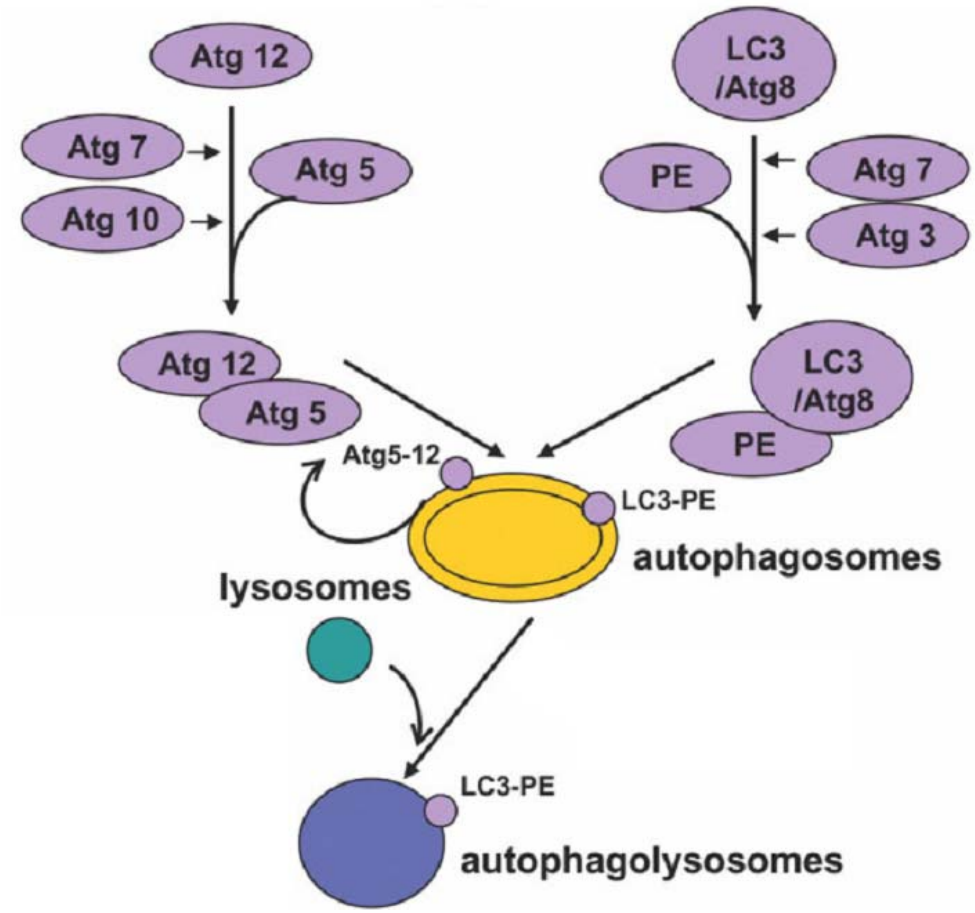

Figure 1.10 Signalling pathways leading to autophagy[106]. Two ubiquitin-like conjugation systems lead to autophagy. In one system, Atg12 is activated by Atg7 and transferred to Atg5 by Atg10. The Atg5-Atg12 complex interacts with Atg16 on the membrane of early autophagosome and is released after the maturation of the autophagosome. In the other system, Atg8/LC3 is transferred to PE by Atg7 and Atg3. The Atg8/LC3-PE complex is localized to the autophagosomal membrane by the Atg5-Atg12-Atg16 complex and stays on the membrane of mature autophagosome until it is degraded by lysosomes. (Taken from reference 100)

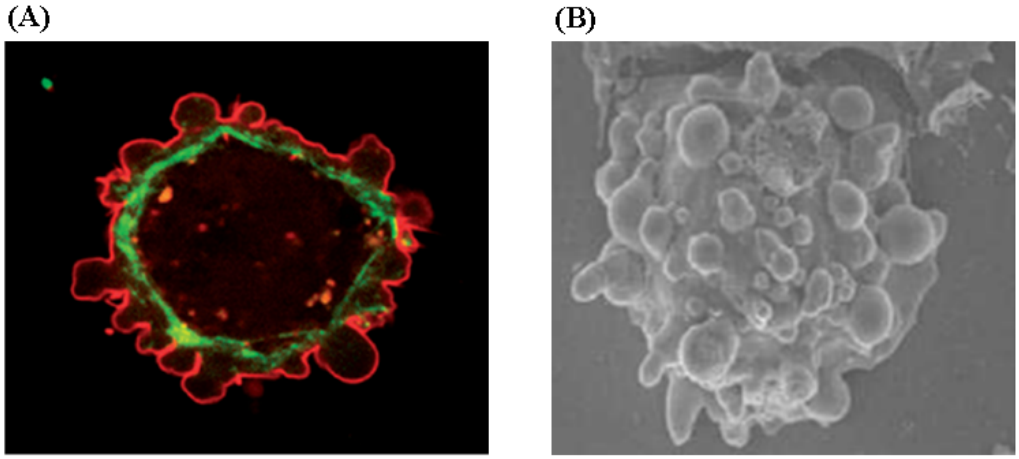

Figure 1.11 Examples of membrane blebbing[133]. (A) Myosin light chain localization in a filamin-deficient melanoma cell. Myosin (in green) localizes to distinct puncta under the blebbing membrane (in red). **(B)** Scanning electron microscopy image of a filamin-deficient melanoma cell. Blebs can clearly be seen over the entire cell surface. Most blebs are spherical, others have elongated into lobopodia or have sprouted a side bleb. (Taken from reference 127)

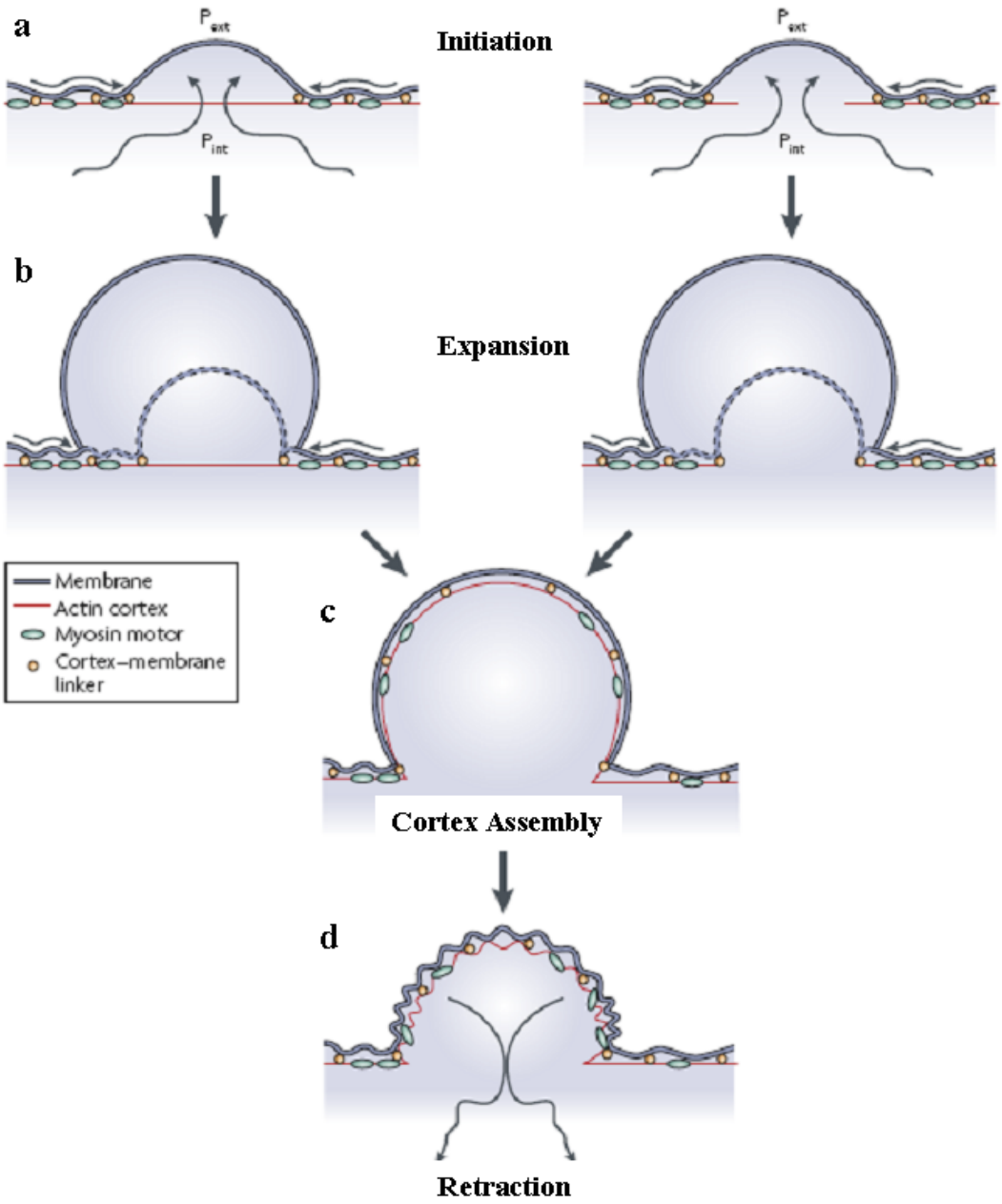

Figure 1.12 The bleb cycle[133]. The life cycle of blebbing can be divided into three phases: bleb initiation, expansion and retraction. **(a)** Bleb initiation can result from a local detachment of the cortex from the membrane (left) or from a local rupture of the cortex (right). **(b)** Hydrostatic pressure in the cytoplasm (P_{int}) then drives membrane expansion by propelling cytoplasmic fluid through the remaining cortex (left) or through the cortex hole (right). Concomitantly, the membrane can detach further from the cortex, increasing the diameter of the bleb base (dashed line). **(c)** As bleb expansion slows down, a new actin cortex reforms under the bleb membrane. **(d)** Recruitment of myosin to the new cortex is followed by bleb retraction. P_{ext}: extracellular hydrostatic pressure. (Taken from reference 127)

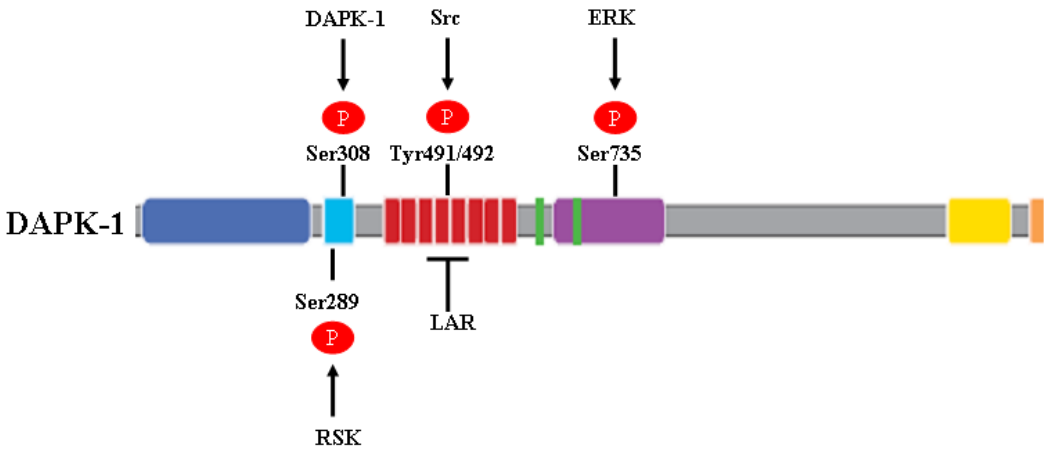

Figure 1.13 A schematic diagram of the phosphorylation sites on DAPK-1. In addition to the autophosphorylation site at Ser308, DAPK-1 can also be phosphorylated by RSK at Ser289, Src at Tyr491/492 and ERK at Ser735. Moreover, LAR can specifically dephosphorylate DAPK-1 at Tyr491/492, thus playing a reciprocal role to Src.

Chapter Two Materials and Methods

2.1 General materials

All reagents were supplied by Sigma unless otherwise stated. All oligonucleotides were synthesized by Sigma-Genosys. All siRNA were ordered from Dharmacon. All restriction enzymes were supplied by New England Biolabs.

PCDNA3.1 plasmid was from Invitrogen. HA-DAPK-1 vector was a gift from Adi Kimchi (Weizmann Institute, Israel), TNFR-1 vector was a gift of Vishva Dixit (Genentech), and cathepsin B-GFP plasmid was a gift from Antonio Baici (University of Zurich). The plasmids for cloning will be described in section 2.4.5. The plasmids for site direct mutagenesis will be described in section 2.4.6.

For tissue culture, Foetal bovine serum (FBS), Dulbecco's modified eagles's medium (DMEM), Roswell Park Memorial Institute (RPMI-1640) medium, McCoy's 5A medium and trypsin-EDTA solution were supplied by Gibco-BRL. All the other materials needed for specific experiments will be addressed in the appropriate sections.

2.2 Transformation and plasmid maintenance

2.2.1 Preparation of competent cells

Glycerol stocks of the required *E.Coli* bacterial strain DH5α or BL21 were inoculated into 3ml Luria-Bertani (LB) medium (1% w/v Tryptone, 0.5% w/v Yeast

extract, 1% w/v NaCl and sterilized by autoclaving at 121°C for 20 minutes) and allowed to grow overnight at 37°C. 250µl of the overnight culture were transferred into 50ml LB and incubated at 37°C until the $O.D._{600nm}$ of the culture reached approximately 0.4. Cells were collected by centrifugation at 1800g for 15 minutes at 4°C, resuspended gently in 16ml ice-cold Buffer 1, pH5.8 (1.2g RbCl, 0.99g $MnCl_2 \cdot 4H_2O$, 0.59g CH_3COOK, 1.5g $CaCl_2 \cdot 2H_2O$ and 15% v/v glycerol in 100ml distilled H_2O) and left on ice for 10 minutes. Then the cells were centrifuged again at 1800g for 15 minutes at 4°C and gently resuspended in 2ml ice-cold buffer 2, pH6.8 (10mM MOPS pH6.8, 0.12g RbCl, 1.1g $CaCl_2 \cdot 2H_2O$ and 15% v/v glycerol in 100ml distilled H_2O). After 10-minute incubation on ice, the cells were aliquoted and snap-frozen in liquid nitrogen and stored at -80°C.

2.2.2 Heat shock transformation

An aliquot of competent cells was incubated on ice with equal amount of 1X KCM (100mM KCl, 30mM $CaCl_2$ and 50mM $MgCl_2$) and appropriate amount of plasmid (usually 50ng) for 30 minutes. The cells were then subject to heat shock by incubating at 42°C for 45 seconds and left at room temperature for 10 minutes. LB medium was added to the competent cell/plasmid mixture and cultured for 1 hour at 37°C to allow the growth of transformed bacteria cells. Finally the cells were plated onto pre-prepared LB agar plates with selection antibiotics specific for the plasmid transformed and the plates were incubated at 37°C overnight for colony formation.

2.2.3 Plasmid maintenance

After transformation, single colonies were selected and allowed to grow overnight at 37^{o}C either in 5ml LB medium for mini-prep or 150ml LB medium for maxi-prep. Before purification, for the plasmids that are transformed for the first time, 750μl of the transformed-cell culture were mixed with 250μl of glycerol and stored at -80^{o}C. Future culture to obtain these plasmids can then avoid the transformation step and start directly from the inoculation of these glycerol stock. To purify plasmids from culture, mini-prep or maxi-prep were carried out using the high speed mini-prep or maxi-prep kits from Qiagen following the manufacturer's protocols. Concentration of the plasmids was measured by ND-3300 Fluorospectrometer (NanoDrop Technologies) at 260nm. Purified plasmids are stored at -20^{o}C.

2.3 Tissue culture and transient transfection

2.3.1 Cell maintenance and sub-culture

Hela (human cervix epithelial carcinoma), A549 (human alveolar epithelial cell), HEK293 (Human embryonic kidney cell line) and A375 (human melanoma) cells were cultured in DMEM, H1299 (human lung carcinoma) cells were cultured in RPMI medium, and HCT116 (human colon carcinoma) cells were cultured in McCoy's 5A medium. The medium were supplemented with 10% FBS and a penicillin and streptomycin mixture from Gibco at 37 °C with 5% CO_2 in a humidified atmosphere.

Cells were usually maintained in 175cm^2 flasks and sub-cultured into different containers dependent on the requirement of individual experiment. When confluent, cells were rinsed with 3ml of PBS twice, followed by the addition of 3ml trypsin-EDTA solution/175 cm^2 flask and incubated at 37^{o}C. After all the cells floated, 7ml medium with FBS were added per 175 cm^2 flask to stop the reaction. The trypsinised cells were then centrifuged at 400g for 1 minute and a portion of the collected cells, which is dependent on the growth rate of individual cell line, was resuspended with fresh medium in a new flask.

In a typical experiment, 10^6 cells were sub-cultured into a 10cm tissue culture plate and left for at least 24 hours to attach to the bottom of the container. Before harvesting, cells were first washed twice with PBS and then scraped into 1ml of PBS.

2.3.2 Long-term storage of cells

For long-term cell storage, a 175cm^2 flask of cells were trypsinised and collected as mentioned in 2.3.1 and resuspended in 5 ml of freezing solution composed of 4ml FBS and 1ml Demethyl sulfoxide (DMSO). The cell solution was then aliquoted into 5 cell storage vials, left at -80^{o}C overnight and kept in liquid nitrogen the next day.

In order to recover a frozen cell culture stock, a vial of cells was rapidly thawed at 37^{o}C in water bath and transferred into a 15ml centrifuge tube with 10ml fresh medium. The cells were then collected by centrifugation at 400g to remove DMSO and resuspended with fresh medium in a 175cm^2 flask.

2.3.3 Cell treatments

In order to induce the required response, cells were treated with certain reagents or cultured with serum free medium. In most cases, reagents were added directly onto the cells. In experiments requiring medium change, cells were first washed twice with serum free medium and then cultured in medium containing certain reagents or serum free medium. The reagents used in cell treatments were listed in Table 2.1.

Table 2.1 Reagents used in cell treatments.

Reagent	Function	Diluent	Concentration
Chloroquine (Sigma)	Lysosome inhibitor	DMSO	10μM
Cycloheximide (Supleco)	Protein translation inhibitor	DMSO	10μM
MG132 (Calbiochem)	26S proteasome inhibitor	DMSO	10μM
pIpC (Sigma)	Virus mimicking reagent	DMSO	50μg/ml
PD 150606 (Calbiochem)	pan-Calpain inhibitor	DMSO	10μM
TNF-α (R&D Systems)	Cytokine	0.1% w/v BSA/PBS	20ng/ml
TPCK (Calbiochem)	Chymotrypsin inhibitor	DMSO	10μM

Z-VAD-FMK (Calbiochem)	pan-Caspase inhibitor	DMSO	10μM
Z-PHE-ALA-FMK (Calbiochem)	Cathepsin B inhibitor	DMSO	10μM

2.3.4 Transient transfection

All transfections were carried out by the liposome-mediated method using Lipofectamine 2000 based on the manufacturer's guide. In plasmid transfection, the exact quantity of transfected plasmid varied in each experiment and was dependent on the expression of individual plasmid. However, in each experiment, carrier plasmid such as PCDNA3.1 was co-transfected to keep the quantity of transfected plasmid consistent in each transfection. In siRNA transfection, the amount of siRNA used depended on the volume of the cell culture medium because a certain concentration of siRNA is compulsory to maintain its activity. Usually 100nM was the final concentration used in the siRNA transfection experiment.

2.4 DNA and mRNA assays

2.4.1 mRNA extraction

mRNA was extracted from cells and tissues using the Qiagen RNeasy Mini kit following the manufacturer's suggested procedures. The optional step of DNase treatment using the Qiagen RNase-free DNase set was also included. The

concentration of the extracted mRNA was measured by ND-3300 Fluorospectrometer (NanoDrop Technologies) at 260nm.

2.4.2 Reverse Transcription (RT) Polymerase Chain Reaction (PCR)

RT of mRNA was performed using the Omniscript RT kit from Qiagen following the manufacturer's suggested protocols. The PCR of the reverse-transcribed cDNA was performed using the pfu polymerase kit from Stratagene according to manufacturer's suggestions. The primers for RT PCR are listed in Table 2.2.

Table 2.2 Primers for RT PCR.

s-DAPK-1 RT PCR primers
Forward: 5'-ATGGCCCTCCACGTGGCAGCTCGCTA-3'
Reverse: 5'-CTAAGGCCACAGGGTCCAGTATAGGC-3'

2.4.3 Agarose gel electrophoresis

DNA samples were mixed with 6X DNA loading buffer (30% v/v glycerol, 0.6% w/v SDS, 60mM EDTA and 0.1% w/v bromophenol blue) before loading on the gel. Agarose gels were created by dissolving agarose in heated 1X Tris/Borate/EDTA (TBE) buffer (90mM Tris, 90mM Boric acid and 2mM EDTA). The percentage of agarose in gel depended on the size of sample DNA. As a size reference, a DNA marker from Invitrogen was loaded next to the DNA samples. Electrophoresis was performed at 100V until a good resolution was observed under a UV transilluminator. The images of the gels were captured using the ChemiGenius^2 Bio-Imaging system from Syngene.

2.4.4 Real-time PCR

Real time PCR was performed using the Qiagen QuantiTect SYBR Green one-step PCR kit following the manufacturer's suggested protocols. The primers used in real-time PCR were designed by Primer3[162] software and listed in Table 2.3.

Table 2.3 Primers for real-time PCR.

DAPK-1 real-time primers Forward: 5'-CGAGGTGATGGTGTATGGTG-3' Reverse: 5'-CTGTGCTTTGCTGGTGGA-3'
s-DAPK-1 real-time primers Forward: 5'-CGTCTCTCCAGCAGGTGTT-3' Reverse: 5'-TAAGGCCACAGGGTCCAGTA-3'
Actin real-time primers Forward: 5'-CTACGTCGCCCTGGACTTCGAGC-3' Reverse: 5'-GATGGAGCCGCCGATCCACACGG-3'

2.4.5 Cloning

In order to clone certain DNA into the required expression vector, two cloning techniques were used. For the cloning of GST-836-947 and GST-s-DAPK-1, Gateway cloning was performed using the Gateway® Cloning kit from Invitrogen following the manufacturer suggested protocols. pDEST27 vector (Figure 2.1) for mammalian cell expression was the destination vector for GST-836-947, whilst

pDEST15 vector (Figure 2.1) for bacterial expression was that for GST-s-DAPK-1. The primers for Gateway cloning were listed in Table 2.4.

Table 2.4 Primers for gateway cloning.

GST-836-947 Gateway cloning primers Forward: 5'-GGGGACAAGTTTGTACAAAAAAGCAGGCTTAATCCATGT TGTTGTCTTTAGTCTAGAA-3' Reverse: 5'-GGGGACCACTTTGTACAAGAAAGCTGGGTCCTAATTTCG AAGTACCTTCATGTCCTTTGA-3'
GST-s-DAPK-1 Gateway cloning primers Forward: 5'-GGGGACAAGTTTGTACAAAAAAGCAGGCTTAATGGCCCT CCACGTGGCAGCTCGCTA -3' Reverse: 5'-GGGGACCACTTTGTACAAGAAAGCTGGGTCCTAAGGCCA CAGGGTCCAGTATAG -3'

For the cloning of s-DAPK-1 into 3XFlag-Myc-CMV-26 expression vector (Sigma) and into pAcGFP-C1 vector (Clontech), traditional cloning techniques were applied by performing RT PCR of s-DAPK-1 and restriction enzyme digestion. For Flag-s-DAPK-1-Myc cloning, EcoR I and Xba I restriction sites were included in the primers; whilst for GFP-s-DAPK-1, EcoR I and Sal I restriction sites were included. The primers for normal cloning are listed in Table 2.5. In a typical cloning reaction, the vectors and PCR product were digested with the same restriction enzymes before agarose gel electrophoresis. The single strand digested bands observed on gel were then purified using the Gel Purification kit from Qiagen. After purification, the digested vector and PCR product were applied for ligation overnight using the T4

DNA ligation kit from Promega. In the end, heat shock transformation of the ligation mixture with competent DH5-α cells was performed to select the vector with the PCR product cloned into it.

Table 2.5 Primers for normal cloing.

Flag-s-DAPK-1-Myc Cloning primers
Forward: 5'-TTGAATTCAATGGCCCTCCACCGTGGCAGCT-3'
Reverse: 5'-TTTCTAGAAGGCCACAGGGTCCAGTATAG-3'
GFP-s-DAPK-1 cloning primers
Forward: 5'-TTGAATTCGATGGCCCTCCACGTGGCAGCTCGCTA-3'
Reverse: 5'-TTGTCGACCTAAGGCCACAGGTCCAGTATAGGC-3'

2.4.6 Site-directed mutagenesis

In order to create certain mutations on specific sites of plasmid, Quickchange™ Site-Directed Mutagenesis kit from Stratagene was used to create all the mutants on HA-DAPK-1, Flag-s-DAPK-1-Myc and GFP-s-DAPK-1 based on the manufacturer's provided protocols. The deletion mutants were generated by inserting stop codons at the respective sites. Primers for site-directed mutagenesis were designed using the PrimerX[163] software and listed in Table 2.6.

Table 2.6 Primers for site-directed mutagenesis.

HA-DAPK-1 mutation primers
Primers for HA-1-378
Forward: 5'-CCAACCCAACAAGCACTAGACACCTCCATTACTC-3'
Reverse: 5'-GAGTAATGGAGGTGTCTAGTGCTTGTTGGGTTGG-3'

Primers for HA-1-641

Forward: 5’-CTGACCACGGACGGATAGACGGCAGAAGATC-3’

Reverse: 5’-GATCTTCTGCCGTCTATCCGTCCGTGGTCAG-3’

Primers for HA-1-835

Forward: 5’-CTGCAAATGATCCCACGTCATAGCATGTTGTTGTCTTTAG TC-3’

Reverse: 5’-GACTAAAGACAACAACATGCTATGACGTGGGATCATTTG CAG-3’

Primers for HA-1-947

Forward: 5’-GACATGAAGGTACTTCGAAATTAACTGCAAGAAATACGA AGCCAG-3’

Reverse: 5’-CTGGCTTCGTATTTCTTGCAGTTAATTTCGAAGTACCTTC ATGTC-3’

Primers for HA-1-1313

Forward: 5’-CACTCGGAGGAAATAGAGTCGCCTGCTGG-3’

Reverse: 5’-CCAGCAGGCGACTCTATTTCCTCCGAGTG-3’

Flag-s-DAPK-1-Myc and GFP-s-DAPK-1 mutation primers

Primers for Myc deletion mutant Flag-s-DAPK-1

Forward: 5’-CTGGACCCTGTGGCCTTAGAGAGAACAAAAACTCATC-3’

Reverse: 5’-GATGAGTTTTTGTTCTCTCTAAGGCCACAGGGTCCAG-3’

Primers for tail deletion (TD) mutant Flag-TD and GFP-TD

Forward: 5’-GGCTTCTAAGCCCACATGAAGGAACCTCCATGCTG-3’

Reverse: 5’-CAGCATGGAGGTTCCTTCATGTGGGCTTAGAAGCC-3’

Primers for Ankyrin-repeats only (AO) mutant Flag-AO and GFP-AO

Forward: 5’-GTCTGATGGGAGCCAGCGTTTAAGCGCTGACCACGGACG GAAAG-3’

Reverse: 5’-CTTTCCGTCCGTGGTCAGCGCTTAAACGCTGGCTCCCATC AGAC-3’

Primers for tail mutation (TM) mutant 1 Flag-TM1 and GFP-TM1

Forward: 5’-CTTCTAAGCCCACAGCTGCGAACCTCCATGCTGGC-3’

Reverse: 5’-GCCAGCATGGAGGTTCGCAGCTGTGGGCTTAGAAG-3’

Primers for Flag-TM2

Forward: 5’-CTAAGCCCACAGGTAGGGCAGCTCATGCTGGCCCCGTCT C-3’

Reverse: 5’-GAGACGGGGCCAGCATGAGCTGCCCTACCTGTGGGCTTA G-3’

Primers for Flag-TM3

Forward: 5’-CAGGTAGGAACCTCGCTGCTGGCCCCGTC-3’

Reverse: 5’-GACGGGGCCAGCAGCGAGGTTCCTACCTG-3’

Primers for Flag-TM4

Forward: 5’-GTAGGAACCTCCATGCTGCCGCAGTCTCTCCAGCAGGTG TTG-3’

Reverse: 5’-CAACACCTGCTGGAGAGACTGCGGCAGCATGGAGGTTCC TAC-3’

Primers for Flag-TM5

Forward: 5’-CATGCTGGCCCCGCAGCTCCAGCAGGTG-3’

Reverse: 5’-CACCTGCTGGAGCTGCGGGGCCAGCATG -3’

2.4.7 DNA sequencing

Automated sequencing was carried out by the DNA sequencing service in Genetics Core, WTCRF, University of Edinburgh, Western General Hospital, Edinburgh, UK.

2.5 Protein assays

2.5.1 Protein extraction from cells

In a typical experiment as described in section 2.3.1, after being collected, the cells were centrifuged at 400g for 1 minute and the supernatant was removed. The cell pellet was lysed in approximately 4 times volume of lysis buffers. Two lysis buffers were used. One is the Nonidet-P (NP)40 lysis buffer (1% v/v NP40, 150mM NaCl, 25mM Tris pH 7.5, 1mM Dithiothreitol (DTT) and 1X protease inhibitor) and the other is the Urea lysis buffer (7 M UREA, 100mM DTT, 50mM Hepes pH 8.0, 25mM NaCl and 0.05% v/v Triton X-100). NP40 lysis buffer was applied in regular experiment and Urea lysis buffer for experiments required to extract insoluble proteins considering its much harsher extracting ability.

2.5.2 Determination of protein concentration

1X Bradford reagent was prepared by dissolving 100mg Coomassie Blue in 50ml 95% ethanol, 100ml 85% phosphoric acid and 850ml distilled H_2O, stored at 4^oC, and filtered using a syringe and 0.45μM filter (Millipore) before use. 1μl protein sample was mixed with 1ml of 1X Bradford reagent, vortexed and incubated at room temperature for 5 minutes to develop colour reaction. The absorbance of the mixture

was tested at 595nm in a disposable cuvette using a spectrometer. The protein concentration was calculated using a Bovine Serum Albumin (BSA) standard curve. 40μg of each sample is usually loaded on the gels for a typical western experiment. When the expression of the interested protein is too high or too low, the respective amount of protein loaded on the gel is reduced or increased according to individual experiment.

2.5.3 Western Blot

Western blot was composed of two main steps: Sodium Dodecyl Sulfate (SDS) polyacrylamide gel electrophoresis (PAGE) and immunoblotting. In SDS-PAGE, equal amount of protein samples were first mixed with 4X SDS sample buffer (4% w/v SDS, 25mM Tris pH 6.8, 20% v/v glycerol, 0.01% w/v bromophenol blue and 200mM DTT) and incubated at 95^{o}C for 2 minutes before loading onto 8, 10, 12 or 15% polyacrylamide gel or 4-12% NuPAGE Bis-Tris gel (Invitrogen). The selection of gels depends on the respective experiments. The running gel of polyacrylamide gel is composed of 25% 1.5M Tris pH8.8, 0.1% SDS, 0.1% w/v Ammonium Persulfate (APS), v/v 0.04% Tetramethylethylenediamine (TEMED) and required amount of 30% w/v acrylamide mixture from National Diagnostics. The stacking gel of polyacrylamide gel is composed of 1/12 1M Tris pH 6.8, 0.1% w/v SDS, 0.1% w/v APS, 0.1% v/v TEMED and 1/6 of 30% w/v acrylamide mixture. The samples on polyacrylamide gels were resolved by electrophoresis in SDS running buffer (0.1% w/v SDS, 0.192M glycine and 25mM Tris) on BioRad mini-protean 3 apparatus. The samples on 4-12% NuPAGE Bis-Tris gels were resolved by

electrophoresis in MOPS buffer (Invitrogen) on a Novex XCell SurelLock gel apparatus.

For immunoblotting, the resolved proteins were first transferred onto Hybond-C nitrocellulose membrane (Amersham Biosciences) in transfer buffer (0.192M glycine, 25mM Tris and 20% v/v methanol) on BioRad transfer kit at 350mA for 2 hours. An ice pack was placed in the transfer tank to maintain low temperature to help protein transfer.

Following transfer, the membrane was incubated in PBS-Tween-20 (0.1% v/v Tween-20 in PBS) (PBST) with 5% w/v dry skimmed milk (MARVEL) for 1 hour at room temperature to block non-specific protein binding. Then after a quick wash with PBST, the membrane was incubated with the primary antibodies at a supplier-recommended dilution in PBST with milk and shaken at $4^{o}C$ overnight. The next morning the blot was washed 3 times for 5 minutes with PBST and incubated with respective horse radish peroxidase (HRP) coupled secondary antibodies from DAKO in PBST with milk to detect specific antibody binding. Finally the blot was washed 3 times with PBST for 5 minutes and then incubated with electrochemiluminescence (ECL) solution mixture. ECL solution I was composed of 2.5mM luminol, 0.4mM coumaric acid and 100mM Tris pH 8.5, and ECL solution II composed of 100mM Tris pH8.5 and 0.018% v/v H_2O_2 (BioRad). ECL solutions were kept in the dark at $4^{o}C$ and mixed at 1:1 ratio prior to incubation with the blot. Specific bands were detected by exposing the membrane to ECL hyperfilm (Amersham Biosciences). The primary antibodies used were listed ini Table 2.7. The blot data was quantified by

densitometry using Scion Image Software (National Institues of Helath) and normalised to the level of the control protein.

Table 2.7 Primary antibodies used in western blot.

Antibody name	Source	Company	Dilution
Cathepsin B antibody	sheep	Serotec	1:1000
DAPK-1 antibody	mouse	BD Bioscience	1:250
DAPK-1 antibody (55)	mouse	Santa Cruz Biotechnology	1:1000
DAPK-2 antibody	goat	Santa Cruz Biotechnology	1:1000
DAPK-3 (ZIP) antibody	goat	Santa Cruz Biotechnology	1:1000
Flag antibody	mouse	Sigma	1:5000
GFP antibody	mouse	Cancer Research UK	1:1000
GST antibody	mouse	Sigma	1:1000
HA.11 antibody	mouse	Covance	1:1000
IRF-1 antibody	mouse	BD Bioscience	1:1000
p53 antibody (DO1)	mouse	Moravian Biotechnology	1:1000
PARP antibody	rabbit	Cell Signalling	1:1000
TNFR-1 antibody	goat	Santa Cruz Biotechnology	1:1000

2.5.4 Fractionation

One 10^6 plate of cells was used for each fractionation. The fractionation samples were extracted using the ProteoExtract® Subcellular Proteome Extraction Kit from Calbiochem in accordance to the manufacturer's protocols.

2.5.5 Immunoprecipitation (IP)

Protein G Sepharose™ 4 Fast Flow or Glutathione-Sepharose™ from GE Healthcare were used in IP reactions. The beads were kept in 70% ethanol in a 1:1 ratio. Each reaction required 25µl of beads, and before the immunoprecipitation, the beads were washed 5 times with 1 ml of IP dilution buffer (0.1% v/v NP40, 25mM Tris pH 7.5, 150mM KCl, 1mM DTT, and 1X complete mini protease inhibitor from Roche Diagnostics). Proteins for IP were extracted by lysing the cells with NP40 lysis buffer described in section 2.5.1. Equal amounts of proteins were added to 1 ml of IP dilution buffer. After that, the antibodies for IP and protein G beads in suspension were added into the tubes, and the mixture was rotated overnight at 4 °C. After rotation, the beads were sedimented at 1200g and the supernatants were discarded. The beads were then washed six times by rotating them in 1 ml of IP dilution buffer for 5 min at room temperature. In the end, proteins bound to the beads were either eluted using elution buffers or extracted directly by adding 4X SDS sample buffer.

2.5.6 *In vitro* synthesis of radioactive protein

^{35}S-labelled protein was synthesized using the TNT® translation kit (Promega) following to the manufacturer's protocols.

2.5.7 *In vitro* cleavage of radioactive HA-DAPK-1 by cathepsin B

^{35}S-labeled HA-DAPK-1 was synthesized as described in section 2.5.6. 2µl of the ^{35}S-labeled HA-DAPK-1 was added to 5µl of 3X cathepsin B reaction buffer

(150mM sodium acetate, pH 6.0, 12mM EDTA and 24mM DTT) with 1µl of purified cathepsin B (0.02 units/µl, U.S. Biological), which was diluted in 50mM sodium acetate pH 5.0 with 1mM EDTA prior to use. The final volume of the reaction was brought to 15µl with distilled water. The cleavage reaction was performed by incubation at 37 °C for indicated time. After incubation, 15µl of 4X SDS sample buffer was added to the samples, and then were boiled and subjected to SDS-PAGE. The gels were then dried, and the signals were detected by autoradiography.

2.5.8 Protein purification from bacterial expression system

Bacteria BL21 cells were transformed as described in section 2.2.2 with the plasmid that is designed for bacterial expression, e.g. pDEST15 (Figure 2.1) from Invitrogen, and cultured in 10ml LB medium with 100µM ampicillin overnight. The next day the transformed bacteria culture was inoculated into 500ml LB medium with 100µM ampicillin and incubated for approximately 3 hours until the $O.D._{600nm}$ of the culture reached 0.6. The culture was then incubated with 0.2% w/v Arabinose for another 3 hours and lysed with 0.2% Triton in PBS. The synthesized protein was then purified from the lysate by IP as mentioned in 2.5.5.

2.5.9 *In vitro* cleavage of recombinant GST-s-DAPK-1 by cell lysate

GST-s-DAPK-1 was synthesized as mentioned in 2.5.8 and purified from the lysate by IP using glutathione-Sepharose™, and eluted with 50mM Glutathione in PBS, pH8.0. For *in vitro* cleavage assay, 2µl of the purified GST fusion protein were

incubated at 30^{o}C with indicated amount of NP40 cell lysis for 30 minutes. The reaction was then stopped by adding 4X SDS sample buffer and the mixture was subject to western blot.

2.6 Immunofluorescent assays

2.6.1 Fluorescent microscopy

For normal protein localization assay, cells were seeded on NUNC LAB-TEK® 4-well chamber slides at a density of approximately 5x10^{4} cells/well. 18 hours later, cells were transfected with the indicated expression vectors for a further 24 hours. Then the slides were washed in 1X PBS and fixed in 4% paraformaldehyde for 15 minutes at room temperature and washed three times in 1X PBS afterwards. The cells were fixed in ice-cold methanol for 5 minutes and air-dried. After that, cells were permeabilized in freshly prepared 0.5% w/v Triton X-100 in 1X PBS, and slides were washed three times with 1X PBS for 10 minutes. Following washes with 1X PBS, non-specific sites were blocked for 1 hour with 3% w/v BSA/PBS at room temperature. After three washes in 1X PBS, the chambers from each slide were removed, and cells were incubated overnight with the primary antibody diluted in 1% v/v BSA/PBS at 4°C. 24 hours post-incubation, the slides were washed in 0.1% v/v PBS-Tween and incubated with the Alexa dye conjugated secondary antibodies from Invitrogen, which are listed on Table 2.8, for 30 minutes at room temperature. After incubation, cells were washed three times in 1X PBST. Nuclei were counterstained with Topro-3 from Invitrogen. Coverslips were mounted with Fluorescent mounting

medium (DakoCytomation). The control for non-specific binding of the secondary antibody was the 1% w/v BSA/PBS, where no primary antibody was added.

Table 2.8 Secondary antibodies for immunofluorescence.

Secondary antibody name	Colour	Dilution
Alexa 488 Goat anti mouse	Green	1:100
Alexa 488 Donkey anti rat	Green	1:100
Alexa 568 Goat anti rabbit	Red	1:100

Microscopy analysis was performed on Zeiss microscope (Zeiss Axionplan Imaging Systems provided by the Medical Research Council, Human Genetics Unit). The photometric CoolSnap HQ camera was used to capture the image.

2.6.2 TUNEL apoptosis assay

Cells were seeded directly onto coverslips in 6-well plates. 18 hours later cells were transfected with indicated amounts of expression vectors for a further 24 hours. Following transfection, cells were fixed in 1% paraformaldehyde for 10 minutes at room temperature. Apoptotic cells were labelled using Apoptag Plus fluorescein *in situ* apoptosis detection kit S7111 (Chemicon International) according to the manufacturer's instructions and viewed by fluorescent microscopy.

2.6.3 Membrane blebbing assay

Cells for membrane blebbing were seeded and transfected as described in section 2.6.1. 24 hours post transfection, cells were fixed with 4% paraformaldehyde in 1X PBS for 10 minutes, washed with 1X PBS for 3 times and blocked with 3% w/v

BSA/PBS for 1 hour. Then after incubation with the appropriate primary antibodies for 1h, cells were washed 3 times with 1X PBS and stained with the appropriate fluorescent secondary antibody for 1 hour before being mounted and ready for observation for membrane blebbing morphology using Zeiss microscope.

2.7 Annexin V staining assay

Cells were seeded into 6 well plates. 18 hours later, cells were transfected with the indicated amounts of expression vectors for a further 24 hours. In order to include any floating cells, medium was collected into fluorescence-activated cell sorting tubes and centrifuged at 360g for 4 minutes to leave a cell pellet. Medium was then discarded from tubes. Plates were then washed once with 2 ml of PBS and 1.5 ml of trypsin was added to each plate and incubated until cells became detached. Following cell detachment, 1.5 ml of McCoy's 5A medium supplemented with 10% FBS was added to each plate to stop the trypsin. The cell suspensions were then added to each of the relevant cell pellets from the floating cells. Samples were centrifuged at 360g for 4 min, and pellets were resuspended in 1 ml of McCoy's 5A medium supplemented with 10% FBS and incubated for 5 min. Samples were centrifuged for a further 4 min at 360g prior to resuspension in 1ml of ice-cold 1X PBS. Apoptotic cells were detected using a TACS^{TM} Annexin V-fluorescein isothiocyanate apoptosis detection kit (R&D systems) according to the manufacturer's instruction and analyzed by flow cytometry.

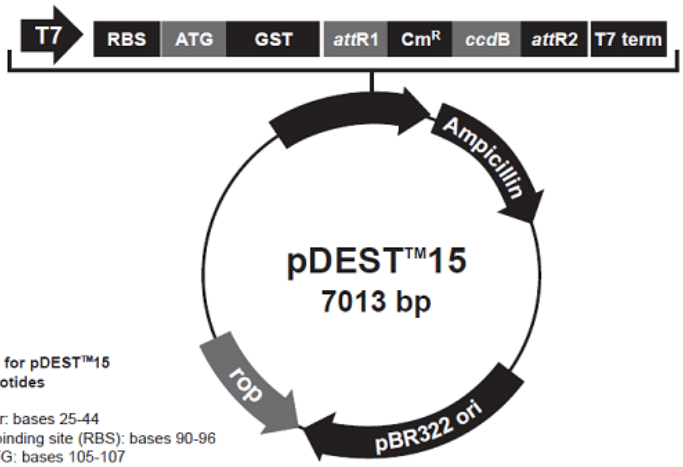

Comments for pDEST™15
7013 nucleotides

T7 promoter: bases 25-44
Ribosome binding site (RBS): bases 90-96
Initiation ATG: bases 105-107
GST tag: bases 108-776
*att*R1: bases 792-916
Chloramphenicol resistance gene (Cm^R): bases 1025-1684
*ccd*B gene: bases 2026-2331
*att*R2: bases 2372-2496
T7 transcription termination region: bases 2518-2646
bla promoter: bases 3134-3232
Ampicillin (*bla*) resistance gene: bases 3233-4093
pBR322 origin: bases 4238-4911
ROP ORF: bases 5282-5473 (C)

C=complementary strand

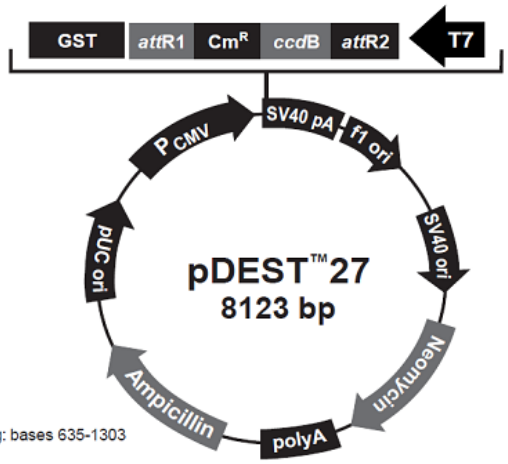

Comments for pDEST™27:
8123 nucleotides

CMV promoter: bases 15-608
Glutathione *S*-transferase (GST) tag: bases 635-1303
*att*R1 site: bases 1313-1437
Chloramphenicol resistance gene (Cm^R): bases 1546-2205
*ccd*B gene: bases 2547-2852
*att*R2 site: bases 2893-3017
T7 promoter: bases 3049-3068 (C)
SV40 early polyadenylation signal: bases 3368-3634
f1 intergenic region: bases 3760-4215
SV40 early promoter and origin: bases 4375-4683
Neomycin resistance gene: bases 4742-5536
Synthetic polyadenylation signal: bases 5600-5648
bla promoter: bases 5960-6058
Ampicillin (*bla*) resistance gene: bases 6059-6919
pUC origin: bases 7064-7737

(C) = complementary strand

Figure 2.1 Schematic maps of pDEST15 and pDEST27 vectors. (Taken from Invitrogen website)

Chapter Three Regulation of TNF-α mediated apoptotic pathway by DAPK-1/cathepsin B complex

3.1 Introduction

DAPK-1 is a member of the CaMK superfamily that includes CHK2 and AMPK. Recent studies highlighted that these kinases play a genetic role in activating the p53 tumour suppressor pathway[132]. Down-regulation of DAPK-1 by CpG methylation has been shown in a variety of tumours, providing tumours with growth advantages[15]. Moreover, a recent study revealed that DAPK-1 is a transcriptional target of p53[157]. Thus the fact that DAPK-1 is linked to the control of p53 expression by phosphorylation[132] and DAPK-1 itself is a transcriptional target of p53 indicates that a feedback loop exists between DAPK-1 and p53. These data suggest that transcriptional regulation of DAPK-1 is important for its function. However, the protein levels of DAPK-1 do not always correlate with the level of mRNA expression[46, 160, 164], therefore, additional mechanisms are important for the control of DAPK-1 activity.

Growing evidence suggests that some post-translational mechanisms control the activity of DAPK-1 in cells[15, 47, 62, 66]. These include RSK-dependent inactivation of DAPK-1, ERK dependent activation of the proapoptotic function of DAPK-1, DIP-1 dependent ubiquitination and proteasomal degradation of DAPK-1 and cathepsin B dependent cleavage of DAPK-1. In addition, a study in renal cell carcinomas demonstrates that the enzyme activity of DAPK-1 in these cells is largely attenuated

although its mRNA and protein are highly expressed[47]. Therefore, post-translational modification of DAPK-1 seems to be very important for its function.

The aim of this part of my project is to investigate how the steady state level of DAPK-1 protein is regulated, and characterize new factors that can control DAPK-1 protein stability. It has been reported that TNF-α can induce the proteasomal degradation of DAPK-1[151]. Therefore, I focused on identifying factors important for TNF-α induced DAPK-1 degradation. Furthermore, the role played by DAPK-1 in the TNF-α induced apoptotic pathway, i.e. a positive or negative regulator, is somewhat controversial. Therefore this will also be investigated in my study.

3.2 Uncoupled DAPK-1 protein level from gene expression

In tumour cell lines with a defined p53 status, we set up experiments to determine whether DAPK-1 protein expression was controlled post-translationally. The mRNA and protein expressions of DAPK-1 in six different tumour cell lines were examined (Figure 3.1). In HCT116 cells, DAPK-1 protein is expressed in both p53 wild type (+/+) and p53 null (-/-) cells (Figure 3.1), whereas in Hela cells, which have an HPV-E6 attenuated wild type p53 pathway, DAPK-1 levels are relatively high (Figure 3.1). These data suggest that the basal expression of DAPK-1 protein is not p53-dependent, which is consistent with previous work[157]. More interestingly, Hela cells actually possess more DAPK-1 protein compared with A549 cells, which have the highest mRNA level (Figure 3.1). This indicates that DAPK-1 can be regulated post-

translationally, and this regulation may be important for determining the basal protein levels of DAPK-1.

DAPK-1 was initially defined as a factor in interferon-γ-induced apoptotic pathway[8]. Therefore, cells were treated with the virus mimetic reagent pIpC (polyinosinic:polycytidylic acid), which is structurally similar to double-stranded RNA and can interact with toll like receptor 3 (TLR3) to activate interferon responsive pathway, to determine whether it can trigger transcriptional or post-translational changes in DAPK-1. The stress-induced expression of a series of endogenous proteins, including interferon-responsive factor-1 (IRF-1) and DAPK-1 were examined (Figure 3.2A). The IRF-1 level increased as expected, but there were no significant changes in the steady-state expression of any DAPK family members or p53.

HCT116 p53+/+ and HCT116 p53-/- cells were then treated with combined serum starvation and pIpC treatment, because the cells respond better to these combined stresses as reported previously[126]. Upon serum starvation or pIpC treatement, DAPK-1 mRNA levels decreased by around 50% in the HCT116 p53+/+ cells (Figure 3.2B). Combinational treatment caused a further decrease in DAPK-1 mRNA level in HCT116 p53+/+ cells (Figure 3.2B), implicating a synergy between these two signals in regulating DAPK-1 transcription. However, despite the changes in mRNA levels, the DAPK-1 protein levels remained the same with or without treatment in HCT116 p53+/+ cells (Figure 3.2B), suggesting again that gene transcription is not the key for reguatling DAPK-1 protein levels in cancer cell lines.

Simiarly, in HCT116 p53-/- cells, although DAPK-1 mRNA level was reduced upon pIpC treatement, its protein levels remained the same. Interestingly, serum starvation didn't change the DAPK-1 mRNA level in HCT116 p53-/- cells, which suggested that factors in the serum may induce DAPK-1 mRNA expression through p53 and supported the idea that p53 can induce DAPK-1 expression in response to stress[157].

3.3 Stability and cleavage of DAPK-1 protein

The stability of DAPK-1 protein was subsequently examined in Hela cells where DAPK-1-dependent signalling pathways operate, by performing a time course of cycloheximide, which inhibits the general protein translation machinery. Surprisingly, DAPK-1 protein level increased after 6h cycloheximide treatment (Figure 3.3), suggesting some regulatory proteins for degrading DAPK-1 may be highly unstable and get depleted very quickly after the treatment of CHX, resulting in the accumulation of DAPK-1 protein. These data suggest that DAPK-1 protein might be stored or assembled into a stable and possibly latent multiprotein complex in cells, since it is not rapidly degraded and resynthesized.

The stability data are in contrast to a previous report demonstrating that DAPK-1 can be controlled post-translationally via a proteasome-dependent pathway that involves the E3 ubiquitin ligase DIP-1[62], since usually proteasome regulates short half-life proteins[50]. Therefore I tested the effect of the proteasome inhibitor MG132 on steady-state levels of endogenous DAPK-1 to determine whether DAPK-1 protein

can be turned over by a proteasome-dependent pathway, despite the fact that it has a relatively high stability. MG132 treatment did increase the DAPK-1 protein levels and rendered higher molecular mass adducts, which might be ubiquitinated DAPK-1 (Figure 3.4A, lane 2 versus lane 1). However, as highlighted by the arrows, MG132 also unexpectedly depleted some lower mass fragments of DAPK-1. This suggests that DAPK-1 protein is actively cleaved in cells by a protease(s) that can be inhibited by MG132.

Several previous reports have described the appearance of DAPK-1 protein cleavage products[65, 66]. These reports are consistent with our data showing that DAPK-1 is cleaved by some proteases *in vivo*. Recently it was reported that the accumulation of a 60-kDa cleavage band of DAPK-1 protein is specifically inhibited by a cathepsin B inhibitor[66]. Moreover, since MG132 can also function as a general inhibitor of cathepsins[165], we compared the effect of cathepsin B inhibitor with MG132 on inhibition of the cleavage of DAPK-1. The cathepsin B inhibitor depleted similar cleavage products as observed using MG132 (Figure 3.4B), albeit to a lesser extent, which possibly reflects the efficacy of the inhibitors.

3.4 Interaction of DAPK-1 and cathepsin B

In order to confirm that cathepsin B is able to cleave DAPK-1, radioactive labelled DAPK-1 protein was incubated with purified cathepsin B protein *in vitro* and a 60KDa cleavage product was also observed (Figure 3.5), suggesting that cathepsin B but not the proteasome is responsible for the accumulation of lower mass adducts

seen in cells. Since cathepsin B and DAPK-1 appear to interact *in vivo*, as defined by cathepsin B-sensitive proteolytic fragments (Figure 3.5), we set out to determine whether they directly bind to each other using co-immunoprecipitation assays. Since both cathepsin B and DAPK-1 are reported to be involved in TNF-α apoptotic pathways and TNF-α have been shown to promote the degradation of DAPK-1[76, 121, 166, 167], we reasoned that TNF-α may mediate the degradation of DAPK-1 via enhancing its interaction with cathepsin B. Therefore, we set out to test whether TNFR-1 transfection altered the stability of the DAPK-1-cathepsin B immune complex. Because cathepsin B is a 29KDa protein, which is in size very close to the light chain in the IP reactions observed in western blot, we examined the expression of transfected TNFR-1 and its effect on endogeous cathepsin B in direct lysate first (Figure 3.6A) and it is clear that overexpressed TNFR-1 does not enhance the exrpression of endogenous cathepsin B. We then carried on to do immunoprecipitation and found that TNFR-1 transfection relative to vector control increased the co-precipitation of endogenous DAPK-1 with cathepsin B in lysates from three cell lines (Fig 3.6, B–D, lane 4 versus lane 3). Surprisingly, there was no detectable decrease in the total levels of DAPK-1 protein in direct lysates (Figure 3.6, B–D, lane 5 versus lane 1), suggesting that the increase in immune complex formation observed may not necessarily lead to a decrease in DAPK-1 protein level. Notably, the control IPs in Hela and A549 cells (lanes 2 in Figure 3B and Figure 3D) are much stronger than that in HCT116 p53+/+ cells (lane 2 in Figure 3.6C). This may be due to differences in the expression level of endogenous DAPK-1 protein in these three cell lines (Figure 3.1).

We next set out to investigate the localization of endogenous DAPK-1 and cathepsin B. Because the commercial antibodies available can not detect endogenous DAPK-1 by immunostaining, a subcellular fractionation kit was used[23, 125]. The fact that TNF-α can induce the permeabilization of lysosomes and thus release cathepsin B into the cytosol[168] led us to consider that TNFR-1 promoted the interaction between DAPK-1 and cathepsin B by localizing both of them to the same cellular compartment. Therefore, we investigated the localization of DAPK-1 and cathepsin B by comparing the proportion of these two proteins in each fraction with or without TNFR-1 transfection (Figure 3.7A). As expected, after TNFR-1 transfection, the proportion of cathepsin B protein was elevated in the cytosolic fraction (Figure 3.7B) and mainly decreased in the "nuclear" fraction (Figure 3.7B). Moreover, the proportion of cytosolic DAPK-1 protein increased after TNFR-1 transfection (Figure 3.7B) and the proportion of DAPK-1 in other fractions, especially the cytoskelaetal fraction, reduced after TNFR-1 transfection (Figure 3.7B). Interestingly, DAPK-1 mobilities varied in different fractions (Figure 3.7A) and a duplex was observed in the "membrane and organelle" fractions (Figure 3.7A, lanes 2 and 6). This may be due the different buffers used in each fraction, or may reflect specific modifications of DAPK-1 such as phosphorylation in the "membrane and organelle" fraction since autophosphorylation of DAPK-1 is a common mechanism for the regulation of DAPK-1 activity as mentioned in Section 1.9. I then performed an immunoprecipitation from subcellular fractions 1–3 (Figure 3.7A) to evaluate the interaction of DAPK-1 and cathepsin B in these fractions (Figure 3.C). Fraction 4 was not used because the protein precipitated in the buffer during the IP proceedure. A mixture of fractions 1, 2 and 3 were used in the control IP to make sure there was

no background detected in any of the fractions. It is clear that although the strongest DAPK-1 and cathepsin B complex is detected in the "nuclear" fraction (Figure 3.7C, lane 4), TNFR-1-mediated signalling elevated the DAPK-1/cathepsin B complex only in the cytosolic fraction since the proportion of DAPK-1/cathepsin B complex in this fraction increased from around 5% to around 40% (Figure 3.7D). Moreover, TNFR-1 mediated reduction of the DAPK-1-cathepsin B immune complex occurred in the "nuclear"fraction (Figure3.7D). Unexpectedly, the membrane and organelle fraction which has the highest levels of cathepsin B (Figure 3.7A, lanes 2 and 6) did not yield formation of a detectable immune complex between DAPK-1 and cathepsin B (Figure 3.7B, lane 6 and lane 3). These data suggest that DAPK-1 and cathepsin B are assembled into a very specific dynamic multiprotein complex. The TNFR-1 mediated increase in DAPK-1/cathepsin B binding observed may be due to the relocalization of the proteins, since the lysis buffer used in the co-immunoprecipitation assays is much more gentle compared to those in the last two fractions of the fractionation kit and TNFR-1 may actually function to drive some insoluble DAPK-1/cathepsin B complex into the cytosol.

3.5 Role of DAPK-1/cathepsin B complex in TNF-α signalling pathway

In order to determine the functional role of the DAPK-1/cathepsin B complex in TNF-α signalling pathway, I set out to define which region on DAPK-1 binds to cathespin B. First I examined whether TNFR-1 could promote the binding of transfected full-length DAPK-1 (1432 amino acids) with endogenous cathepsin B.

Similar to the previous results, TNFR-1 stimulated the formation of a DAPK-1/cathepsin B complex as determined by immunoprecipitation (Figure 3.8A, lanes 3 versus lane 2). Four DAPK-1 mutants with deletion of key functional domains were then created by site-directed mutagenesis (Figure 3.8B) When co-transfecting the DAPK-1 deletion mutants (Figure 3.9A, lanes 1–5) with TNFR-1 followed by immunoprecipitation with the cathepsin B antibody, only the longest DAPK-1 mutant (residues 1–1313) bound to endogenous cathepsin B (Figure 3.9A, lane 10 versus lanes 6–9). These data suggest that the region between 836 and 1313 is important for the binding of cathepsin B to DAPK-1.

In addition the inverse IP experiment by performed, DAPK-1 was immunoprecipitated from cell extract and immunoblotting with cahtpesin B antibody. However, no complex could be observed. We considered it may be due to the masking of the binding site of DAPK-1 and cathepsin B by the antibody. Because the antibody was generated by using a fragment of DAPK-1 protein (694-947), which partially overlapps with the interaction domain that we mapped to amino acids (846-1313). We therefore generated another DAPK-1 deletion construct (residues 1-947) in order to map further the cathepsin B binding site. When co-transfecting the DAPK-1 deletion mutants (residues 1–835 and residues 1–947 with TNFR-1 followed by immunoprecipitation with the cathepsin B antibody, only the DAPK-1 mutant (residues 1–947) bound to endogenous cathepsin B (data not shown). This interaction was weak and the blot we obtained is not very clear. However, the fact that the antibody immunogen overlapped with the domain we mapped convinced us that the 836-947 is the major component on DAPK-1 that cathepsin B interacts with.

The use of small peptide domains derived from full-length polypeptides to manipulate cell signalling is an emerging field called chemical genetics or peptide therapeutics[169]. Such mini-modules often reveal novel insights into signalling as a result of disrupting a specific protein interaction, and they can be expected to provide leads for drug design and development. To determine whether the minimal cathepsin B binding region of DAPK-1 acts in a gain-of-function or in a dominant negative fashion on TNFR-1-dependent apoptosis, the DAPK-1(836–947) miniprotein was transfected into cells to evaluate effects on cell signalling. A dose-dependent expression of DAPK-1(836–947) miniprotein can be observed after transfection (Figure 3.10A). Further, transfection of the cathepsin B expression vector results in reduction in levels of the DAPK-1(836–947) miniprotein (Figure 3.10B, lanes 4 versus lanes 2), indicating an interaction between the two proteins in cells. An *In vitro* cleavage assay whereby I incubated purifed GST only with cathepsin B further confirmed that cathespin B downregulates GST-836-947 specifically via the 836-947 minidomian rather than the GST-tag (Figure 3.10C). Furthermore, the transfection of the vector encoding the DAPK-1(836–947) miniprotein resulted in a stimulation of TNFR-1-dependent PARP cleavage (Figure 3.11, lane 4 versus lanes 2 and 3). Interestingly, in this experiment the level of the unprocessed form of PARP is very similar despite the dramatic difference in the level of cleaved PARP (Figure 3.11). This may be due to the stimulation of the expression of unprocessed PARP by death signals like TNFR-1 via unknown mechanisms. Surprisingly, a significant decrease in endogenous DAPK-1 protein level was observed when combined with the transfection of TNFR-1 (Figure 3.11, lane 4 versus lanes 1–3), suggesting that

disruption of the endogenous DAPK-1/cathepsin B complex actually sensitises DAPK-1 to TNFR-1 mediated degradation. Therefore, although cathepsin B is capable of cleaving DAPK-1 and can form a stable complex with DAPK-1, TNFR-1 mediated DAPK-1 degradation does not appear to be cathepsin B dependent. Moreover, endogenous cathepsin B may protect DAPK-1 from degradation in response to TNF-α treatment.

In order to determine whether changes in PARP cleavage correlated with changes in apoptosis, Annexin V staining and a TUNEL assay were used to quantify DAPK-1 (836–947) miniprotein apoptotic function. The transfection of TNFR-1 resulted in increased apoptosis as defined by Annexin V staining (Figure 3.12A) that was further stimulated by the co-transfection of the DAPK-1(836–947) miniprotein (Figure 3.12A). The transfection of TNFR-1 also resulted in apoptosis, as defined by TUNEL staining (Figure 3.12B), that was similarly stimulated by the co-transfection of DAPK-1(836–947) miniprotein (Figure 3.12B; quantitated in Figure 3.12C). This maximal level of apoptosis therefore correlated with the appearance of cleaved PARP and a reduction in endogenous DAPK-1 protein levels (Figure 3.11).

Given that cathepsin B may have an inhibitory effect on TNF-α signalled DAPK-1 degradation, we used siRNA to cathepsin B to determine the actual role of the endogenous protein in regulating the rate of TNF-α-dependent apoptosis and DAPK-1 degradation. Because the protein translation inhibitor cycloheximide can block NF-κB activity and greatly enhances the apoptotic effect of TNF-α[170] and it has been shown that TNF-α and CHX combinatonal treatment degrades DAPK-1 much better

than TNF-α alone[62, 151], the cells were treated with TNF-α plus CHX and the levels of apoptosis were evaluated by monitoring PARP cleavage (Figure 3.13A, lane 2 versus lane 1). Treatment of cells with siRNA to cathepsin B led to depletion of cathepsin B protein (Figure 3.13A, lanes 5 and 6 versus lanes 2 and lanes 1) and a concomitant stimulation of PARP cleavage (Figure 3.13A, lane 6 versus lane 2). These data suggest that cathepsin B is a negative regulator of TNF-α dependent apoptosis. Further, consistent with previous work, TNF-α and CHX combinational treatment was able to degrade DAPK-1 better than TNF-α or CHX alone, although TNF-α treatment is enough to stimulate apoptosis (Figure 3.13B). In fact, DAPK-1 levels increased slightly after TNF-α or CHX treatment alone, suggesting a strong rather than subtle cell death signal may be necessary for the degradation of DAPK-1 or the proteins involved in the inhibition of TNF-α induced apoptosis such as Bcl-2 are required to maintain DAPK-1 level upon TNF-α stimulation. Moreover, the TNF-α/CHX induced decrease was enhanced in combination with cathepsin B siRNA treatment (Figure 3.13B). These data support the idea that cathepsin B negatively regulates TNF-α mediated DAPK-1 degradation and both cathepsin B and DAPK-1 might function as negative regulators of TNF-α-dependent apoptosis. In agreement, DAPK-1 protein depletion in response to TNF-α treatment coincides with the appearance of PARP cleavage (Figure 3.13A, lane 6 versus lane 2). Further, attenuation of DAPK-1 expression failed to block the potent PARP cleavage observed in response to TNF-α and CHX combined treatment (Figure 3.13C, lane 8 versus lane 4) and actually increased PARP cleavage slightly in combination with TNF-α treatment (Figure 3.13C, lane 6 vs lane2). This suggests that DAPK-1

negatively regulates TNF-α-mediated cell death and is consistent with a previous report showing that although DAPK-1 mediates interferon-γ-dependent apoptosis, DAPK-1 protein depletion using morpholino technologies sensitizes cells to TNF-α-dependent apoptosis[18].

Taken together, these data suggest that although cathepsin B is capable of cleaving DAPK-1, the physiological role of cathepsin B is to protect DAPK-1 from degradation. The activity of proteases can vary depending on the pH of the environment[171], therefore it is possible that the DAPK-1/cathepsin B complex is formed *in vivo*, but the protease activity of cathepsin B is inhibited and the cleavage may actually occur during cell lysis. Therefore, lysis buffer was supplemented with MG132 or cathepsin B inhibitor to investigate whether the cleavage of DAPK-1 was blocked (Figure 3.14). Indeed inhibitors in the lysis buffer blocked the cleavage of endogenous DAPK-1, which confirmed that the majority of the cleavage occurred *in vitro* (Figure 3.14).

3.6 Conclusion

My study shows that DAPK-1 protein levels can be controlled post-translationally. While cathepsin B can interact with and cleave DAPK-1 protein during cell lysis *in vitro* (Figure 3.4, 3.5, 3.14), it appears the function of cathepsin B in cells is to protect DAPK-1 from TNFR-1 induced degradation since TNF-α and CHX combinational treatment degrades DAPK-1 better in the absence of cathepsin B (Figure 3.13). It is not clear whether cathepsin B protects DAPK-1 simply by binding to it or through alternative pathways that requires its protease activity. The fact that

the DAPK-1 miniprotein GST-836-947 can be depleted by cathepsin B (Figure 3.10) and promote TNFR-1 induced DAPK-1 degradation suggestes that interaction between DAPK-1 and cathepsin B may be the key for this protection. An IP experiment has been performed to examine the interaction between GST-836-947 and cathepsin B, but no stable complex could be observed (data not shown). This suggested that cathepsin B may not mediate the depletion of GST-836-947 via direct cleavage, but thorugh other unidentified degradation components such as the lysosome. Of note, it cannot be ruled out that the activity of cathepsin B still plays a role in this protection. Further experiments using cathepsin B inhibitor together with TNFR-1 may help to investigate this aspect more deeply.

The siRNA experiment (Figure 3.13C) and other published work[62, 151] suggest that DAPK-1 acts as a survival factor in the TNF-α signalling pathway. Cathepsin B functions to protect DAPK-1 from TNFR-1 induced degradation. Considering that the expression of the ubiquitin E3 ligase DIP-1 for DAPK-1 promotes TNF-α-induced apoptosis[62], there may be a link between the ubiquitination of DAPK-1, its interaction with cathepsin B, and TNF-α apoptotic responses.

DAPK-1 is known to bind to early responsive components in the TNF-α pathway, including TNFR-1 and FADD after brain seizures, although the physiological functions of these interactions are still unclear[76, 166]. Morpholino depletion of DAPK-1 protein sensitizes cells to TNF-α-induced apoptosis, whereas a depletion of DAPK-1 protein attenuates interferon-γ-induced apoptosis (Figure 3.15A)[18]. These data indicate that DAPK-1 can exhibit prosurvival as well as proapoptotic signalling

properties. The discovery here of a TNFR-1-regulated interaction between cathepsin B and DAPK-1 raises the question of whether this complex would be prosurvival or proapoptotic. The stimulation of TNFR-1-induced apoptosis by either DAPK-1 or cathepsin B depletion using siRNA (Figure 3.13) suggests that this complex could be regulating the rate of TNF-α-dependent apoptosis by virtue of attenuating the apoptotic program. Using the cathepsin B binding domain of DAPK-1 as a tool to further test the mechanism of TNF-α-apoptotic signaling, we show that the DAPK-(836–947) miniprotein can function in a dominant negative manner, resulting in a stimulation of DAPK-1 protein degradation and an increase in TNF-α-dependent apoptosis (Figure 3.15B). These data provide a genetic tool with which to dissect the mechanism of how DAPK-1 links to TNF-α signalling in the future.

The fractionation studies have demonstrated that there are distinct pools of DAPK-1 that may have distinct functions (Figure 3.7A). These pools of DAPK-1 presumably will have distinct functions, possibly responding to ERK or other cytoskeleton-responsive signalling pathways or regulate the autophagy pathways, Moreover, the duplex in the "membrane and organelle" fraction may be the caused by the autophosphorylation of DAPK-1. It will be interesting to test the activity of DAPK-1 in each fraction to further investigate this observation.

In addition to cathepsin B, several other proteases, such as cathepsin D and cathepsin L, are reported to be involved in TNF-α-induced apoptotic pathways[100, 172, 173]. Further, cathepsin D also mediates the interferon-γ-triggered programmed cell death

like DAPK-1[8, 173]. It will be interesting to investigate whether DAPK-1 has any connections with these cathepsin family members.

DAPK-1 has been reported to bind to distinct proteins, such as ERK[77], RSK[155], and myosin light chain[174]. Our studies indicate that cathepsin B is a new member of this growing family of DAPK-1 binding partners with a novel binding domain localized in the C-terminal domain of DAPK-1 between the ankyrin repeats and the death domain. Given the ability of TNF-α-dependent pathways to induce apoptosis[175, 176], studying how this DAPK-1/cathepsin B complex integrates with MEK-ERK-DAPK-1[131], RSK-DAPK-1, and DAPK-1-p53 signalling axes will shed light on signal transduction mechanisms that modify the apoptotic response[177].

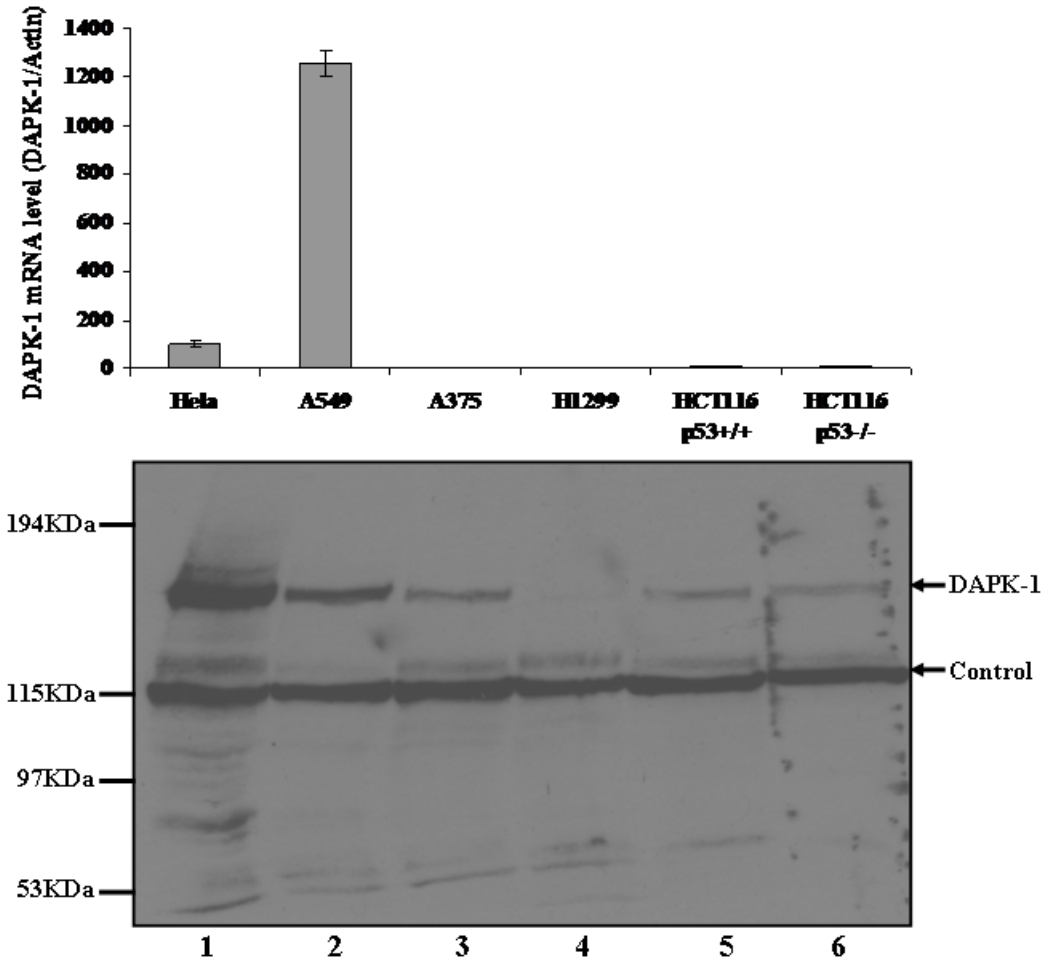

Figure 3.1 DAPK-1 protein and mRNA quantification in cycling cells. Six different tumour cells, as indicated, were harvested, and each cell sample was split into two halves. Half was used for mRNA level test using one-step SYBR green real time PCR (top); the other was lysed in UREA buffer and used for DAPK-1 protein level quantification using immunoblotting. The relative mRNA level is depicted as a ratio of DAPK-1/actin. The non-specific control band was used as loading control. This experiment has been performed twice.

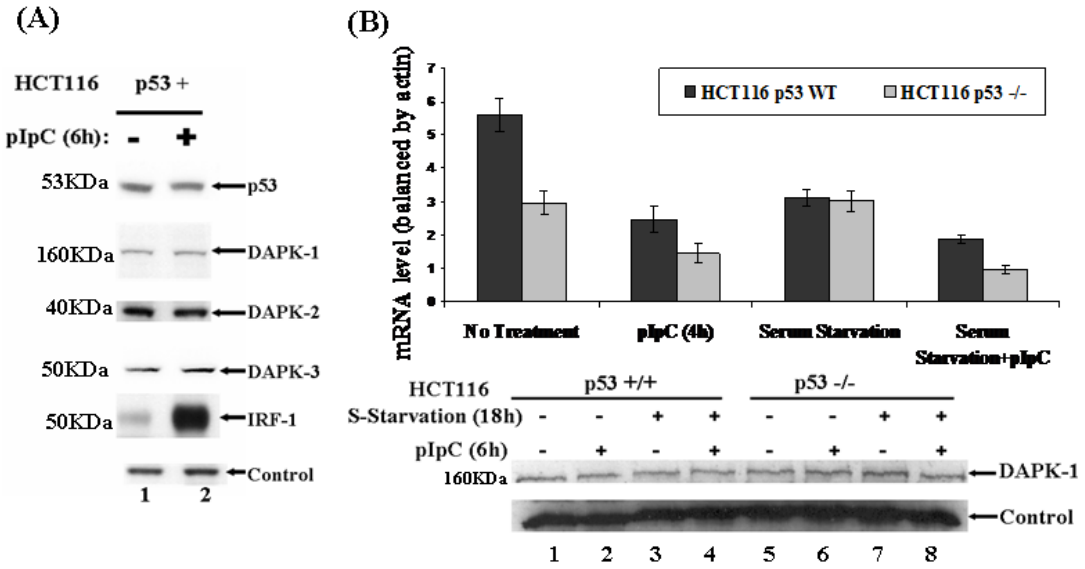

Figure 3.2 DAPK-1 protein and mRNA quantification upon viral stress. (A) The pIpC response of the p53 pathway. HCT116 p53+/+ cells were treated with and without pIpC for 6h (lanes 1 versus lanes 2), and the endogenous protein was extracted in UREA buffer and the expressions (as indicated; p53, DAPK-1, DAPK-2, DAPK-3, IRF-1, and loading control) were detected using the respective antibodies. **Same non-specific band as in Figure 3.1 was used as control. This experiment has been performed more than 3 times. (B) DAPK-1 protein and mRNA quantification in stress responses.** HCT116 p53+/+ and p53-/- cells were treated with pIpC for 6 h under normal culture or serum-starved conditions. Each cell sample was split into two halves. One was used for mRNA level quantification using real time PCR (top) and the other for DAPK-1 protein quantification using UREA lyssis and immunoblotting (bottom). The relative change in mRNA level is depicted as a ratio of DAPK-1/actin. **The non-specific band as shown in Figure 3.1 was used as control.** This experiment has been performed twice.

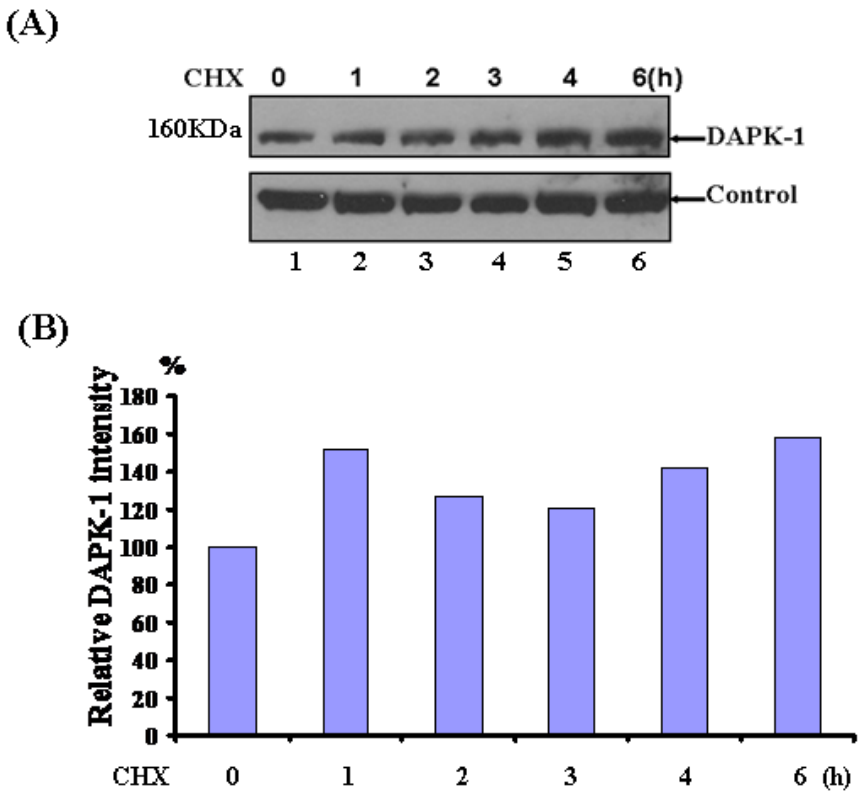

Figure 3.3 DAPK-1 has a higher stability. (A) The stability of DAPK-1 protein in Hela cells was determined by CHX treatment for 1 h, 2 h, 3 h, 4 h, and 6 h and the protein expression in (A) was quantified in (B). DAPK-1 was extracted in UREA buffer and detected using a DAPK-1-specific antibody. **The non-specific band as shown in Figure 3.1 was used as control. This experiment have been observed more than 3 times.**

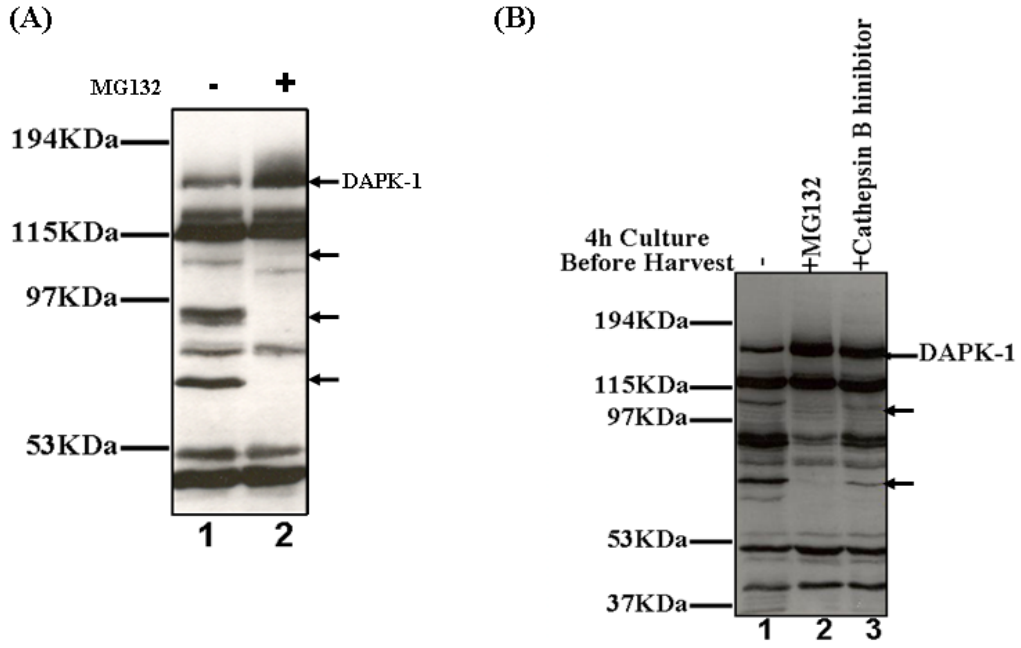

Figure 3.4 Blockage of the cleavage bands of DAPK-1. (A) Endogenous DAPK-1 protein cleavage in MG132-treated cells. The effect of MG132 on endogenous DAPK-1 protein levels was analyzed in A549 cells treated with and without MG132 for 6 h before harvesting (lanes 1 versus lanes 2). DAPK-1 protein was extracted in UREA buffer and immunoblotted and the MG132-dependent cleavage changes are depicted using. **(B) The effect of a cathepsin B inhibitor on DAPK-1 protein cleavage.** A549 cells were treated with MG132 (lane 2) or a cathepsin B inhibitor (benzyloxycarbonyl-FA-fluoromethyl ketone) (lane 3) for 4 h before harvesting. The endogenous DAPK-1 was extracted in UREA buffer and detected by immunoblotting. Both experiments have been performed more than 3 times.

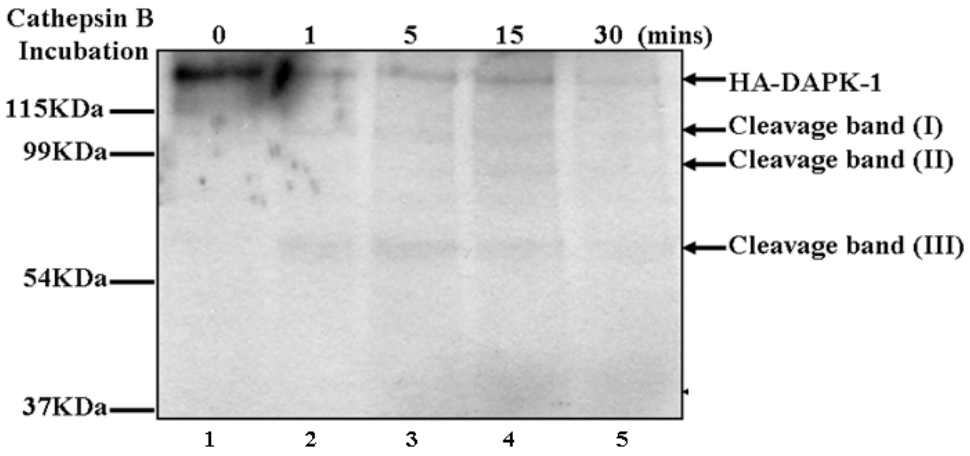

Figure 3.5 *In vitro* cleavage of DAPK-1 by cathepsin B. ^{35}S-labeled HA-DAPK-1 (2 μg) was incubated with purified cathepsin B (0.1 units) in a 15μl reaction volume for the indicated time points. The reaction was stopped with SDS-containing sample buffer, and protein was separated using SDS-PAGE. The cleavage bands of DAPK-1 are depicted using arrows as I, II and III. (Radioacive HA-DAPK-1 made by Dr. Jennifer Fraser) This experiment has been performed twice.

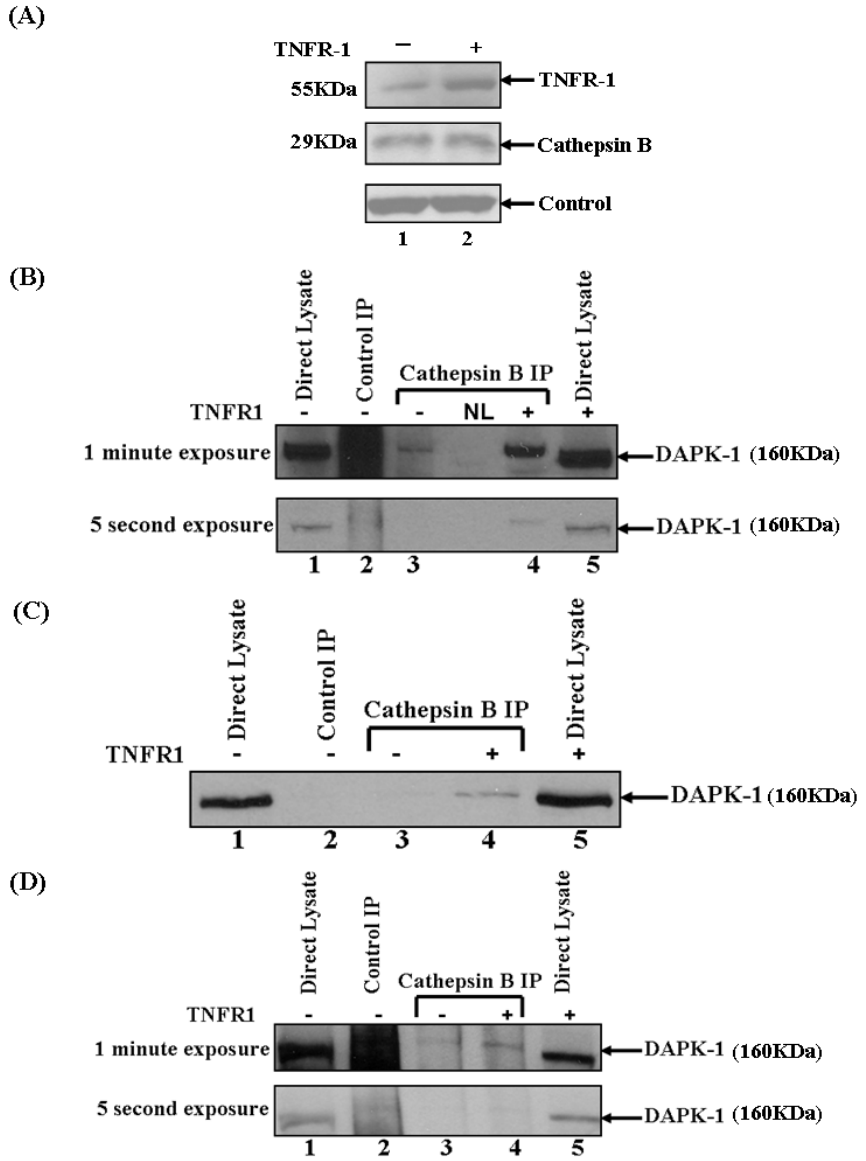

Figure 3.6 TNFR-1 enhances the complex formation between DAPK-1 and cathepsin B. (A) Hela cells were transfected with PCDNA3 (-) or vectors encoding TNFR-1 for 18h before harvesting. The lysates were extracted in NP40 buffer and then subjected to immunoblotting. The expression of TNFR-1 and cathepsin B was detected by respective antibodies. B-actin was used as the loading control. This experiment has been observed more than 3 times. (B) Hela; (C) HCT116 p53+/+; (D) A549 cells were transfected with PCDNA3 (-) or vectors encoding TNFR-1 for 18 h before harvesting. The lysates were extracted in NP40 buffer and then subjected to immunoprecipitation with a cathepsin B antibody and then probed with anti-DAPK-1 antibody. Mouse secondary antibody was used in the control immunoprecipitation. Lane 1, direct lysate with vector only transfection; lane 2, control immunoprecipitation; lane 3 and 4, immunoprecipitation in vector only or TNFR-1-transfected cells; lane 5, direct lysate with TNFR-1 transfection). In **(B)**, a no lysate control (lane NL) immunoprecipitation was also performed to check the background of the antibody. Cathepsin B IP for endogeous DAPK-1 experiments have been performed more than 3 tims.

(A)

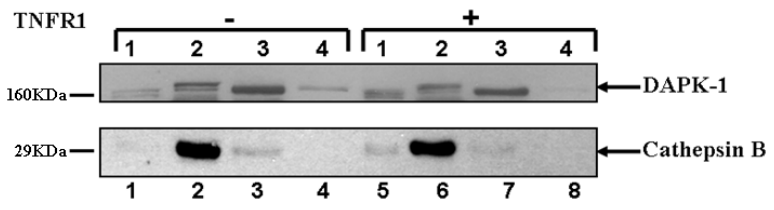

1=cytosol; 2=membrane and organelle; 3=nucleus; 4=cytoskeleton;

(B)

	PCDNA3 transfection		TNFR-1 transfection	
Fractions	DAPK-1	Cathepsin B	DAPK-1	Cathepsin B
1	11.59%	3.79%	29.75%	10.13%
2	33.05%	85.44%	28.44%	84.56%
3	45.91%	10.43%	39.41%	4.68%
4	9.45%	0.35%	2.4%	0.63%

(C)

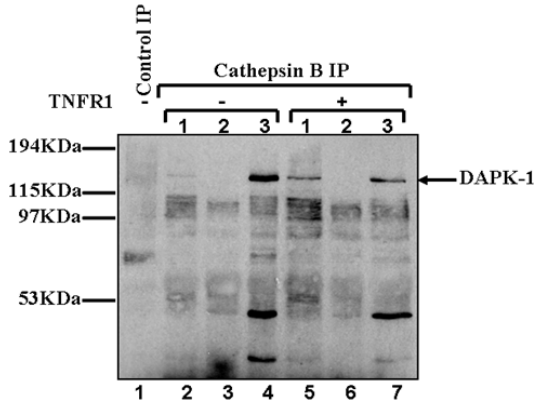

(D)

	PCDNA3 transfection	TNFR-1 transfection
Fractions	DAPK-1	DAPK-1
1	5.89%	38.15%
2	0.01%	0.01%
3	94.10%	61.84%

Figure 3.7 TNFR-1 switches the localization of the DAPK-1/cathepsin B complex. (A) TNFR-1 induces a DAPK-1 and cathepsin B mobilization to the cytosolic fraction. Hela cells were transfected with PCNDA3 (-) or vectors encoding TNFR-1 for 18 h before harvesting. The subcellular fractionation was performed using the fractionation kit from Calibiochem. DAPK-1 and cathepsin B were detected with respective antibodies. Lanes 1–4, DAPK-1 and cathepsin B levels in fractions 1–4 in vector-only transfectants; lanes 5–8, DAPK-1 and cathepsin B levels in fractions 1–4 in TNFR-1 transfectants. **The proportion of DAPK-1 and cathepsin B in each fraction in (A) was quantified in (B). (C) TNFR-1 switches DAPK-1/cathepsin B complex to the cytosolic fraction.** The lysates of each fraction from (A) were immunoprecipitated with cathepsin B antibody and then probed with DAPK-1 antibody. Lanes 2–4, cathepsin B bound DAPK-1 levels in fractions 1–3 in vector-only transfectants; lanes 5–7, cathepsin B bound DAPK-1 levels in fractions 1–3 in TNFR-1 transfectants. A mixture of fractions 1,2 and 3 in vector only transfectant and a non-specific anti-mouse secondary antibody were used in the control IP. The proportion of pulled-out DAPK-1 in each fraction in (C) was quantified in (D). These experiments have been performed once.

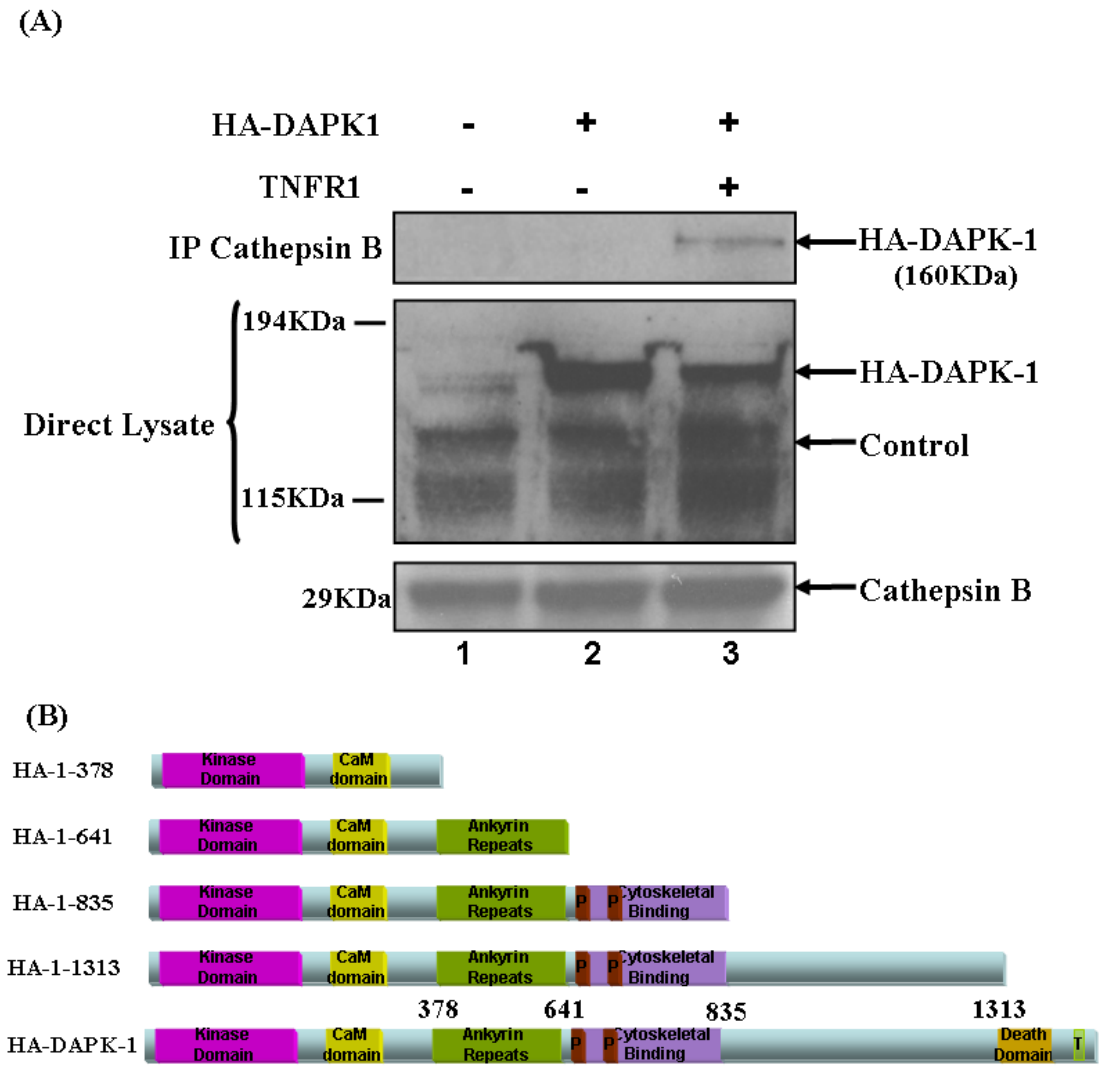

Figure 3.8 Generation of HA-DAPK-1 mutants. (A) TNFR-1 increases the binding between transfected HA-DAPK-1 and endogenous cathepsin B. HCT116 p53+/+ cells were transfected with PCNDA3 (-) or vectors encoding HA-DAPK-1 for 36 h and TNFR-1 for 18 h prior to harvest. The lysates were extracted in NP40 buffer and then subjected to immunoprecipitation with a cathepsin B antibody, and then both direct lysates and eluates were probed with an anti-HA antibody to quantify DAPK-1 binding. The expression of cathepsin B was detected by a cathepsin B antibody. The non-specific band was used as a loading control. This experiment has been performed more than 3 times. **(B) A schematic diagram of DAPK-1 mutants made from the full-length HA-DAPK-1 construct.**

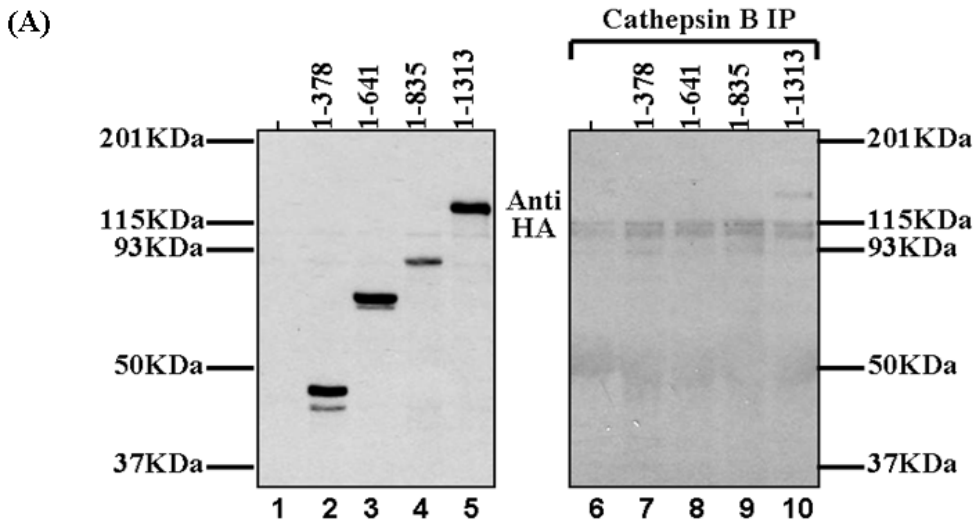

Figure 3.9 Mapping the binding region of cathepsin B on DAPK-1. (A) DAPK-1 C-terminal domain deletion prevents cathepsin B binding in cells. HCT116 p53+/+ cells were transfected with PCNDA3 (-) or the indicated HA-DAPK-1 expression vectors for 36 h. The TNFR-1-encoding vector was transfected 18 h post-transfection of HA-DAPK-1 mutants. The cell lysates were extracted in NP40 buffer and then immunoprecipitated with a cathepsin B antibody and then probed with HA antibody to quantify DAPK-1 protein levels. **This experiment has been performed more than 3 times.**

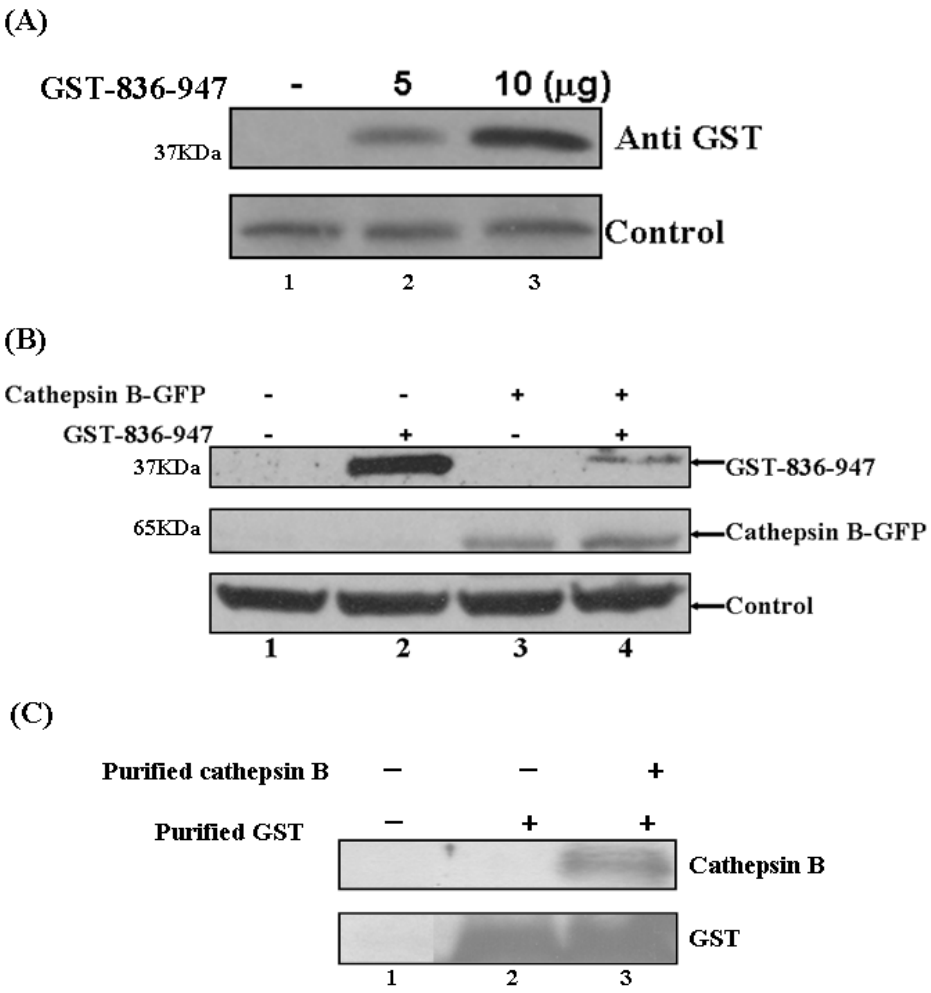

Figure 3.10 Characterization of DAPK-1-(836-947) mutant. (A) Expression of DAPK-1-(836–947) in cells. HCT116 p53+/+ cells were transfected with PCDNA3 (-) or vectors encoding GST-DAPK-1-(836–947) for 36 h before harvest. The lysates were extracted in NP40 buffer and the expression of GST-DAPK-1-(836–947) was detected by GST antibody. β-Actin was used as a loading control. **This experiment has been performed more than 3 times. (B) Cathepsin B transfection depletes the DAPK-1-(836–947) miniprotein.** HCT116p53+/+ cells were transfected with PCDNA3 (-) or vectors encoding GST-DAPK-1-(836–947) and cathepsin B-GFP for 36 h before harvest. The lysates were extracted in NP40 buffer and the expression of GST-DAPK-1-(836–947) was detected by GST antibody, and cathepsin B was detected by GFP antibody. β-Actin was used as a loading control. **This experiment has been performed more than 3 times. (C)** Purified GST (2 μg) was incubated with purified cathepsin B (0.1 units) in a 15μl reaction volume for 30 minutes. The reaction was stopped with SDS-containing sample buffer, and protein was separated using SDS-PAGE. Cathepsin B and GST were detected with respective antibodies. **This experiment has been performed once.**

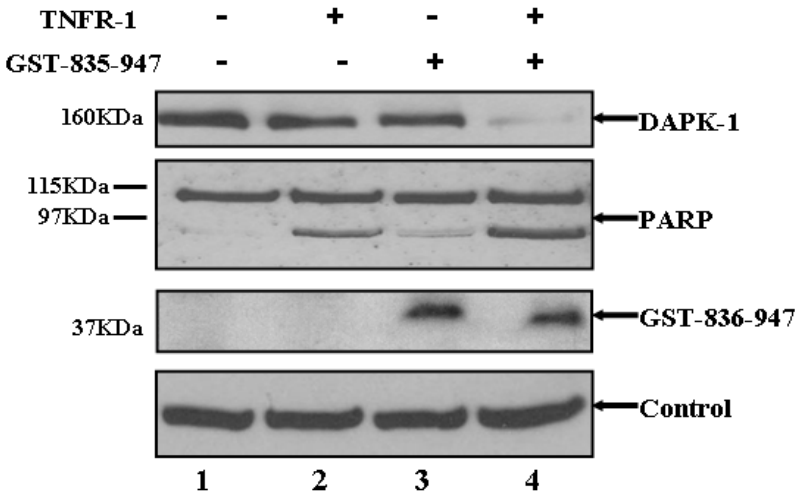

Figure 3.11 DAPK-1-(836–947) miniprotein promotes TNFR-1-dependent DAPK-1 degradation in cells. Hela cells were transfected with PCNDA3 (-) or vectors encoding GST-DAPK-1-(836–947) and TNFR-1 for 24h before harvest. The lysates were extracted in NP40 buffer and the expression of endogenous DAPK-1 and PARP were detected by respective antibodies. GST-836-947 was detected by GST antibody and its detection was performed in a separate western blot experiment. **The non-specific band as shown in Figure 3.1 was used as control. This experiment has been performed more than 3 times.**

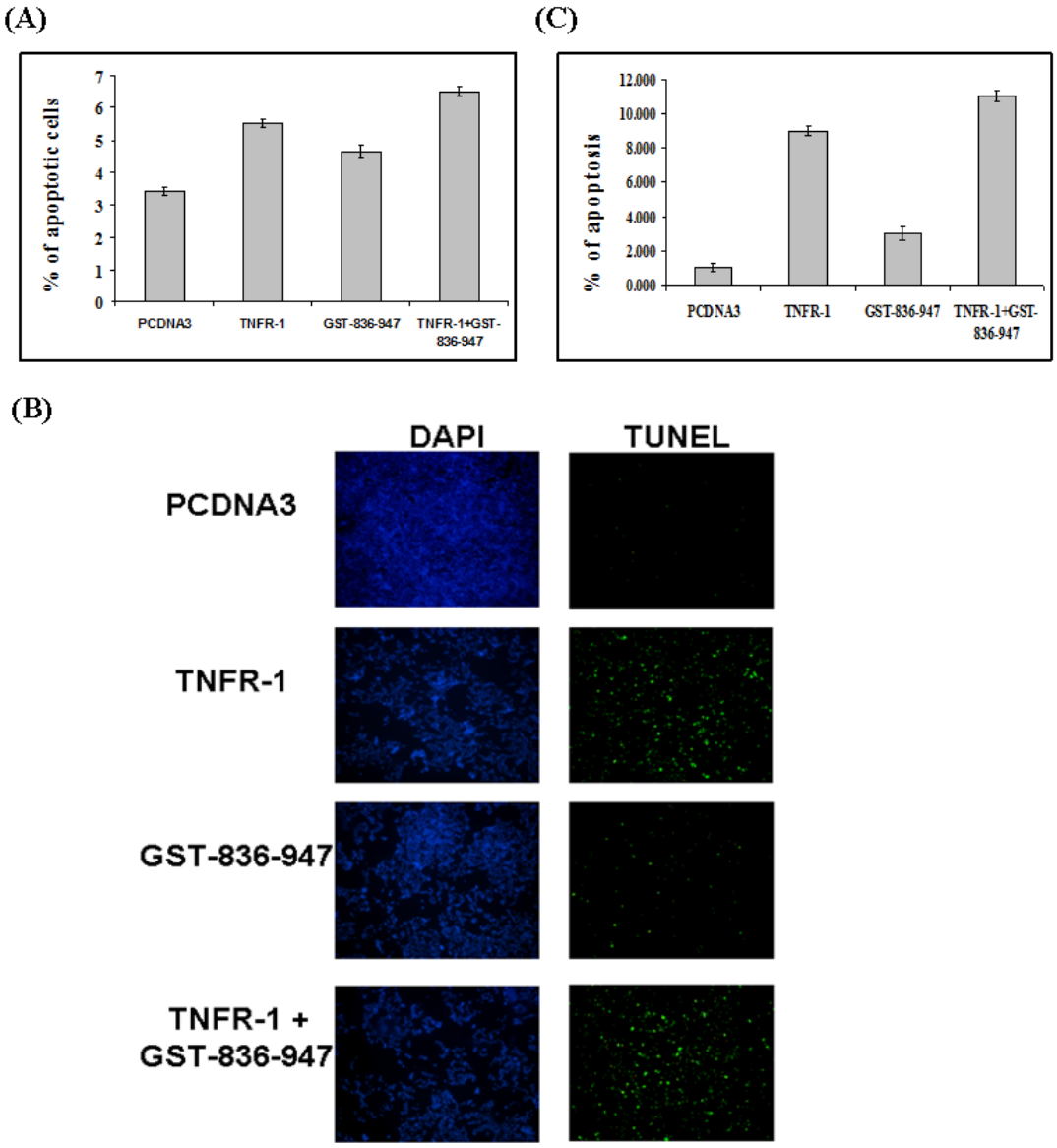

Figure 3.12 DAPK-1-(836–947) miniprotein enhances TNFR-1-dependent apoptosis in cells (Performed by Dr. Craig Stevens). (A) Annexin V quantitation of apoptosis stimulated by DAPK-1-(836–947). HCT116 p53+/+ cells were transfected with the indicated expression vectors for 24 h before harvest. The apoptotic cells were then detected using the TACS Annexin V-fluorescein isothiocyanate apoptosis detection kit. The percentages of the apoptotic cells are presented in bar graphs. **(B) TUNEL assay for quantifying apoptosis stimulated by DAPK-1-(836–947).** HCT116p53+/+cells were transfected with the indicated expression vectors for 24h before staining. Apoptotic cells were labelled using an Apoptag Plus fluorescein *in situ* apoptosis detection kit S7111 (Chemicon International). **(C) The result of the TUNEL assay was analyzed by Image J, and the percentages of apoptotic versus total cells are presented in bar graphs. These experiments have been performed twice.**

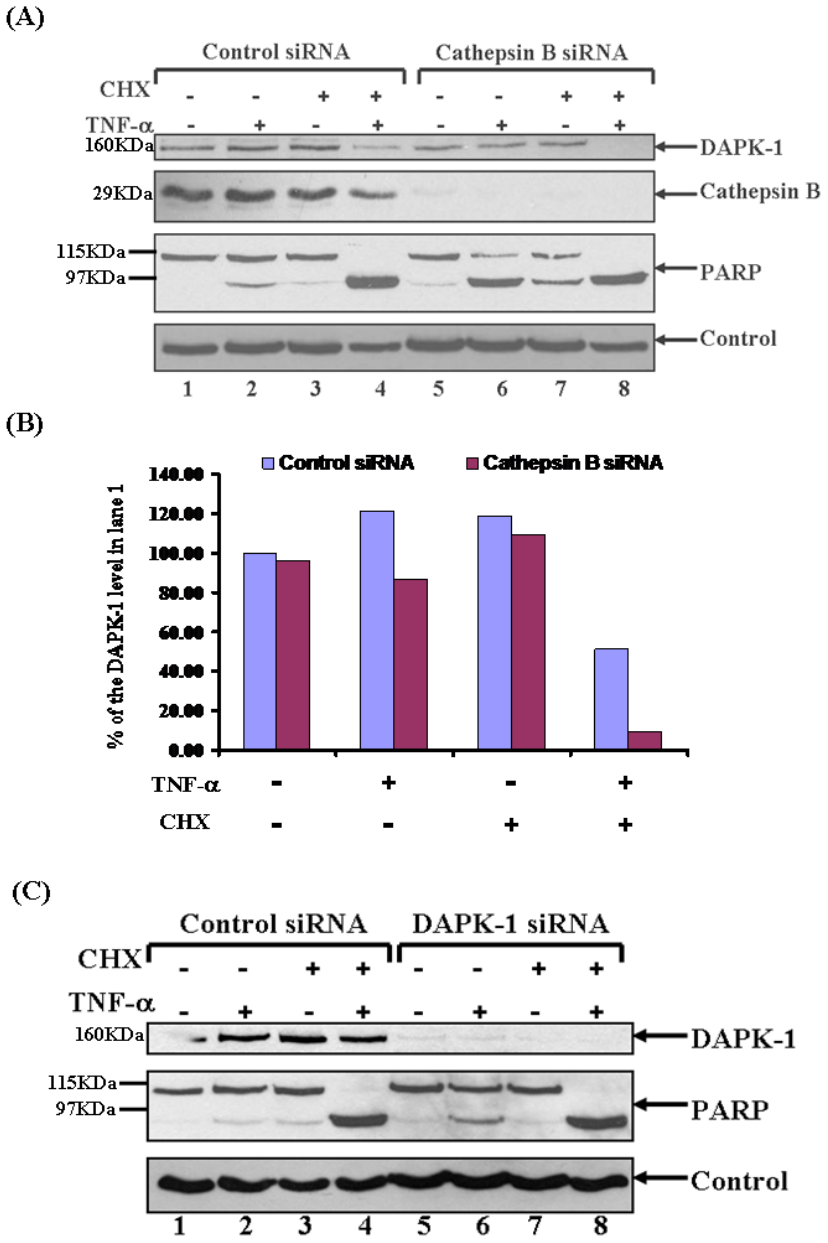

Figure 3.13 Roles of endogenous DAPK-1 and cathepsin B in TNF-α induced apoptosis. (A) Effects on TNF-α induced DAPK-1 degradation and PARP cleavage after cathepsin B protein reduction using siRNA. siRNA knockdown of cathepsin B was performed in Hela cells in combination with the TNF-α and CHX treatments. DAPK-1, cathepsin B, and PARP were extracted in NP40 buffer and detected with the respective antibodies, as indicated. **The non-specific band as shown in Figure 3.1 was used as control. The expression of DAPK-1 protein in (A) was quantified in (B). (C) Effects on TNF-α induced PARP cleavage after DAPK-1 protein reduction using siRNA.** siRNA knock-down of DAPK-1 was performed in Hela cells in combination with the TNF-α and CHX treatments. DAPK-1 and PARP were extracted in NP40 buffer and detected with the respective antibodies, as indicated. **The non-specific band as shown in Figure 3.1 was used as control. These experiments have been observed twice.**

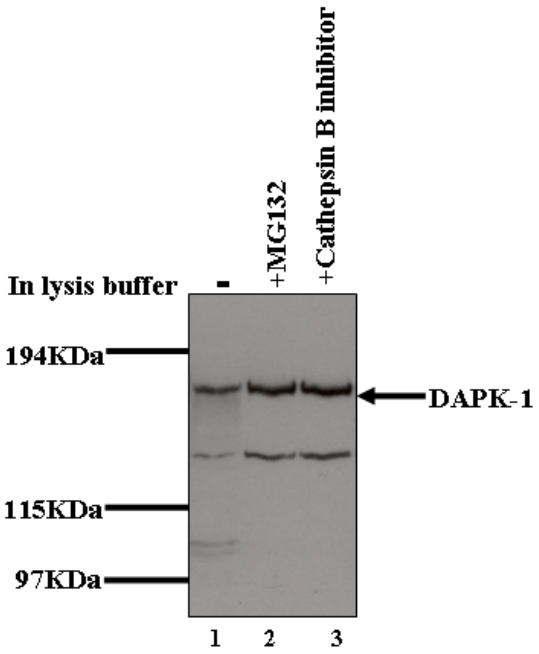

Figure 3.14 DAPK-1 cleavage can be blocked *in vitro* by cathepsin B inhibitor and MG132. 10μM MG132 or 10μM cathepsin B inhibitor was added to the UREA lysis buffers before lysing Hela cells. The endogenous DAPK-1 and its cleavage bands were detected by DAPK-1 antibody. **This experiment has been performed more than 3 times.**

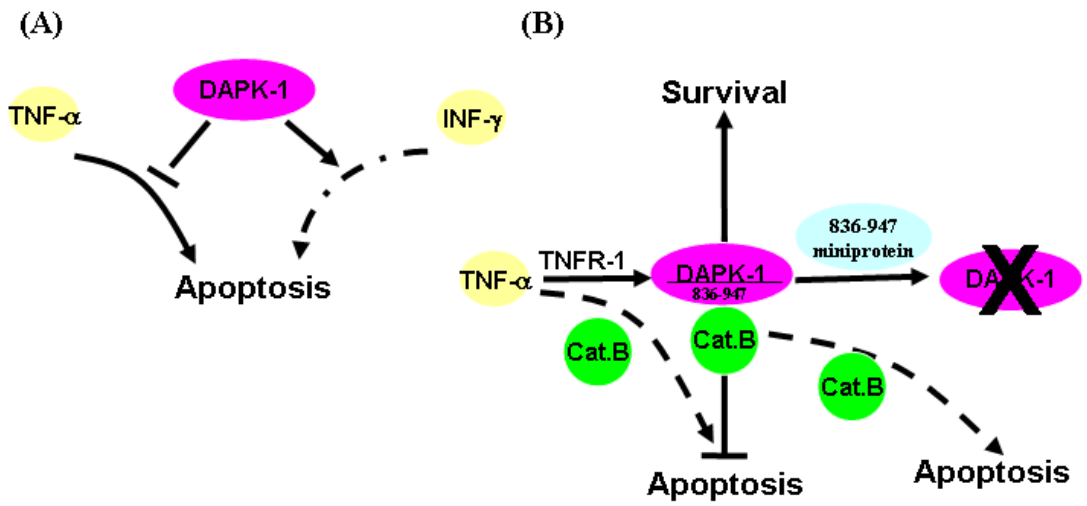

Figure 3.15 Models for DAPK-1/cathepsin B complex in apoptosis pathways. (A) A model highlighting the two distinct pathways involving DAPK-1: a DAPK-1 survival function antagonizing TNF-dependent apoptosis and a DAPK-1 proapoptotic function in interferon-γ dependent apoptosis. **(B) A model highlighting the mechanism of DAPK-1 dependent attenuation of TNF-α dependent apoptosis.** Although cathepsin B has been reported to stimulate TNF-α-mediated apoptosis [99, 100], this current study shows that the depletion of either cathepsin B or DAPK-1 using siRNA can stimulate TNF-α-mediated PARP cleavage, suggesting the binding of DAPK-1 to cathepsin B attenuates TNF-α-mediated apoptosis. The induction of a DAPK-1/cathepsin B complex in the cytosol by TNF-α signalling suggests that it may be the complex itself that has such prosurvival activity. Moreover, the ability of the DAPK-1 binding region for cathepsin B (miniprotein amino acids 836–947) to degrade endogenous DAPK-1, thus stimulating apoptosis, further suggests that it is this dimeric complex that can counter rates of TNF-α-mediated apoptosis. We propose that the DAPK-1 domain from amino acids 836–947 can interact with an "anchoring" factor (like cathepsin B) that normally keeps DAPK-1 in a stable state with a very slow turnover (Figure 3.3). This region is required to maintain the DAPK-1/cathepsin B complex, and the DAPK-1 miniprotein (amino acids 836–947) can bind to this endogenous anchor (possibly cathepsin B), releasing cathepsin B from DAPK-1 and resulting in TNF–α-dependent DAPK-1 protein degradation and enhanced apoptosis.

Chapter Four Identification of an alternative transcript from DAPK-1 locus

4.1 Introduction

DAPK-1 is relatively large for a protein kinase, and its independent functional domains are involved in various regulatory activities. The DAPK-1 kinase domain is required to mediate cytoskeleton remodeling by phosphorylating MLC 2[23], inhibiting cell migration[150] and inducing membrane blebbing[125]. Furthermore, MAP1B interaction with the kinase domain of DAPK-1 stimulates membrane blebbing and autophagy[25]. The roles of its other functional domains in its regulatory effects are being characterized. For example, the death domain of DAPK-1 forms a docking site for its interaction with ERK, and is thus required for DAPK-1's proapoptotic effect in response to the MEK/ERK signaling pathway[77]. Moreover, a germline mutation in the death domain of DAPK-1 has been found to reduce intrinsic oligomerization of the death domain, disrupt the binding of ERK, and thus prevent MEK/ERK-induced apoptosis[131]. The death domain of DAPK-1 also promotes its interaction with the netrin-1 receptor UNC5H2, whose proapoptotic effect when unbound to netrin-1 is partially attenuated in the absence of DAPK-1[81]. The ankyrin-repeat region of DAPK-1 is required for its proper localization to the actin stress fibers[23] and for stable binding with DAPK-1's ubiquitin E3 ligase DIP-1 [62]. Recently, it was shown that the LAR interacts with the ankyrin-repeat region of DAPK-1 and dephosphorylates DAPK-1 at pY491 / 492 to stimulate its proapoptotic and antimigration activities[79]. There are many regions/minidomains on DAPK-1 without

an ascribed function, and it is likely that further biochemical characterization will result in a greater understanding of the DAPK-1 gene product in autophagic and apoptotic cell signaling.

In this part of my project, I identified an mRNA product of the DAPK-1 locus that encodes a small miniprotein (which I have named s-DAPK-1), that shares some domains with full-length DAPK-1: part of the ankyrin-repeat region, through to part of the cytoskeleton binding domain, but also includes with a unique tail extension of 42 amino acids that is not present in full-length DAPK-1. The functions of s-DAPK-1 compared to full-length DAPK-1 will be investigated. Furthermore, the roles of the unique tail of s-DAPK-1 in the regulation of its activity and stability will be investigated.

4.2 Identification of s-DAPK-1

Ankyrin repeats are versatile protein–protein interaction motifs[178], thus proteins that contain ankyrin repeats have the potential to cross-talk with the DAPK-1 pathway. Therefore, we evaluated the homology of the ankyrin-repeat region of DAPK-1 with other genes in the human genome using the NCBI nucleotide blast tool. One Homo sapiens cDNA was identified: FLJ45958 fis, clone PLACE7011559, from the NEDO human cDNA sequencing project. The start of this expression clone matches intron 13–14 of the DAPK-1 gene and stops on intron 20–21 (Figure 4.1A). The start codon, ATG, of this expression clone is located on the 10–12th base pairs of exon 15 within the DAPK-1 gene, which makes the translation of this clone in-frame with that of

DAPK-1 mRNA. After the start codon, this expression clone shares the same sequence as DAPK-1 mRNA through the end of exon 20, as indicated in Figure 4.1B, and its stop codon, TAG, is located on the 124–126th base pairs of intron 20–21 (Figure 4.1A). Thus, the first 295 amino acids of this 337 amino acid protein are identical to the region of the DAPK-1 protein from residues 447–743, whereas the last 42 amino acids are unique for this product (Figure 4.1B). These data suggest that this product is highly similar to and may be a splice variant of DAPK-1. Because of its smaller size as compared to full-length DAPK-1, we have named it short-DAPK-1 (s-DAPK-1).

The transcription of s-DAPK-1 was demonstrated further by RT-PCR using the Stratagene QPCR Human Reference Total RNA and the primers located on both ends of the coding region of s-DAPK-1 mRNA (Figure 4.2A). In order to determine the expression of s-DAPK-1, we compared its mRNA expression with that of DAPK-1 in three widely used tumour cell lines, and we saw a general correlation between full-length DAPK-1 and s-DAPK-1 mRNA levels (Figure 4.2B).

4.3 Cleavage of s-DAPK-1 on its tail region

To begin functional studies of s-DAPK-1, the s-DAPK-1 cDNA was reverse transcribed from the Stratagene QPCR Human Reference Total RNA and cloned into a Flag–Myc vector (Figure 4.3A), which contains an N-terminal Flag tag and a C-terminal Myc tag, and this was followed by expression in HCT116 p53+/+ cells. Two major transfected bands were observed: a 44 kDa upper band, and a 40 kDa lower

band (Figure 4.3B). In order to determine which band corresponded to s-DAPK-1, the C-terminal Myc tag was deleted (Figure 4.3A). Upon transfection, the same lower protein band was observed in the Flag–s-DAPK-1- and the Flag–s-DAPK-1-Myc-transfected cells, whereas the upper band in the Flag–s-DAPK-1 transfection lane was slightly smaller (Fig. 4.3C, lane 2 versus lane 1). This suggests that the depletion of the Myc tag only changes the size of the upper band, and that therefore the upper band represents the 'full-length' s-DAPK-1.

Since the upper band is full-length s-DAPK-1, the appearance of the 40 kDa lower band in both Flag-s-DAPK-1 and Flag-s-DAPK-1-Myc transfected cells suggests a cleavage on s-DAPK-1. This is further suggested by the *in vitro* cleavage assay, in which the purified GST–s-DAPK-1 was incubated with HCT116 p53+/+ cell lysates. With increasing amount of cell lysates, GST–s-DAPK-1 was cleaved *in vitro* at a faster rate than GST alone (Figure 4.4), supporting the existence of a protease that cleaves s-DAPK-1 protein *in vivo*. The reason why the cleavage band was not observed in this assay may be the rapid degradation of the purified protein from the cell lysate. When subjected to a longer exposure, the blot showed multiple bands below GST–s-DAPK-1, which may mask the actual cleavage band.

Two s-DAPK-1 deletion mutants, Flag-AO (Ankyrin repeat Only) and Flag-TD (Tail Deletion) were created (Figure 4.3A) to further investigate why the lower molecular mass protein was observed. Upon transfection, the Flag-TD vector produces only one major band of lower molecular mass (Figure 4.5, lane 3), which is similar to the 40 kDa lower band produced from the full-length s-DAPK-1 (Figure 4.5, lane 4 versus

lane 3). This suggests that the lower band might be a cleavage product of the full-length s-DAPK-1, and that the cleavage signal is within the C-terminal tail extension. The higher molecular mass protein band (~54 kDa) observed in Flag-s-DAPK-1 transfected cells (Figure 4.5, lane 4) might result from a covalent adduct resulting from ubiquitin-like modification; nevertheless, this apparent adduct is dependent upon the integrity of the C-terminal tail extension.

Having identified that the cleavage occurs within the tail region, I next investigated which sites within the tail are the critical targets for cleavage. Because the transfected Flag-TD vector is similar to the *in vivo* cleaved form of Flag–s-DAPK-1 in size, five tail mutants (TMs) of s-DAPK-1 were created to screen the first 10 amino acids on the tail for proteolytic susceptibility (Figure 4.6A). Upon transfection, only Flag-TM1 exhibited a loss of proteolytic band, and Flag-TM2 showed a weakened cleavage band (Figure 4.6B). These data suggest that the first two amino acids of the tail are critical for proteolytic susceptibility, and that the third and fourth amino acids are involved in the regulation of this cleavage. This also further fine-maps the site of cleavage, and indicates that the tail deletion Flag-TD may be used as a mimic of the *in vivo* processed form of full-length s-DAPK-1. Flag-TM3 surprisingly produced a specific shift in size under denaturing conditions, suggesting that the modification of the fifth amino acid on the tail may alter its secondary structure in denaturing polyacryl-amide gels or might yield an undefined covalent adduct (Figure 4.6B, lane 4).

As described in Chapter Three, cathepsin B is capable of cleaving DAPK-1. Although the binding site of cathepsin B does not lie on the ankyrin repeats region of DAPK-1, it is still possible that cathepsin B can interact with this region on DAPK-1. Therefore, I set out to test whether the cleavage of the tail region of s-DAPK-1 is induced by cathepsin B by treating the Flag-s-DAPK-1 transfected cells with cathepsin B inhibitor. No difference of the s-DAPK-1 cleavage pattern was observed between the treated (Figure 4.7, lane 3) and the untreated cells (Figure 4.7, lane 2), suggesting cathepsin B is not responsible for the observed cleavage of s-DAPK-1.

4.4 Functions of s-DAPK-1

The proapoptotic effect in response to MEK⁄ERK signaling and the membrane-blebbing-promoting effect upon transfection are two readily measurable functions of DAPK-1[77, 125, 131]. Therefore, we set out to define the role of s-DAPK-1 in these two pathways. Unlike DAPK-1, overexpression of s-DAPK-1 does not induce PARP cleavage in response to the MEK⁄ERK signal input (Figure 4.8, lane 6 versus lane 5). Interestingly, when co-transfected with ERK, the expression level of DAPK-1 reduces dramatically, while that of s-DAPK-1 remains the same, suggesting that ERK may regulate the degradation of DAPK-1 via its interaction with the death domain of DAPK-1. Further research will be needed to investigate this ERK-indued reduction of DAPK-1 in the future. We next compared the effect s-DAPK-1 in membrane blebbing with full-length DAPK-1. The transfection of Flag–s-DAPK-1 was able to cause significant membrane blebbing, however the effect was weaker than observed with full-length DAPK-1 (Figure 4.9).

4.5 Regulation of s-DAPK-1 by its tail region

Since s-DAPK-1 exhibits biological activity in the membrane-blebbing assay, I evaluated the activity of the mutant with the tail deletion (Flag-TD) and the protease-resistant substitution (Flag-TM1). When compared to full-length s-DAPK-1, Flag-TM1 showed a reduced membrane-blebbing effect (Figure 4.10), whereas Flag-TD was almost as active as full-length DAPK-1 (Figure 4.10). These data indicate that the 'tail' of s-DAPK-1 has a negative regulatory function with regard to s-DAPK-1 activity, and that its removal serves to enhance the membrane-blebbing effect of s-DAPK-1.

To determine the mechanism that underlies the effect of the tail on the membrane-blebbing-promoting ability of s-DAPK-1, the localization and half-lives of the full-length s-DAPK-1, Flag-TD and Flag-TM1 were examined. As compared to DAPK-1, s-DAPK-1 shows more specific localization in the cytoplasm (Figure 4.11). TD predominantly localizes around the nucleus, and TM1 spreads throughout the cytosol and tends to form some 'aggregating bodies' (Figure 4.11). It is still not clear what these bodies are. Co-staining of TM1 with other speicifc antibodies for distinct structural bodies such as lysosome may help to clarify this in the future. Moreover, the stability of TD is much higher than those of s-DAPK-1 and Flag-TM1 (Figure 4.12 A–E), suggesting that the increased membrane-blebbing function of TD may be due to its increased stability (Figure 4.12E).

4.6 Conclusion

DAPK-1 is a stress-regulated kinase whose downstream functions are linked to a variety of diverse signalling pathways, including ERK kinase activation, autophagic signalling, and oncogene-mediated p53 transcriptional responses. DAPK-1 is also regulated by TNF-α signalling, RSK, and L, which alter the specific activity of the kinase as a prosurvival or proapoptotic factor. Although the DAPK-1 protein is now known to be regulated post-translationally, the gene is also subject to methylation, which has the potential to reduce the specific activity of DAPK-1[43]. In this work, I have identified another function of the DAPK-1 locus: it can express a message whose product possesses part of DAPK-1's ankyrin-repeat region, P-loop, and cytoskeletal binding domain, and a unique tail of 42 amino acids encoded by intron 20–21 of the DAPK-1 gene. In our examination of DAPK-1 and s-DAPK-1 expression using real-time PCR, we found a significant correlation in their expression, whether using cancer cell lines or normal human tissues, suggesting that mRNA from the locus is coordinately produced. Future work will be required to understand the regulation of the translation of these mRNAs and whether stress-regulated signaling pathways regulate these two proteins differently in cell growth control.

Despite the many functions attributed to DAPK-1, the two standard cellular assays for defining its function include proapoptotic pathways and membrane blebbing. Therefore, we have examined the ability of the s-DAPK-1 protein to play a role in these two processes. We found that although s-DAPK-1 cannot induce apoptosis in response to the activated MEK⁄ERK signal like DAPK-1, it can mimic DAPK-1 and

induce membrane blebbing. A function was also attributed to the unique tail of s-DAPK-1: it can regulate the localization and stability of the protein and can be subjected to proteolytic cleavage in cells. Thus proteolytic cleavage of the tail relocalizes s-DAPK-1 to increase its stability and membrane blebbing activity (Figure 4.12).

DAPK-1 has been shown to induce membrane blebbing and promote the formation of actin stress fibers and disassembly of focal adhesions[22]. These biological events can occur in cooperation with MAP1B[25], for which the ability of DAPK-1 to phosphorylate MLC 2[23] and tropomyosin-1[73] are considered to be important. However, it was also shown that the ankyrin-repeat region deletion mutant of DAPK-1 mislocalized to focal contacts and lost its ability to induce morphological changes[23], indicating a functional role of this region in DAPK-1's activity. This might explain the membrane-blebbing-promoting effect of s-DAPK-1, as it shares a portion of the ankyrin-repeat region of DAPK-1. However, the functional significance of the s-DAPK-1-induced membrane blebs is not clear, as s-DAPK-1 cannot induce MEK/ERK-stimulated apoptotic signals (Figure 4.8). A recent study has provided a novel insight into membrane blebbing[138]; it was shown that membrane blebbing is due to the reassembly of the contractile cortex. Therefore, distinct from the alternative models showing that membrane blebbing is linked to autophagic or cell death pathways, membrane blebbing may also be part of a normal cell division processes such as cytokinesis. Considering that ankyrin B plays an important role in the membrane-blebbing process[138], DAPK-1 and s-DAPK-1 may be able to interact with ankyrin B via their ankyrin repeats and thus promote membrane blebbing. Although

these data provide an explanation for the significance of the ankyrin-repeat region of DAPK-1 in inducing morphological changes, they do not necessarily indicate that DAPK-1- or s-DAPK-1-induced membrane blebbing is part of a normal cell division cycle. Considering that physiological membrane blebbing is a transient process[138], it also remains possible that DAPK-1 and s-DAPK-1 arrest the cells at the blebbing stage and thus halt the cell division cycle. Therefore, the actual biological significance of the s-DAPK-1- and DAPK-1-induced membrane blebbing requires further investigation.

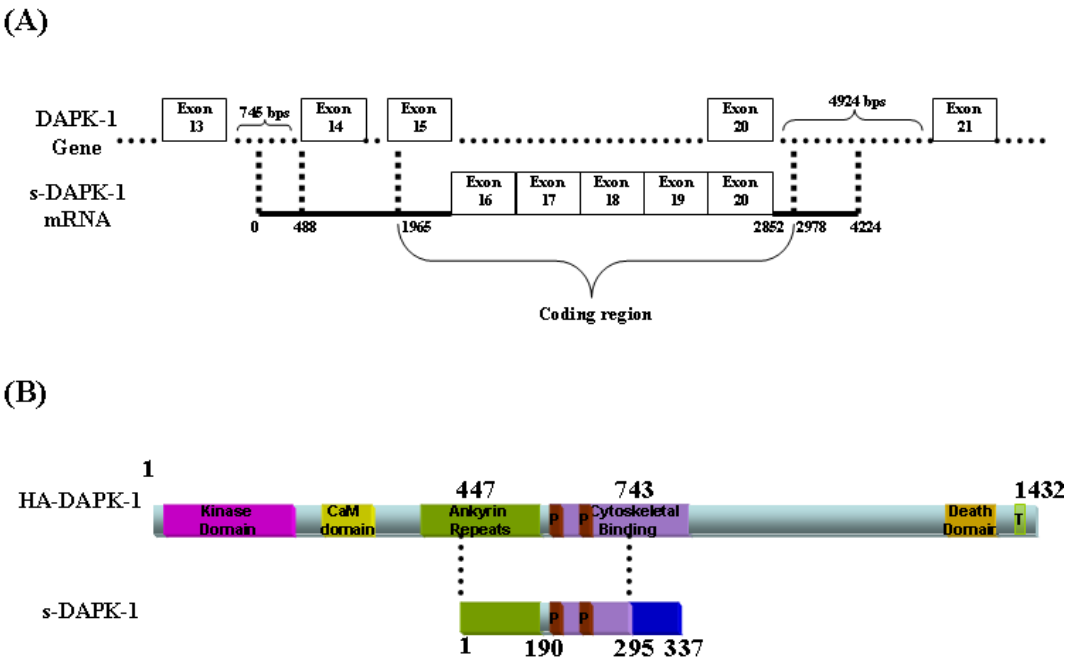

Figure 4.1 Identification of a small transcript from the DAPK-1 locus. (A) A schematic map of s-DAPK-1 mRNA in relation to the DAPK-1 gene structure. The mRNA of s-DAPK-1 starts in intron 13–14 of the DAPK-1 gene. Its coding region starts from the 10th base pair on exon 15 of the DAPK-1 gene, and shares the same splicing as full-length DAPK-1 through the rest of exons 15, 16, 17, 18, 19 and 20. s-DAPK-1's coding region stops at the 126th base pair of intron 20–21 of the DAPK-1 gene, and the 3'-UTR extends through the middle of intron 20–21. **(B) Comparison of the protein sequences of DAPK-1 and s-DAPK-1.** The first 295 amino acids of s-DAPK-1 are identical to amino acids 447–743 of full-length DAPK-1; however, the last 42 amino acids comprise a unique tail.

(A)

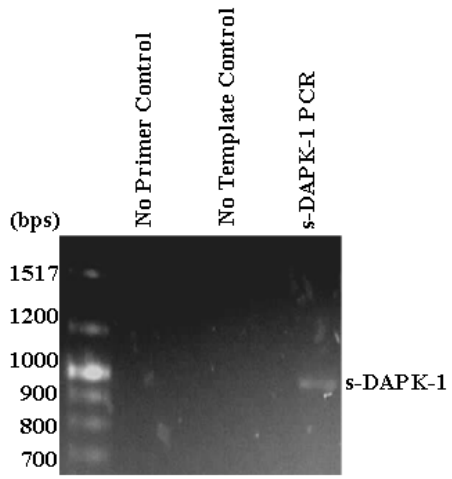

(B)

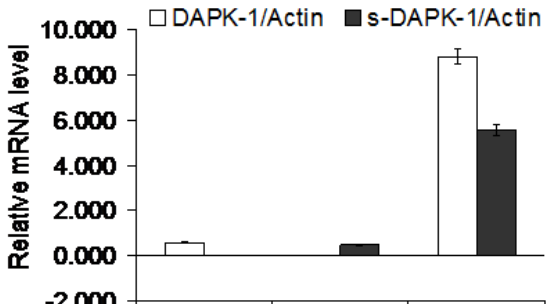

	HCT116	A375	HEK293
DAPK-1/Actin	0.575	0.012	8.793
s-DAPK-1/Actin	0.000	0.455	5.517

Figure 4.2 Expression of s-DAPK-1 mRNA. (A) Identification of s-DAPK-1 mRNA. RT-PCR was performed using the Stratagene QPCR Human Reference Total RNA, and the products were subjected to electrophoresis and staining with ethidium bromide. **(B) mRNA level test using SYBR Green real-time PCR.** The relative mRNA level is depicted as a ratio of DAPK-1／s-DAPK-1 to actin.

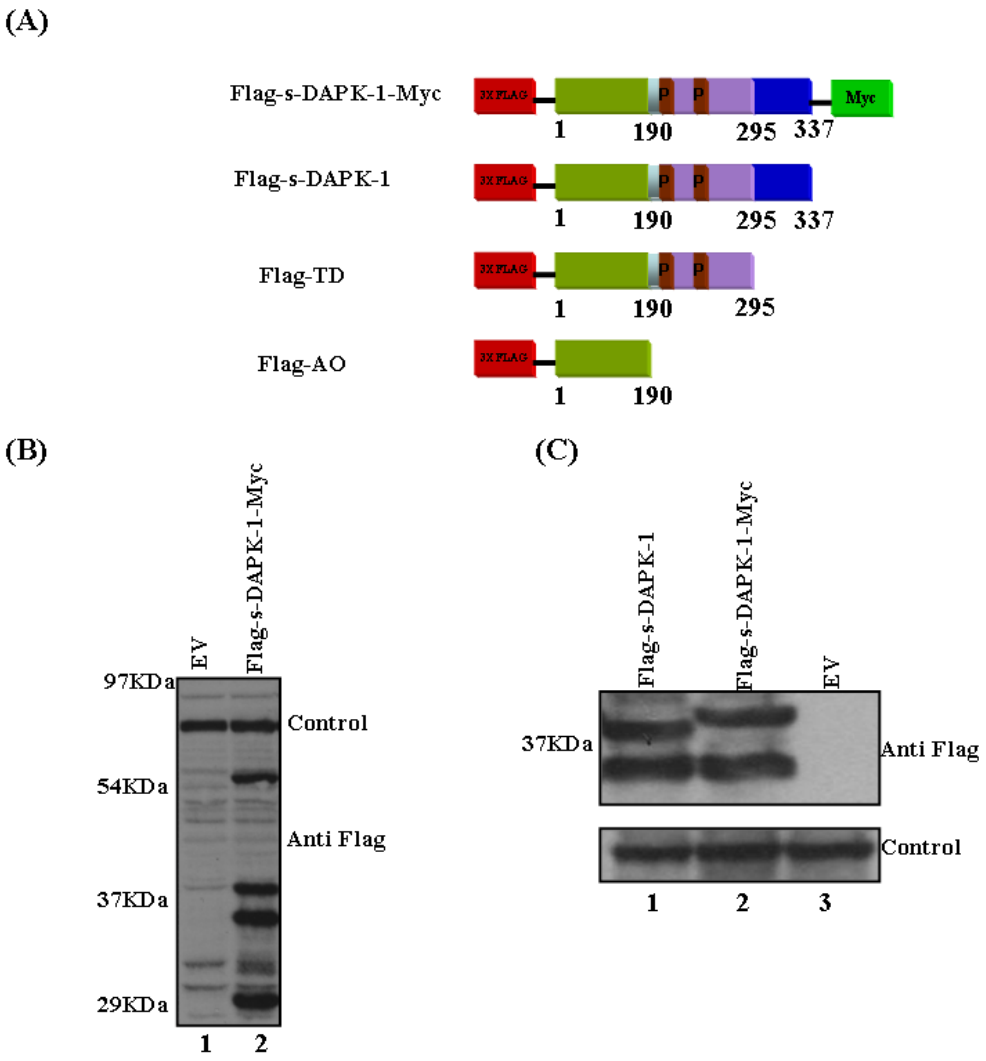

Figure 4.3 Identification of a proteolytic cleavage of s-DAPK-1 protein. (A) A schematic diagram of the Flag–Myc vector with the s-DAPK-1 clone and its mutants created by site-directed mutagenesis. The vector encoding the s-DAPK-1 with a 42 amino acid tail deletion is named Flag-TD. The vector encoding only the ankyrin repeats region of s-DAPK-1 is named Flag-AO. **(B,C) Transfected s-DAPK-1 and its mutants identified a cleavage on s-DAPK-1.** HCT116 p53+/+ cells were transfected with empty Flag vector (EV) or the respective vectors, as indicated, for 24 h prior to harvesting. Expression of the ectopically expressed s-DAPK-1 and its mutants was detected using an antibody to Flag tag. The non-specific band in 4.3 (B) was used as the control. **These experiments have been performed more than 3 times.**

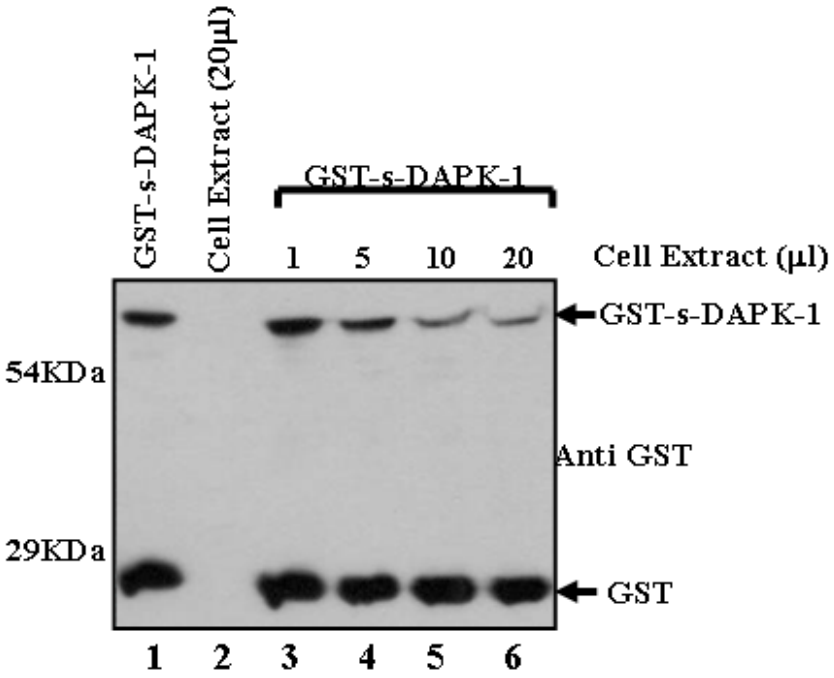

Figure 4.4 In vitro cleavage of purified GST–s-DAPK-1. Recombinant GST–s-DAPK-1 was purified from Bl21 cells and incubated at 30^{o}C with increasing amounts of HCT116 p53 +/+ cell lysates (0, 1, 5, 10 and 20 μL). The sample mixtures after in vitro cleavage were subjected to immunoblotting as indicated. **This experiment has been performed more than 3 times.**

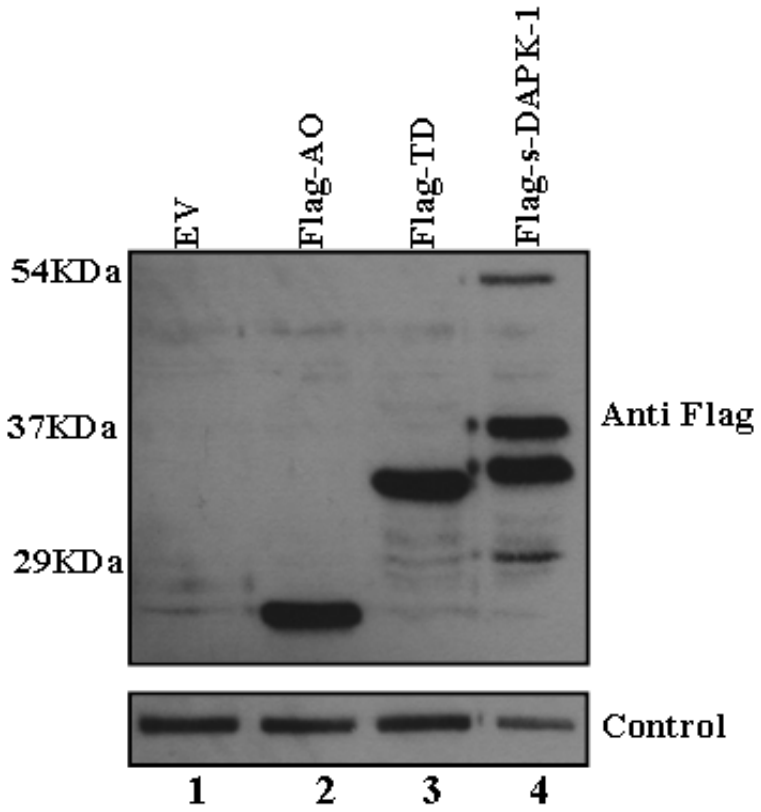

Figure 4.5 Identification of the cleavage site of s-DAPK-1 within its tail. Transfected s-DAPK-1 and its mutants identified a cleavage within its tail. HCT116 p53 +/+ cells were transfected with empty Flag vector (EV) or Flag-s-DAPK-1 and its mutants Flag-AO (Ankyrin repeat only) and Flag-TD (Tail deletion) for 24 h prior to harvesting. Expression of the ectopically expressed s-DAPK-1 and its mutants was detected using an antibody to Flag tag. The non-specific band as shown in 4.3 (B) was used as the control. **This experiment has been performed more than 3 times.**

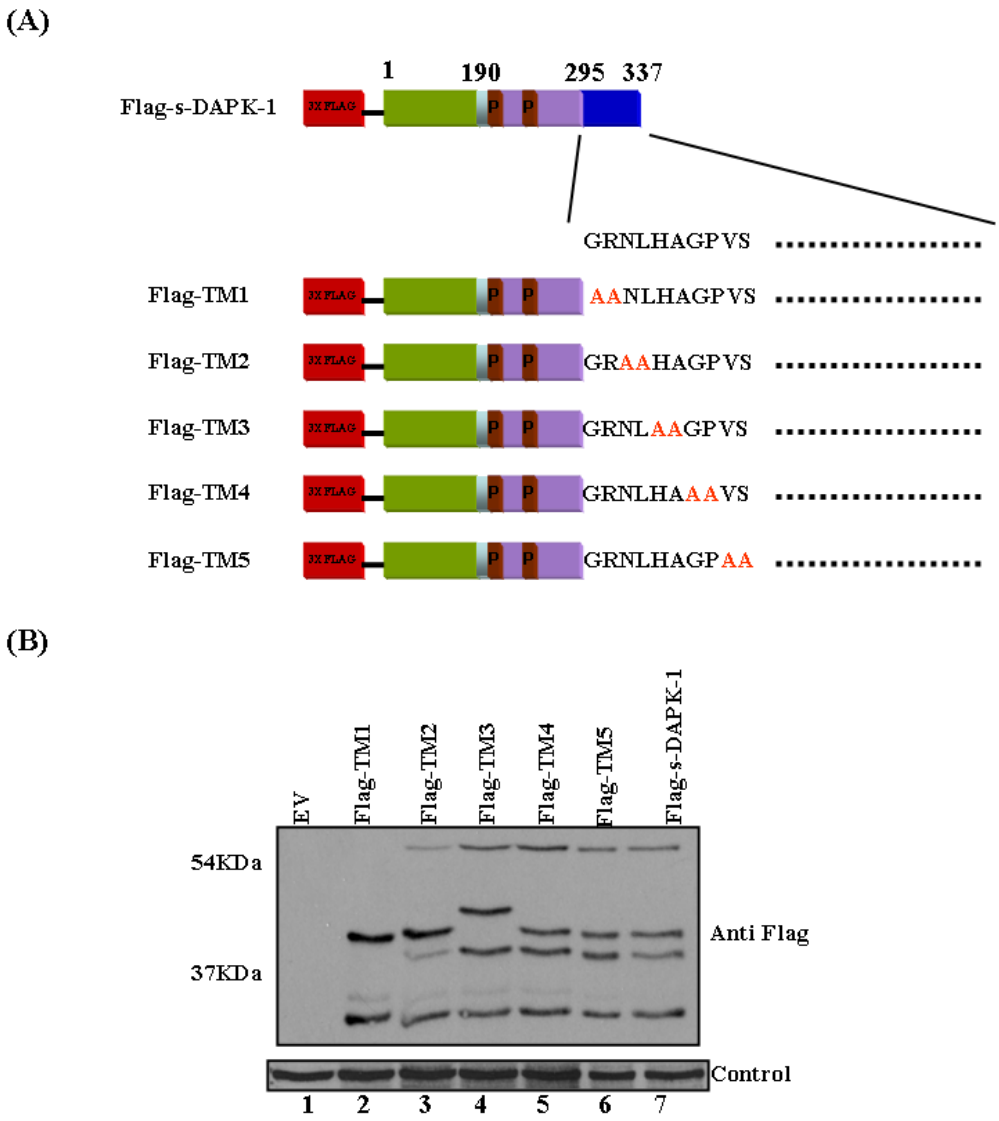

Figure 4.6 Identification of the critical sites for proteolytic cleavage of the C-terminal tail of s-DAPK-1. (A) A schematic diagram of the tail mutants of s-DAPK-1 created by site-directed mutagenesis. (B) Expression of the tail mutants of s-DAPK-1. HCT116 p53 +/+ cells were transfected with empty Flag vector (EV) or the respective vectors, as indicated, for 24 h prior to harvesting. Expression of the s-DAPK-1 tail mutants was detected by immunoblotting. The non-specific band as shown in 4.3 (B) was used as the control. **This experiment has been performed more than 3 times.**

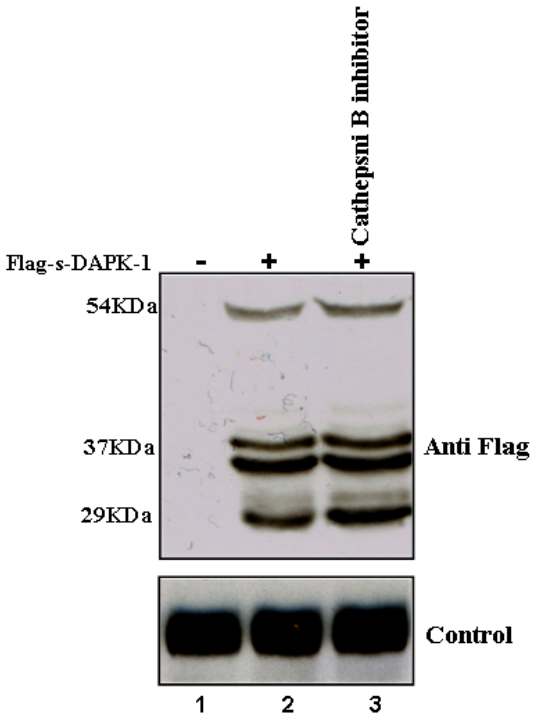

Figure 4.7 Cleavage of s-DAPK-1 is not inhibited by cathepsin B inhibitor. HCT116 p53 +/+ cells were transfected with empty Flag vector (-) or the Flag-s-DAPK-1 vectors for 24h and treated with cathepsin B inhibitor for 6h prior to harvesting. The Flag-s-DAPK-1 protein was detected by immunoblotting. The non-specific band as shown in 4.3 (B) was used as the control. **This experiment has been performed more than 3 times.**

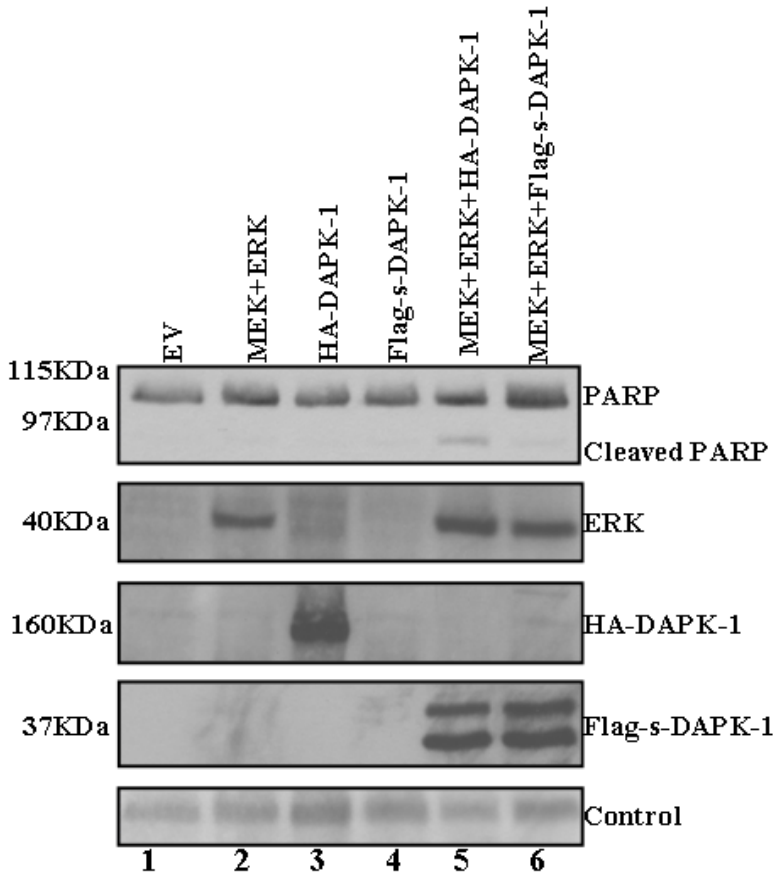

Figure 4.8 s-DAPK-1 does not induce apoptosis in response to MEK／ERK signaling. HEK293 cells were transfected with the PCDNA3 (EV) or the respective vectors, as indicated, for 24 h prior to harvesting. The unprocessed form and cleaved form of PARP were detected with a PARP-specific antibody.β-actin was used as the control. **This experiment has been observed more than 3 times.**

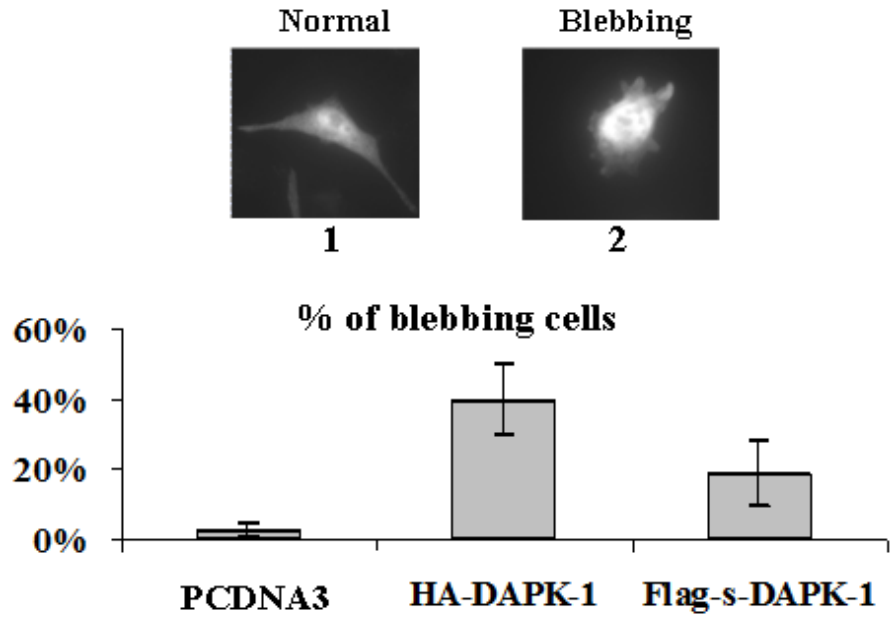

Figure 4.9 s-DAPK-1 induces membrane blebbing. A375 cells were transfected with GFP in addition to the respective vectors as indicated, and evaluated for membrane blebbing in transfected cells as described previously[125] . The top panel shows the normal (1) and the blebbing (2) morphology. The bar graph in the bottom panel summarizes the mean percentage of blebbing cells upon each transfection. Each experiment was repeated four times. **This experiment has been performed more than 3 times.**

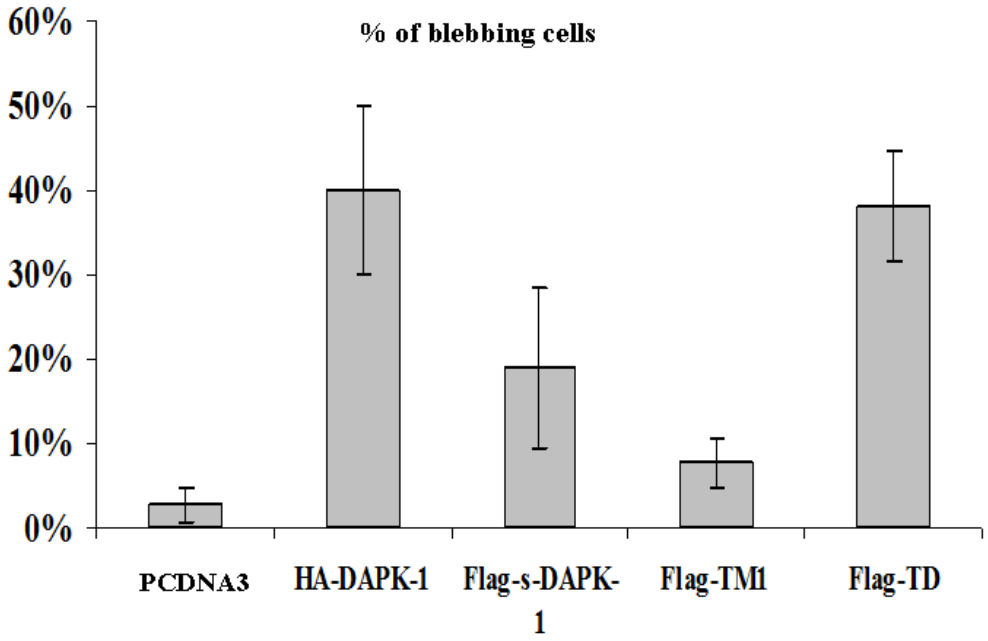

Figure 4.10 The C-terminal tail of s-DAPK-1 regulates its membrane-blebbing function. A375 cells were transfected with GFP in addition to the respective vectors as indicated (wt, TM1, and TD) and evaluated for membrane blebbing in transfected cells as described previously[125]. The bar graph summarizes the mean percentage of blebbing cells upon each transfection. Each experiment was repeated four times. **This experiment has been performed more than 3 times.**

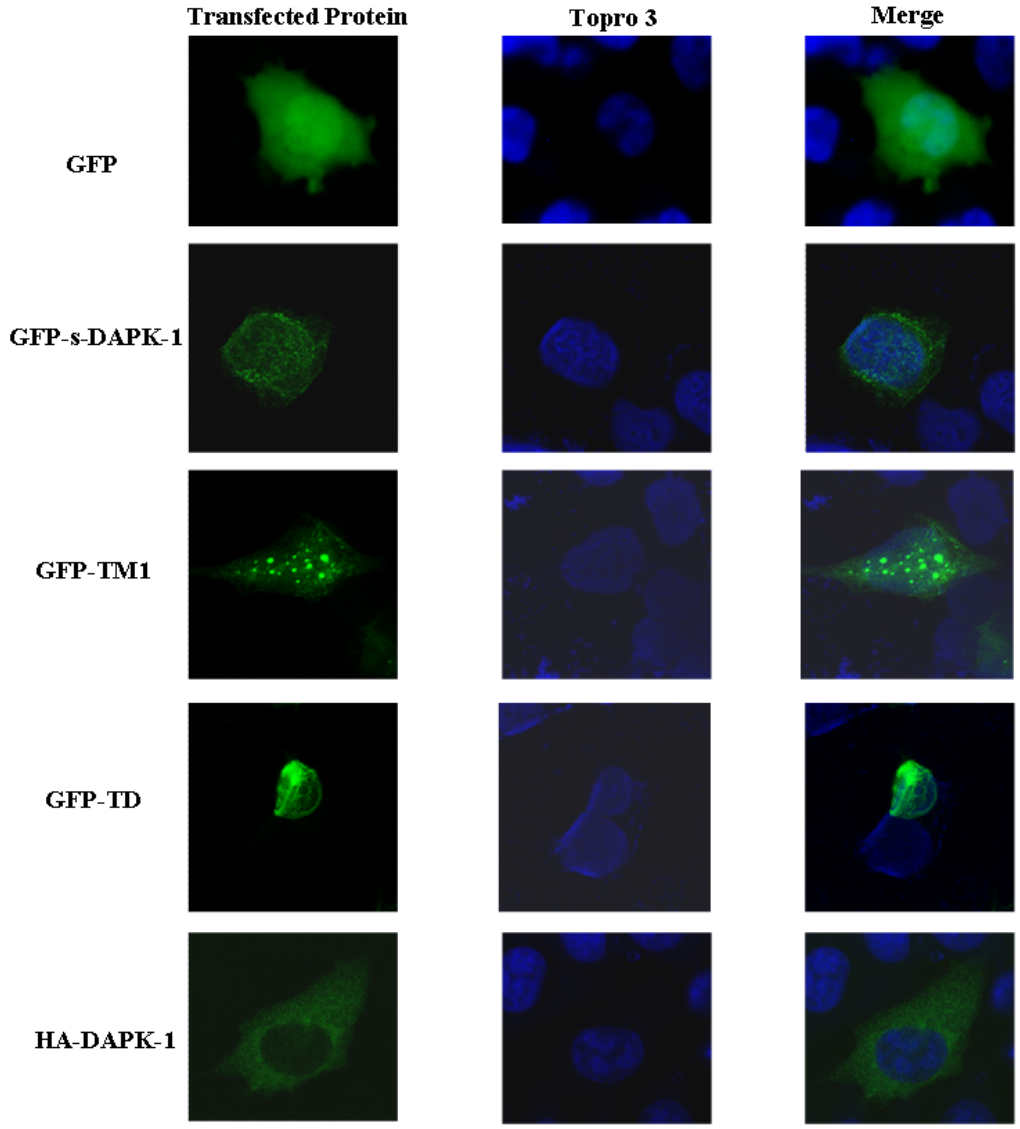

Figure 4.11 The C-terminal tail of s-DAPK-1 regulates its localization. A375 cells were transfected with the respective vectors as indicated (GFP control, GFP-wt s-DAPK, GFP-TM1, GFP-TD, and HA-DAPK-1). The localization of GFP and GFP-tagged proteins were detected using fluorescent microscopy. HA–DAPK-1 protein expression was detected using an antibody to HA tag. The nucleus of cells were stained with Topro3. **This experiment has been performed more than 3 times.**

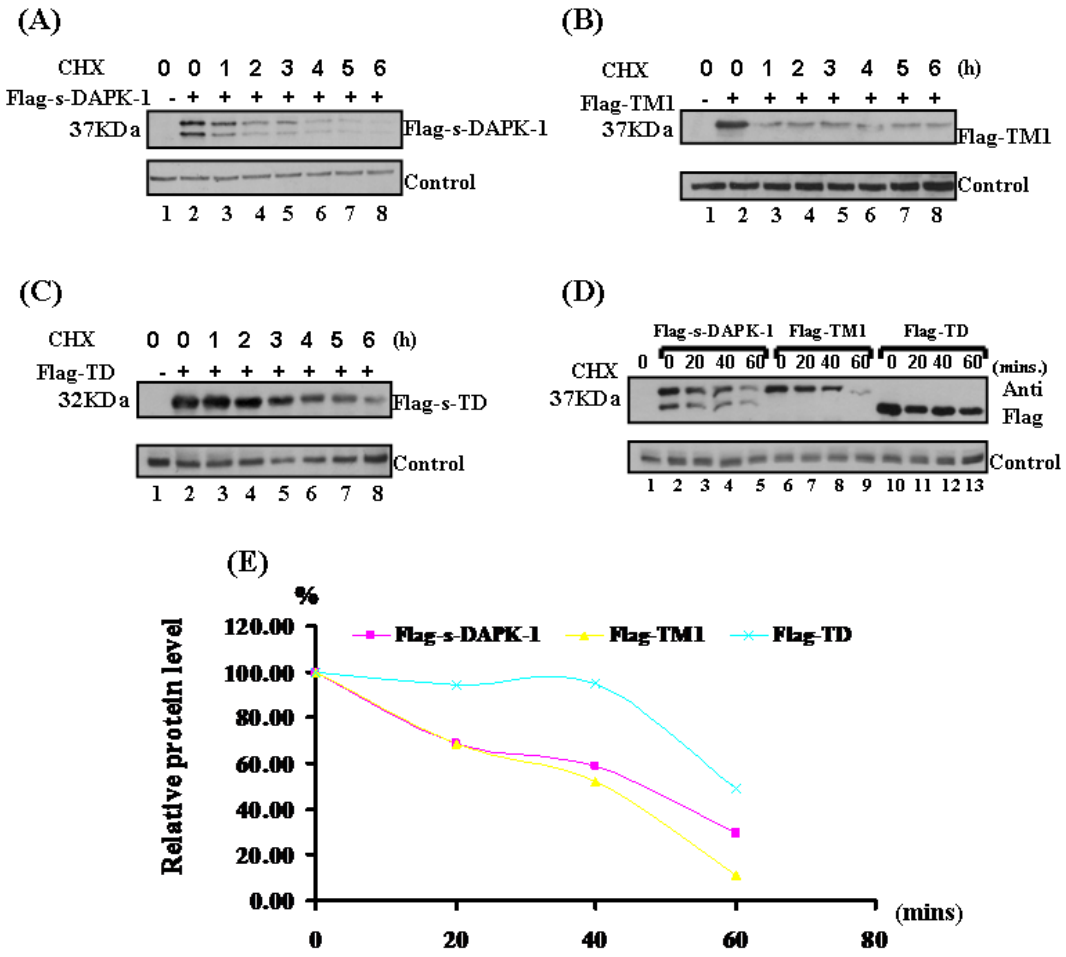

Figure 4.12 The C-terminal tail of s-DAPK-1 regulates its stability. (A–D) HCT116 p53 +/+ cells were transfected with empty Flag vector (-) or the respective vectors as indicated for 24 h, then treated with cycloheximide for the indicated times, prior to harvesting. Expression of the Flag-tagged proteins was evaluated by immunoblotting. The non-specific band as shown in 4.3 (B) was used as the control. Quantification of the level of Flag-s-DAPK-1, Flag-TD and Flag-TM1 in (D) is summarized in (E). **These experiments have been performed more than 3 times.**

Chapter Five s-DAPK-1 induces lysosome-dependent DAPK-1 destabilization

5.1 Introduction

In unstressed cells DAPK-1 is relatively stable [151]. DAPK-1 stability can be regulated through the action of two ubiquitin E3 ligases, MIB1 and CHIP, which target DAPK-1 for proteasomal degradation [64]. It has been demonstrated previously that reduction of either MIB1 or CHIP can efficiently rescue the DAPK-1 degradation induced by the binding of Geldanamycin to Hsp90[64], however there is no evidence that either of these E3s control the steady state levels of DAPK-1 protein, or are responsible for the DAPK-1 degradation in response to stresses such as TNF-α or ceramide [62, 151]. Therefore, it is possible that other ubiquitin E3s or alternative degradation pathways can regulate the degradation of DAPK-1 protein.

As shown in Chapter Four, the splice variant of DAPK-1, s-DAPK-1, can mimic the membrane blebbing promoting ability of full-length DAPK-1, which is regulated by the tail region of s-DAPK-1. I next set out to investigate whether s-DAPK-1 can influence the activity or expression of full-length DAPK-1 when co-expressed with DAPK-1. In this chapter, I show that s-DAPK-1 is able to promote the degradation of full-length DAPK-1, which is dependent upon the ankyrin repeats region of s-DAPK-1 and the kinase domain of DAPK-1. In addition, s-DAPK-1 does not target DAPK-1 for proteasomal degradation, although s-DAPK-1 itself is rapidly degraded by the proteasome. These data suggest that one function for s-DAPK-1 is to regulate

the steady-state levels of full-length DAPK-1 and implicates a proteasome-independent degradation pathway for DAPK-1.

5.2 s-DAPK-1 decreases DAPK-1 level

The Ankyrin repeat is a common protein-protein interaction domain in a wide range of proteins[178]. As both s-DAPK-1 and DAPK-1 contain ankyrin repeats, I first set out to investigate whether they can interact with each other using immunoprecipitation. Although GFP-s-DAPK-1 was successfully immunoprecipitated by the GFP antibody, no co-immunoprecipitated HA-DAPK-1 was detected in s-DAPK-1 immune complexes (Figure 5.1). These data indicate that s-DAPK-1 and DAPK-1 cannot form stable immune-complexes. However, a significant decrease in HA-DAPK-1 protein expression was observed in direct lysates after GFP-s-DAPK-1 was co-transfected into cells (Figure 5.1, lane 4 vs lane 2), suggesting that s-DAPK-1 can downregulate DAPK-1 protein levels. This is further confirmed by a titration experiment showing increasing amounts of GFP-s-DAPK-1 leads to a reduction of HA-DAPK-1 protein (Figure 5.2).

5.3 Domains responsible for s-DAPK-1 mediated DAPK-1 decrease

Using deletion mutants of s-DAPK-1, I have demonstrated in Chapter Four that the tail region of s-DAPK-1 attenuates its ability to induce membrane blebbing, most likely due to the decreased stability of the full-length s-DAPK-1 compared to its tail-

deleted form. Therefore, we next investigated which domain on s-DAPK-1 can influence its new function to downregulate DAPK-1 using the TD and AO mutants of s-DAPK-1 (Figure 4.3). Interestingly, although the ankyrin repeats region of s-DAPK-1 does not mediate the interaction between DAPK-1 and s-DAPK-1, it is capable of inducing the decrease in DAPK-1 protein levels (Figure 5.3A). To further confirm this effect and find out whether the recombinant polypeptide tags influence this new function of s-DAPK-1, HA-DAPK-1 was co-transfected with s-DAPK-1 and the same TD and AO mutants in Flag-tagged vectors, which resulted in a similar destabilization of HA-DAPK-1 protein (Figure 5.3B). These data suggest the ankyrin repeat region of s-DAPK-1 is critical for its ability to mediate the downregulation of DAPK-1 protein. Moreover, the TD mutant is more able to destabilize DAPK-1 protein level compared to full-length s-DAPK-1, which is consistent with our previous finding that the tail possesses an inhibitory effect towards s-DAPK-1 activity.

Since the ankryin repeat region on s-DAPK-1 is identical to part of the ankyrin repeats region of DAPK-1, and is important for its ability to downregulate DAPK-1 protein (Figure 5.3), it is of interest to see whether the ankyrin repeat region on DAPK-1 is also critical for its regulation by s-DAPK-1. Two deletion mutants of DAPK-1 HA-1-378 (containing the end of CaM binding region of DAPK-1) and HA-1-641 (containing the end of ankyrin repeat region of DAPK-1) (Figure 3.8B) were co-transfected with GFP-s-DAPK-1. Surprisingly, s-DAPK-1 not only decreases the level of the DAPK-1(1-641) mutant, but also that of the DAPK-1(1-378) mutant (Figure 5.4). As this recombinant DAPK-1 deletion mutant 1-378 does

not contain the ankyrin repeat region, these data suggest that the determinant responsible for s-DAPK-1 induced downregulation of DAPK-1 lies within the DAPK-1 core kinase domain.

5.4 s-DAPK-1 targets DAPK-1 for lysosome-dependent degradation

In order to determine the mechanisms underlying this s-DAPK-1 mediated downregulation of DAPK-1 protein, we investigated the half-lives of DAPK-1 in the presence or absence of s-DAPK-1 using the translation inhibitor cycloheximide. As is shown, DAPK-1 by itself is still very stable after 4 hours of treatment with cycloheximide (Figure 5.5A), which is consistent with previous findings showing DAPK-1 is stable in Chapter Three. When s-DAPK-1 was co-transfected into cells with DAPK-1, the stability of DAPK-1 was reduced substantially after 4-hour treatment of cycloheximide (Figure 5.5B), suggesting s-DAPK-1 could downregulate DAPK-1 by stimulating its degradation. Interestingly, although s-DAPK-1 was depleted by cycloheximide after around 1h treatment (Figure 5.5B), DAPK-1 level continued to drop afterwards, which again suggests that s-DAPK-1 mediates the degradation of DAPK-1 protein via an indirect pathway rather than direct binding to it.

As discussed in Chapter One, lysosomal and ubiquitin-proteasomal degradation pathways are the two pathways responsible for protein destruction inside cells and the latter usually applies to short half-life proteins[50]. Therefore, we set out to test

whether s-DAPK-1 promotes DAPK-1 degradation by targeting DAPK-1 towards the proteasome using the proteasome inhibitor MG132. MG132 greatly enhanced the level of s-DAPK-1 (Figure 5.6), which suggests s-DAPK-1 itself is degraded by proteasome, and is consistent with its rapid turnover (Figure 5.5B). However, MG132 didn't rescue DAPK-1 from s-DAPK-1 mediated degradation (Figure 5.6), implicating an alternative proteasome-independent degradation pathway for DAPK-1 by s-DAPK-1.

Next I used the lysosome inhibitor chloroquine instead of MG132 in the same experiments to test whether this alternative degradation pathway for DAPK-1 is via lysosome. Chloroquine successfully rescues DAPK-1 from s-DAPK-1 induced degradation while has little effect on s-DAPK-1 (Figure 5.7, lane 5 vs lane 4). Interestingly, even in the absence of s-DAPK-1, chloroquine greatly enhanced the level of DAPK-1 (Figure 5.7, lane 3 vs lane 2), suggesting this lysosomal degradation pathway is important in regulating the steady state of DAPK-1.

5.5 Conclusion

An interesting observation we found is that the *in vivo* cleavage of the tail region of s-DAPK-1 is reduced substantially when s-DAPK-1 is cloned into GFP vectors and expressed in cells (Figure 5.3, lane 5 in (A) vs lane 5 in (B)). Previous reports have shown that protein tags are capable of changing the conformational structures of their fusion proteins[179, 180]. The inhibition of the proteolytic cleavage of the tail region of GFP-s-DAPK-1 in *vivo* may be due to the conformational changes brought by the

much bigger GFP tag compared to Flag tag, which masks the sites for cleavage on the tail and prevent the protease from binding. Alternatively, GFP has been reported to have some toxic effects in some biological assays[181] and therefore may change the signalling networks that control the s-DAPK proteolytic processing pathway.

In this study, we have demonstrated that s-DAPK-1 protein can be turned over relatively rapidly (Figure 5.5B) and be degraded by a proteasome-dependent pathway (Figure 5.6), which is consistent with Chapter Four showing s-DAPK-1 is unstable. The DAPK-1 ubiquitin E3 ligase, MIB1, binds to the ankyrin repeats region of DAPK-1 composed of 265 amino acids[62], the last 190 of which consist of the ankyrin repeats region of s-DAPK-1. Therefore, it remains possible that MIB1 might be the ubiquitin E3 ligase that targets s-DAPK-1 for proteasomal degradation. If so, s-DAPK-1 may actually protect DAPK-1 from degradation when MIB1 become the main factor activated to degrade DAPK-1 under certain stresses. Such potential stresses implicated in MIB1 function are not yet defined.

The ankyrin repeats region of s-DAPK-1 are sufficient to promote the degradation of DAPK-1 (Figure 5.3). Ankyrin repeat containing proteins are widely expressed in cells, and some of them are even contained within ubiquitin E3 ligases such as the HECT domain and ankyrin repeat containing, E3 ubiquitin protein ligase 1 (HACE1)[182]. It is possible that s-DAPK-1 can crosstalk with some of these ankyrin repeat containing proteins and actually activate a general rather than a DAPK-1 specific degradation pathway. Therefore, it will be interesting to investigate whether s-DAPK-1 can affect the stability of other proteins in the cell. Further, as a tumour

suppressor, the expression level of DAPK-1 is very important for growth suppression in some cancer types[15]. Under certain stresses such as that induced by TNF-α, DAPK-1 actually acts as an anti-apoptotic factor and is targeted for degradation [151]. Our study provides a new angle for studying the regulation of DAPK-1 protein degradation and suggests a potentially central role for s-DAPK-1 in DAPK-1 biology.

Another ubiquitin E3 ligase, CHIP, binds to DAPK-1 via Heat Shock protein 90 (Hsp90), which recognizes the kinase domain of DAPK-1[78]. The fact that the kinase domain of DAPK-1 is responsible for s-DAPK-1 mediated DAPK-1 degradation (Figure 5.4) suggests s-DAPK-1 might function via a CHIP-dependent pathway. However, the proteasome inhibitor MG132 cannot rescue DAPK-1 from s-DAPK-1 induced degradation (Figure 5.6), suggesting s-DAPK-1 doesn't degrade DAPK-1 through CHIP-proteasome pathway, and implicating the existence of an alternative proteasome independent degradation pathway for DAPK-1. Considering the relatively high stability of DAPK-1 protein [62], it is likely that there is a proteasomal-independent and lysosomal-mediated degradation pathway regulating the steady state levels of DAPK-1 protein, which is confirmed by the observation that chloroquine stabilized DAPK-1 in the absence and presence of s-DAPK-1 (Figure 5.7).

Interestingly, even in the absence of s-DAPK-1, MG132 doesn't seem to greatly stabilize DAPK-1 protein (Figure 5.6, lane 3 vs lane 2). This is different from what is demonstrated in Chapter Three that MG132 can stabilize DAPK-1 protein and induce high molecular mass adducts in a denaturing polyacrylamide gel, which may be due to the difference of endogenous and exogenous DAPK-1 proteins used in each

experiment. Moreover, the effect of MG132 on DAPK-1 protein levels may vary in different tumour cell lines, for tumour cell lines could lose or gain degradation pathways because of the different mutations occurring in each cell line.

In addition, it has been reported recently that inhibition of the proteasome degradation pathway leads to activation of autophagy[183]. Moreover, DAPK-1 was found to actively participate in the induction of autophagy, partially through binding to its interactive partner MAP1B[25]. Therefore, it is possible that MG132 activates an additional autophagy-lysosomal degradation pathway for the destruction of DAPK-1, which can engulf the ubiquitinated DAPK-1 created by the inhibition of proteasome. Thus, it still can not be ruled out that CHIP-proteasome degradation pathway is involved in s-DAPK-1 mediated DAPK-1 degradation and MG132 does stop some degradation pathways for DAPK-1. In order to better understand the degradation of DAPK-1, further experiments will be required to investigate the degradation pathways for DAPK-1 at mechanistic level.

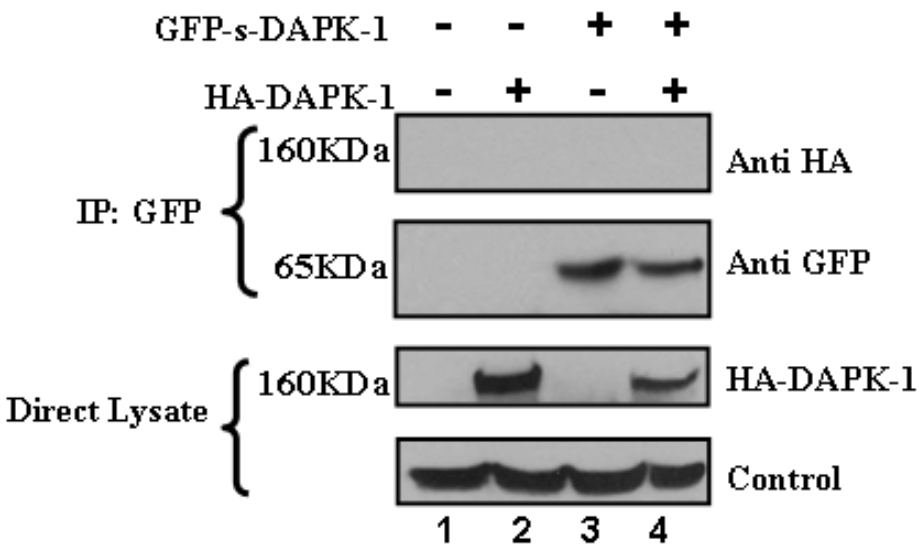

Figure 5.1 s-DAPK-1 doesn't bind to DAPK-1, but decreases its level. A375 cells were transfected with PCDNA3 (-) or the respective vectors as indicated, for 24h, prior to harvesting. The lysates were subjected to immunoprecipitation with a GFP antibody and then probed with anti-HA and anti-GFP antibody. Expression of HA-DAPK-1 and GFP-s-DAPK-1 were evaluated by immunoblotting. The non-specific band as shown in Figure 3.8 (A) was used as the loading control. **This experiment has been performed more than 3 times.**

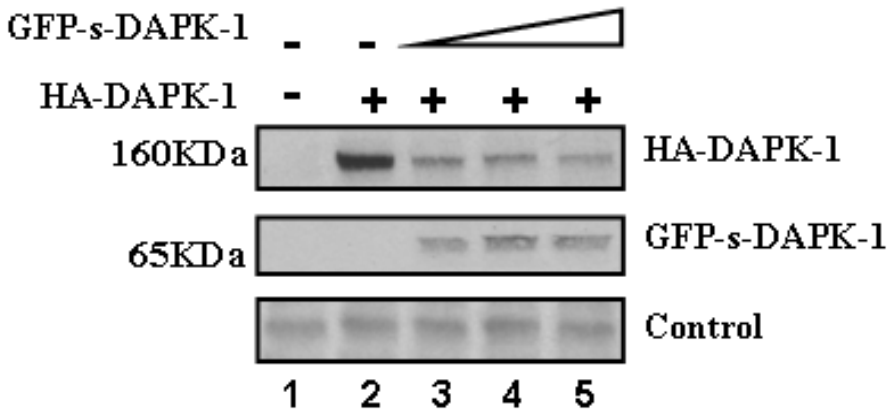

Figure 5.2 Titration of s-DAPK-1 with DAPK-1 overexpression. A375 cells were transfected with PCNDA3 (-) or 1μg of HA-DAPK-1 vector together with increasing amount of GFP-s-DAPK-1 vector (0, 1, 2, 3μg in lanes 2-5 respectively) as indicated, for 24h, prior to harvesting. Expression of HA-DAPK-1 and GFP-s-DAPK-1 were evaluated by immunoblotting. The non-specific band as shown in Figure 3.8 (A) was used as the loading control. **This experiment has been performed more than 3 times.**

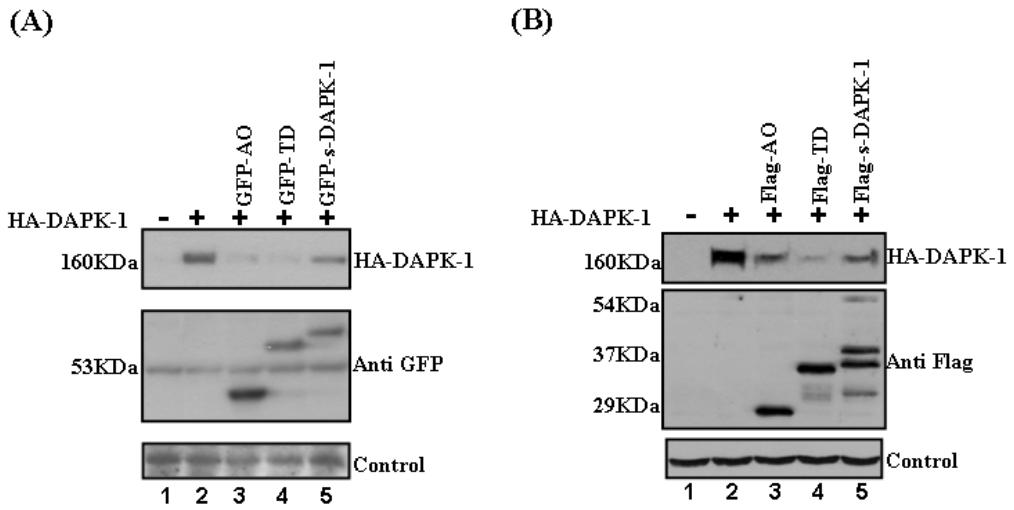

Figure 5.3 The ankyrin repeat region of s-DAPK-1 is sufficient to stimulate the decrease in DAPK-1 protein levels. (A) s-DAPK-1(GFP-tagged) destabilizes DAPK-1. A375 cells were transfected with PCDNA3 (-) or the expression vector [GFP-tagged s-DAPK-1 and its mutants] for 24h, prior to harvesting. The lysates were subjected to immunoblotting using anti-HA and anti-GFP antibody. The non-specific band as shown in Figure 3.8 (A) was used as the loading control. **(B) s-DAPK-1(FLAG-tagged) destabilizes DAPK-1.** A375 cells were transfected with PCDNA3 (-) or the expression vector [FLAG-tagged s-DAPK-1 and its mutants] for 24h, prior to harvesting. The lysates were subjected to immunoblotting using anti-HA and anti-FLAG antibody. The non-specific band as shown in Figure 3.8 (A) was used as the loading control. **These experiments have been performed more than 3 times.**

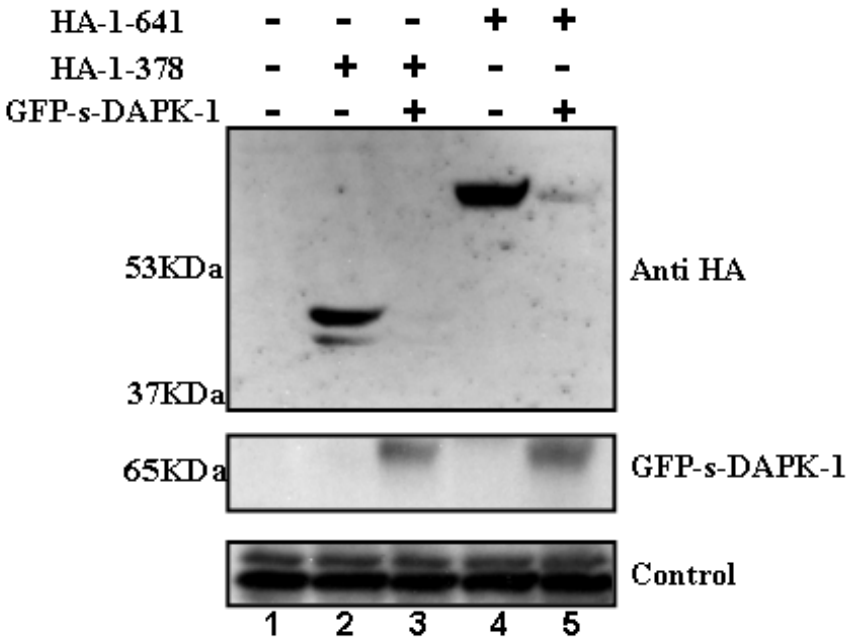

Figure 5.4 The kinase domain of DAPK-1 is the minimal determinant for s-DAPK-1 stimulated decrease in DAPK-1 protein levels. A375 cells were transfected with PCDNA3 (-) or HA-DAPK-1 mutants and GFP-s-DAPK-1 expression vectors as indicated, for 24h, prior to harvesting. Expression of the HA-tagged proteins and GFP-s-DAPK-1 were evaluated by immunoblotting. The non-specific band as shown in Figure 3.8 (A) was used as the loading control. **This experiment has been performed more than 3 times.**

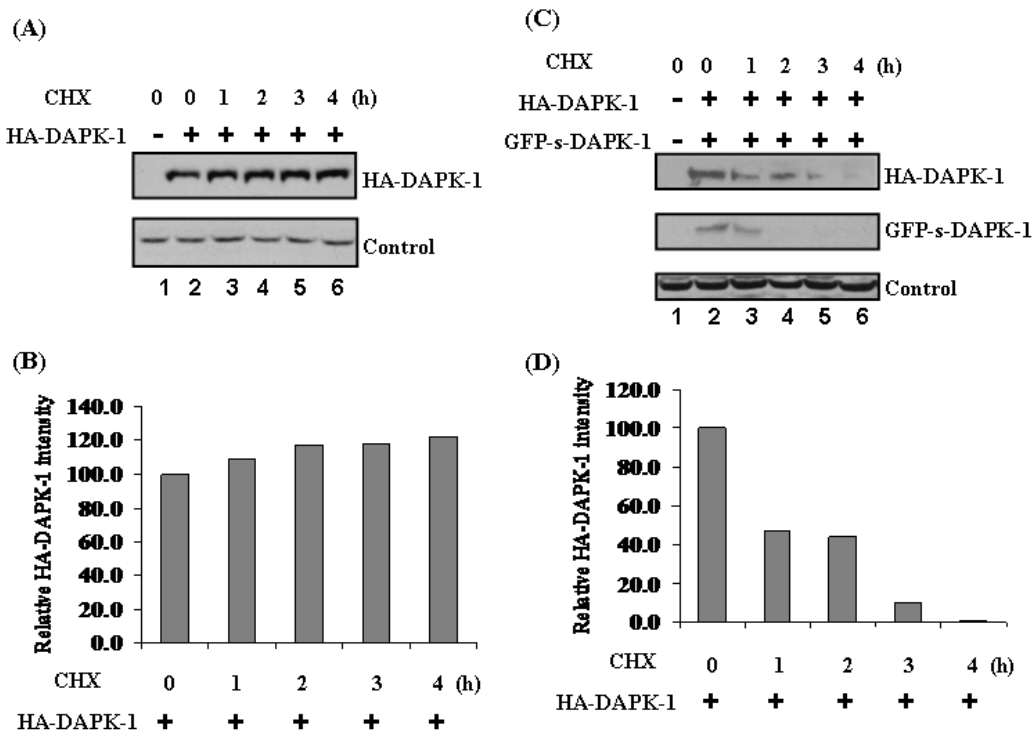

Figure 5.5 s-DAPK-1 decreases DAPK-1 stability. (A, C) HEK293 cells were transfected with PCNDA3 (-) or expression vectors as indicated, for 24h, in combination with cycloheximide treatment for indicated time, prior to harvesting. Expression of HA-DAPK-1 and GFP-s-DAPK-1 were evaluated by immunoblotting. The non-specific band as shown in Figure 3.8 (A) was used as the loading control. Quantification of DAPK-1 levels in (A) and (C) is summarized in (B) and (D). **These experiments have been performed more than 3 times.**

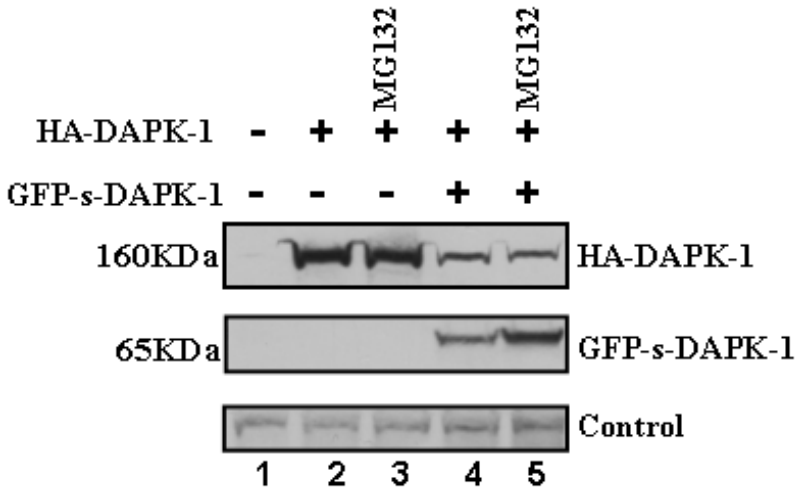

Figure 5.6 s-DAPK-1 stimulated DAPK-1 degradation is proteasome independent. HEK293 cells were transfected with PCDNA3 (-) or the respective expression vectors as indicated, for 24h, in combination with MG132 (lanes 3 and 5) treatments for 6h, prior to harvesting. Expression of HA-DAPK-1 and GFP-s-DAPK-1 was evaluated by immunoblotting. The non-specific band as shown in Figure 3.8 (A) was used as the loading control. **This experiment has been performed more than 3 times.**

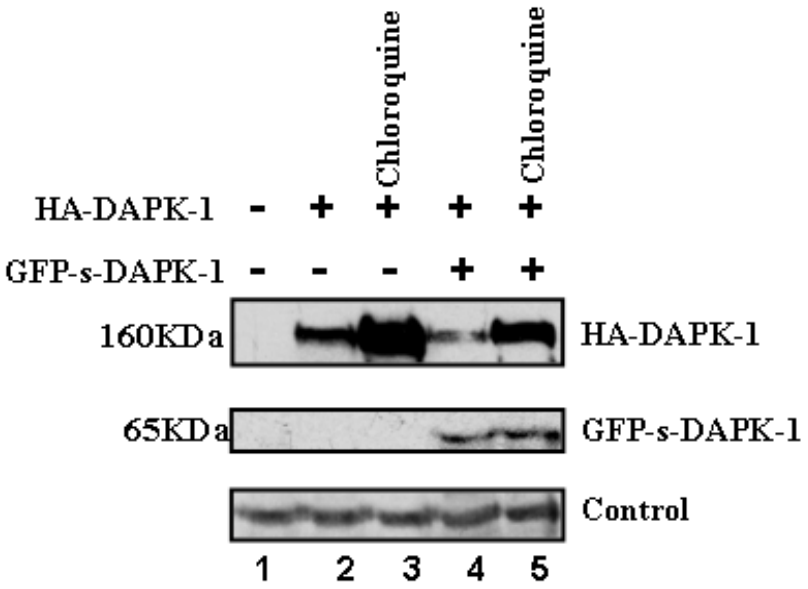

Figure 5.7 s-DAPK-1 stimulated DAPK-1 degradation is lysosome dependent. HEK293 cells were transfected with PCDNA3 (-) or the respective expression vectors as indicated, for 24h, in combination with chloroquine (lanes 3 and 5) treatments for 20h, prior to harvesting. Expression of HA-DAPK-1 and GFP-s-DAPK-1 was evaluated by immunoblotting. The non-specific band as shown in Figure 3.8 (A) was used as the loading control. **This experiment has been performed more than 3 times.**

Chapter Six Discussion

6.1 Result discussion

As described in Chapter One, the role of cathepsin B in TNF-α induced apoptosis is controversial and the mechanism through which TNF-α kills the cells is still unclear. My observations may provide a new angle to investigate the function of cathepsin B in the TNFR-1-induced apoptotic pathways and demonstrate that DAPK-1 also needs to be considered. Interestingly, cathepsin B has long been known to be involved in cell malignancy. Tumour cells tend to have higher expression of cathepsin B, and the secretion of high levels of cathepsin B results in the degradation of cell extracellular matrices[184]. Moreover, it was reported that DAPK-1 can inhibit cell motility by blocking the integrin-mediated polarity pathway[150]. DAPK-1 is also reported to be highly expressed in invading tumour-associated macrophages in colorectal cancer, however DAPK-1 does not kill the cells[185]. The interaction between DAPK-1 and cathepsin B may shed light on explaining the dual function of both DAPK-1 and cathepsin B on the malignancy in tumours.

As shown in Chapter Three (Figure 3.1), post-translational regulation is critical for the expression level of DAPK-1 protein. The result chapters demonstrate that DAPK-1 can be degraded through both a cathepsin B-antagonized TNF-α induced proteasomal degradation pathway and an s-DAPK-1 stimulated lysosomal degradation pathway. The mechanisms through which cathepsin B protects DAPK-1 from TNF-α induced degradation is still not clear. It has been reported that TNF-α induces the degradation of the sphingosine kinase-1 (SK1) in a cathepsin B

dependent manner[186]. Interestingly, the authors showed that only the SK1 bound with motile cathepsin B released from leaking lysosomes get degraded, whilst the SK1 around the contact lysosomes remained unprocessed[186], suggesting that cathepsin B may not be a optimal protease for SK1 in the acidic environment in the lysosome. In contrast, cathepsin B may promote the degradation of DAPK-1 in the lysosome, while it becomes inactive as a DAPK-1 protease in the neutral environment in the cytosol. Thus when the proteasomal degradation pathway for DAPK-1 is activated by TNF-α, the inactive cathepsin B acts to protect DAPK-1 from components of the proteasomal degradation pathway.

Although cathepsin B is not responsible for the degradation of DAPK-1 in the context of my experiments and actually protects it from degradation, it may still promote DAPK-1 lysosomal degradation or cleave DAPK-1 under other environmental conditions. For example, it has been shown that in response to 2h of oxygen glucose deprivation, DAPK-1 is cleaved by cathepsin B in primary neuronal cells[66], confirming that cathepsin B is able to degrade DAPK-1 *in vivo* under certain stresses or in specific cell types. Moreover, my results in chapter three also show that cathepsin B can interact and cleave DAPK-1 *in vitro* (Figure 3.5). Therefore, instead of being a negative regulator, cathepsin B may play a positive role in the s-DAPK-1 stimulated lysosomal degradation pathway for DAPK-1. For example, cathepsin L is a highly redundant functional homologue of cathepsin B, and the mice with double knock-out of both cathepsin B and L have severe brain atrophy associated with selective neuronal loss in the cerebral cortex and in the cerebellar Purkinje and granule cell layers[172, 187]. Considering the apoptotic role of DAPK-1 in neuronal

death[15] and that cathepsin B can cleave DAPK-1 protein, it raises the possibility that the neuronal loss in the cathepsin B and cathepsin L double knock-out mouse may be due to increased abundance of DAPK-1, further implicating a positive role of cathepsin B in regulating the degradation of DAPK-1.

6.2 Degradation pathways for DAPK-1

In addition to the data presented in the results chapters, there is some other work that I have done in collaboration with colleagues, mainly Dr. Craig Stevens, in the laboratory. We have identified another protein TSC2 (tuberous sclerosis 2) as a novel DAPK-1 death domain interacting protein that can mediate the degration of DAPK-1 via both lysosome and proteaome dependent pathways (Unpublished data). Reciprocally, DAPK-1 can phosphorylate and inactivate TSC2, leading to the activation of the mTORC1 (mammalian target of rapamycin complex 1) signlling pathway, which is a major regulator of cell growth[188].

My own data along with other work from our laboratory clearly demonstrates the existence of an alternative lysosomal degradation pathway for DAPK-1 in addition to the existing ubiquitin-proteasome pathway. It is also clear that the steady state level of DAPK-1 is mainly controlled through this lysosomal pathway, and that both s-DAPK-1 and TSC2 target DAPK-1 towards degradation through the lysosomal pathway. In contrast, upon cell treatment with stresses such as TNF-α or Hsp90 inhibition, the proteasomal degradation pathway is activated and rapidly degrades DAPK-1.

The TSC2 null mice and cathepsin B and L double knock-out mice die from distinct developmental defects and both TSC2 and cathepsin B are involved the regulation of DAPK-1 stability. If overexpression of DAPK-1 is responsible for the lethality of these mice, then in neuronal cells, cathepsin B is the major factor controlling DAPK-1 degradation; while in liver cells, TSC2 is be the predominant regulator. Thus, the regulation of DAPK-1 is stability may vary dramatically in a tissue and cell-type specific manner.

Taken together, several factors in the proteasomal and lysosomal degradation pathways for DAPK-1 have been discovered (Figure 6.1). However, unlike the proteasomal degradation pathway, not much is known about the mechanisms underlying the lysosomal degradation of DAPK-1, except the link between cathepsin B and the lysosome. Importantly, DAPK-1 is a positive regulator of IFN-γ induced autophagy[15] and can induce autophagy when overexpressed[25]. The mechanism through which DAPK-1 induces autophagy is still not clear. Our data demonstrates that DAPK-1 can be degraded by the lysosome, thus it is possible that DAPK-1 can be sequestered into autophagolysosme and get degraded by atuophagy. Although more data is required, it may provide a potential mechanism for lysosome dependent degradation of DAPK-1.

6.3 Physiological role of DAPK-1

The discovery that full activation of mTORC1 by EGF requires DAPK-1 indicates that DAPK-1 acts as a survival factor during EGF signalling. This is inconsistent with published data showing that in response to PMA, the DAPK-1-ERK complex induces apoptosis[77]. However, the apoptosis promoting effect of DAPK-1 induced by the ERK activator PMA was only observed in suspended cells[77], and in the overexpression system, the constitutively active MEK signal is required for DAPK-1 to induce apoptosis[131]. Therefore, the apoptosis function of the ERK-DAPK-1 complex may only exist under aberrant conditions, such as when the growth signal is above the limit tolerated by cells. However, under physiological growth conditions, DAPK-1 acts as a survival factor, and promotes cell growth.

As discussed in Section 1.9.1, Src may possess dual functions, and when the EGF signal is over the tolerated limit, Src directly phosphorylates and inactivates DAPK-1. This role of Src may make it a checkpoint in the cells to attenuate the growth signal when it starts to stress the cells. In the overexpression system, MEK/ERK/DAPK-1 may bypass the limit that endogenous Src can cope with, which leads to apoptosis. As shown in Figure 6.5, sustained high levels of DAPK-1 are not tolerated by the cells. This supports the notion that active DAPK-1 is a positive regulator of cell growth, but during long-term culture, the growth signal induced by DAPK-1 must be restrained below a certain level, otherwise the cells will die. This is also consistent with the finding that long-term activation of the EGF pathway leads to cell death[189]. To investigate further the relationship between DAPK-1, Src and ERK in EGF

signalling pathway, a careful time and dose dependent titration of EGF in the presence and absence of DAPK-1 overexpression will be required.

The data in chapter three confirmed that DAPK-1 can act as a survival factor in the TNF-α signalling pathway. However, the mechanism underlying how DAPK-1 antagonizes TNF-α induced apoptosis and acts as a survival factor is still not clear. The discovery of the DAPK-1-TSC2 interaction may provide a clue. It has been shown that TNF-α treatment induces phosphorylation of TSC1 at Ser487 and Ser511 via IKKβ, leading to inactivation of the TSC complex and the subsequent angiogenesis and tumour development[190]. The ability of DAPK-1 to activate mTORC1 places DAPK-1 on the survival side of the TNF-α pathway, and provides a mechanism to explain why DAPK-1 needs to be eliminated for cells to undergo apoptosis. Of note, the TNF-α induced DAPK-1 degradation became obvious only after 2-4 hours of combined TNF-α and CHX treatment[151], whereas the mTORC1 activation by TNF-α was observed within 30 minutes of treatment[190]. Moreover, it was shown that in the early stage of TNF-α/CHX treatment, the kinase activity of DAPK-1 is significantly increased, however this is not accompanied by changes in its protein level[151]. Therefore, it is possible that DAPK-1 activity is initially upregulated by TNF-α to activate the mTORC1 pathway, and is then targeted for degradation at a later time when the apoptotic signal becomes dominant. Importantly, in most papers published about TNF-α, the experiments were carried out in cells growing in serum containing medium, while in most papers on EGF, the experiments were performed in a serum free environment. It is possible that the anti-apoptotic effect of DAPK-1 in TNF-α pathway is due to the activation of mTORC1 via

DAPK-1 by EGF in the medium. Extra caution is needed when trying to interpret the role of DAPK-1 in the TNF-α and EGF pathways.

6.4 Future perspectives

As shown in chapter five, s-DAPK-1 can efficiently target DAPK-1 for degradation. It will be interesting to see whether s-DAPK-1 can facilitate TNFR-1 mediated DAPK-1 degradation similar to the 836-947 miniprotein. Moreover, in addition to CHX, a Smac mimetic can turn TNF-α signalling towards apoptosis[191]. It will be interesting to see whether s-DAPK-1 or 836-847 miniprotein can further enhance apoptosis induced by TNF-α in combination with CHX or Smac mimetic. If so, it may be worthwhile to map the minimal domain on the 836-947 miniprotein and the ankryrin repeat regions on DAPK-1, so that a potential drug-like peptide may be developed for future clinical trial.

In addition, the TSC2 null mouse dies during embryonic development. Considering the tight connection between TSC2 and the expression level of DAPK-1, and the relation of DAPK-1 expression to cell death, it will be interesting to see whether knock-out of DAPK-1 can rescue the TSC2 null mouse from embryonic lethality. If so, it would provide a strong genetic link and physiological significance for the feedback loop between TSC2 and DAPK-1.

In conclusion, my study has added s-DAPK-1, cathepsin B and TSC2 to the group of proteins that can regulate DAPK-1 stability (Figure 6.1). In addition, our discovery

that DAPK-1 acts as a survival factor suggests that under normal growth conditions, DAPK-1 may act as an oncogene. Given that the traditional notion of DAPK-1 as a tumour suppressor, and loss of DAPK-1 expression in some tumours leads to cancer, our study provides a new way of interpreting DAPK-1 expression in tumour cells. It also highlights the importance of studying the degradation control of DAPK-1. The observation that DAPK-1 expression is vital for some tumours to grow or resist certain stresses such as TNF-α, may provide an important potential drug lead that can enhance the efficiency of current therapeutic strategies aimed at eliminating tumour cells.

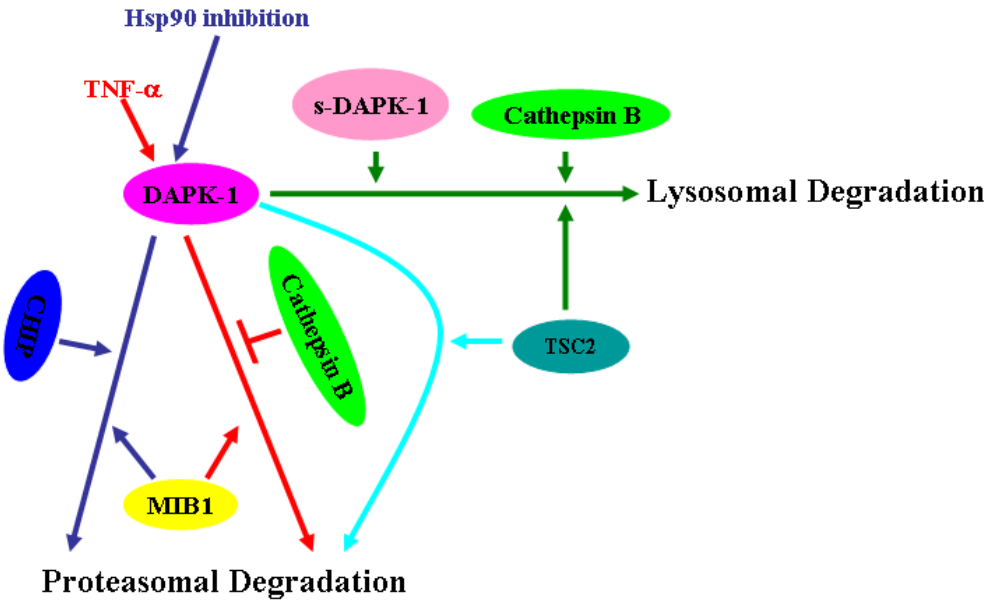

Figure 6.1 Degradation pathways for DAPK-1. It has been published that DAPK-1 can be targeted for ubiquitin-proteasome degradation in response to TNF-α and inhibition of Hsp90, the former of which may be induced by MIB1 and the latter is induced by MIB1 and CHIP. Moreover, our laboratory found that TSC2 can target DAPK-1 for both lysosomal and proteasomal degradation. In this work, I found that cathepsin B can inhibit the TNF-α induced proteasomal degradation of DAPK-1, and s-DAPK-1 promotes lysosomal degradation of DAPK-1.

References

1. Lippman, S.M. & Hawk, E.T. Cancer prevention: from 1727 to milestones of the past 100 years. *Cancer Res* **69**, 5269-5284 (2009).

2. Smith, J.A. & Martin, L. Do cells cycle? *Proc Natl Acad Sci U S A* **70**, 1263-1267 (1973).

3. Danial, N.N. & Korsmeyer, S.J. Cell death: critical control points. *Cell* **116**, 205-219 (2004).

4. Levine, A.J. p53, the cellular gatekeeper for growth and division. *Cell* **88**, 323-331 (1997).

5. Hollstein, M., Sidransky, D., Vogelstein, B. & Harris, C.C. p53 mutations in human cancers. *Science* **253**, 49-53 (1991).

6. Dranoff, G. Cytokines in cancer pathogenesis and cancer therapy. *Nat Rev Cancer* **4**, 11-22 (2004).

7. Deiss, L.P., Feinstein, E., Berissi, H., Cohen, O. & Kimchi, A. Identification of a novel serine/threonine kinase and a novel 15-kD protein as potential mediators of the gamma interferon-induced cell death. *Genes Dev* **9**, 15-30 (1995).

8. Cohen, O., Feinstein, E. & Kimchi, A. DAP-kinase is a Ca2+/calmodulin-dependent, cytoskeletal-associated protein kinase, with cell death-inducing functions that depend on its catalytic activity. *Embo J* **16**, 998-1008 (1997).

9. Mosavi, L.K., Cammett, T.J., Desrosiers, D.C. & Peng, Z.Y. The ankyrin repeat as molecular architecture for protein recognition. *Protein Sci* **13**, 1435-1448 (2004).

10. Saraste, M., Sibbald, P.R. & Wittinghofer, A. The P-loop--a common motif in ATP- and GTP-binding proteins. *Trends Biochem Sci* **15**, 430-434 (1990).

11. Hoeflich, K.P. & Ikura, M. Radixin: cytoskeletal adopter and signaling protein. *Int J Biochem Cell Biol* **36**, 2131-2136 (2004).

12. Chaigne-Delalande, B., Moreau, J.F. & Legembre, P. Rewinding the DISC. *Arch Immunol Ther Exp (Warsz)* **56**, 9-14 (2008).

13. Feinstein, E., Kimchi, A., Wallach, D., Boldin, M. & Varfolomeev, E. The death domain: a module shared by proteins with diverse cellular functions. *Trends Biochem Sci* **20**, 342-344 (1995).

14. Raveh, T., Berissi, H., Eisenstein, M., Spivak, T. & Kimchi, A. A functional genetic screen identifies regions at the C-terminal tail and death-domain of death-associated protein kinase that are critical for its proapoptotic activity. *Proc Natl Acad Sci U S A* **97**, 1572-1577 (2000).

15. Bialik, S. & Kimchi, A. The death-associated protein kinases: structure, function, and beyond. *Annu Rev Biochem* **75**, 189-210 (2006).

16. Kogel, D., Prehn, J.H. & Scheidtmann, K.H. The DAP kinase family of pro-apoptotic proteins: novel players in the apoptotic game. *Bioessays* **23**, 352-358 (2001).

17. Jin, Y., *et al.* Identification of a new form of death-associated protein kinase that promotes cell survival. *J Biol Chem* **276**, 39667-39678 (2001).

18. Jin, Y. & Gallagher, P.J. Antisense depletion of death-associated protein kinase promotes apoptosis. *J Biol Chem* **278**, 51587-51593 (2003).

19. Swulius, M.T. & Waxham, M.N. Ca(2+)/Calmodulin-dependent Protein Kinases. *Cell Mol Life Sci* (2008).

20. Velentza, A.V., Schumacher, A.M. & Watterson, D.M. Structure, activity, regulation, and inhibitor discovery for a protein kinase associated with apoptosis and neuronal death. *Pharmacol Ther* **93**, 217-224 (2002).

21. Shohat, G.*, et al.* The pro-apoptotic function of death-associated protein kinase is controlled by a unique inhibitory autophosphorylation-based mechanism. *J Biol Chem* **276**, 47460-47467 (2001).

22. Kuo, J.C., Lin, J.R., Staddon, J.M., Hosoya, H. & Chen, R.H. Uncoordinated regulation of stress fibers and focal adhesions by DAP kinase. *J Cell Sci* **116**, 4777-4790 (2003).

23. Bialik, S., Bresnick, A.R. & Kimchi, A. DAP-kinase-mediated morphological changes are localization dependent and involve myosin-II phosphorylation. *Cell Death Differ* **11**, 631-644 (2004).

24. Pan, X., Luhrmann, A., Satoh, A., Laskowski-Arce, M.A. & Roy, C.R. Ankyrin repeat proteins comprise a diverse family of bacterial type IV effectors. *Science* **320**, 1651-1654 (2008).

25. Harrison, B.*, et al.* DAPK-1 binding to a linear peptide motif in MAP1B stimulates autophagy and membrane blebbing. *J Biol Chem* **283**, 9999-10014 (2008).

26. Sakagami, H. & Kondo, H. Molecular cloning and developmental expression of a rat homologue of death-associated protein kinase in the nervous system. *Brain Res Mol Brain Res* **52**, 249-256 (1997).

27. Yamamoto, M.*, et al.* Developmental changes in distribution of death-associated protein kinase mRNAs. *J Neurosci Res* **58**, 674-683 (1999).

28. Esteller, M. CpG island hypermethylation and tumor suppressor genes: a booming present, a brighter future. *Oncogene* **21**, 5427-5440 (2002).

29. Kissil, J.L., *et al.* DAP-kinase loss of expression in various carcinoma and B-cell lymphoma cell lines: possible implications for role as tumor suppressor gene. *Oncogene* **15**, 403-407 (1997).

30. Raveh, T. & Kimchi, A. DAP kinase-a proapoptotic gene that functions as a tumor suppressor. *Exp Cell Res* **264**, 185-192 (2001).

31. Gozuacik, D. & Kimchi, A. DAPk protein family and cancer. *Autophagy* **2**, 74-79 (2006).

32. Chan, M.W., *et al.* Hypermethylation of multiple genes in tumor tissues and voided urine in urinary bladder cancer patients. *Clin Cancer Res* **8**, 464-470 (2002).

33. Rosas, S.L., *et al.* Promoter hypermethylation patterns of p16, O6-methylguanine-DNA-methyltransferase, and death-associated protein kinase in tumors and saliva of head and neck cancer patients. *Cancer Res* **61**, 939-942 (2001).

34. Chang, H.W., *et al.* Evaluation of hypermethylated tumor suppressor genes as tumor markers in mouth and throat rinsing fluid, nasopharyngeal swab and peripheral blood of nasopharygeal carcinoma patient. *Int J Cancer* **105**, 851-855 (2003).

35. Wong, T.S., *et al.* Quantitative plasma hypermethylated DNA markers of undifferentiated nasopharyngeal carcinoma. *Clin Cancer Res* **10**, 2401-2406 (2004).

36. Yamaguchi, S., Asao, T., Nakamura, J., Ide, M. & Kuwano, H. High frequency of DAP-kinase gene promoter methylation in colorectal cancer specimens and its identification in serum. *Cancer Lett* **194**, 99-105 (2003).

37. Dulaimi, E., Hillinck, J., Ibanez de Caceres, I., Al-Saleem, T. & Cairns, P. Tumor suppressor gene promoter hypermethylation in serum of breast cancer patients. *Clin Cancer Res* **10**, 6189-6193 (2004).

38. Belinsky, S.A., *et al.* Aberrant promoter methylation in bronchial epithelium and sputum from current and former smokers. *Cancer Res* **62**, 2370-2377 (2002).

39. Soria, J.C., *et al.* Aberrant promoter methylation of multiple genes in bronchial brush samples from former cigarette smokers. *Cancer Res* **62**, 351-355 (2002).

40. Fujiwara, K., *et al.* Identification of epigenetic aberrant promoter methylation in serum DNA is useful for early detection of lung cancer. *Clin Cancer Res* **11**, 1219-1225 (2005).

41. Reesink-Peters, N., *et al.* Detecting cervical cancer by quantitative promoter hypermethylation assay on cervical scrapings: a feasibility study. *Mol Cancer Res* **2**, 289-295 (2004).

42. Gustafson, K.S., Furth, E.E., Heitjan, D.F., Fansler, Z.B. & Clark, D.P. DNA methylation profiling of cervical squamous intraepithelial lesions using liquid-based cytology specimens: an approach that utilizes receiver-operating characteristic analysis. *Cancer* **102**, 259-268 (2004).

43. Raval, A., *et al.* Downregulation of death-associated protein kinase 1 (DAPK1) in chronic lymphocytic leukemia. *Cell* **129**, 879-890 (2007).

44. Inbal, B., *et al.* DAP kinase links the control of apoptosis to metastasis. *Nature* **390**, 180-184 (1997).

45. Lehmann, U., Celikkaya, G., Hasemeier, B., Langer, F. & Kreipe, H. Promoter hypermethylation of the death-associated protein kinase gene in breast cancer is associated with the invasive lobular subtype. *Cancer Res* **62**, 6634-6638 (2002).

46. Toyooka, S., *et al.* Epigenetic down-regulation of death-associated protein kinase in lung cancers. *Clin Cancer Res* **9**, 3034-3041 (2003).

47. Wethkamp, N., *et al.* Expression of death-associated protein kinase during tumour progression of human renal cell carcinomas: hypermethylation-independent mechanisms of inactivation. *Eur J Cancer* **42**, 264-274 (2006).

48. Simpson, D.J., Clayton, R.N. & Farrell, W.E. Preferential loss of Death Associated Protein kinase expression in invasive pituitary tumours is associated with either CpG island methylation or homozygous deletion. *Oncogene* **21**, 1217-1224 (2002).

49. Kawaguchi, K., *et al.* Death-associated protein kinase (DAP kinase) alteration in soft tissue leiomyosarcoma: Promoter methylation or homozygous deletion is associated with a loss of DAP kinase expression. *Hum Pathol* **35**, 1266-1271 (2004).

50. Ciechanover, A. Intracellular protein degradation: from a vague idea thru the lysosome and the ubiquitin-proteasome system and onto human diseases and drug targeting. *Exp Biol Med (Maywood)* **231**, 1197-1211 (2006).

51. Fehrenbacher, N. & Jaattela, M. Lysosomes as targets for cancer therapy. *Cancer Res* **65**, 2993-2995 (2005).

52. Chwieralski, C.E., Welte, T. & Buhling, F. Cathepsin-regulated apoptosis. *Apoptosis* **11**, 143-149 (2006).

53. Rawlings, N.D., Morton, F.R., Kok, C.Y., Kong, J. & Barrett, A.J. MEROPS: the peptidase database. *Nucleic Acids Res* **36**, D320-325 (2008).

54. Rubinsztein, D.C. The roles of intracellular protein-degradation pathways in neurodegeneration. *Nature* **443**, 780-786 (2006).

55. Wang, J. & Maldonado, M.A. The ubiquitin-proteasome system and its role in inflammatory and autoimmune diseases. *Cell Mol Immunol* **3**, 255-261 (2006).

56. Weissman, A.M. Themes and variations on ubiquitylation. *Nat Rev Mol Cell Biol* **2**, 169-178 (2001).

57. Hibbert, R.G., Mattiroli, F. & Sixma, T.K. Structural aspects of multi-domain RING/Ubox E3 ligases in DNA repair. *DNA Repair (Amst)* **8**, 525-535 (2009).

58. Aravind, L. & Koonin, E.V. The U box is a modified RING finger - a common domain in ubiquitination. *Curr Biol* **10**, R132-134 (2000).

59. Hatakeyama, S., Matsumoto, M., Yada, M. & Nakayama, K.I. Interaction of U-box-type ubiquitin-protein ligases (E3s) with molecular chaperones. *Genes Cells* **9**, 533-548 (2004).

60. Peng, J.*, et al.* A proteomics approach to understanding protein ubiquitination. *Nat Biotechnol* **21**, 921-926 (2003).

61. Wertz, I.E. & Dixit, V.M. Ubiquitin-mediated regulation of TNFR1 signaling. *Cytokine Growth Factor Rev* **19**, 313-324 (2008).

62. Jin, Y., Blue, E.K., Dixon, S., Shao, Z. & Gallagher, P.J. A death-associated protein kinase (DAPK)-interacting protein, DIP-1, is an E3 ubiquitin ligase that promotes tumor necrosis factor-induced apoptosis and regulates the cellular levels of DAPK. *J Biol Chem* **277**, 46980-46986 (2002).

63. Connell, P.*, et al.* The co-chaperone CHIP regulates protein triage decisions mediated by heat-shock proteins. *Nat Cell Biol* **3**, 93-96 (2001).

64. Zhang, L., Nephew, K.P. & Gallagher, P.J. Regulation of death-associated protein kinase. Stabilization by HSP90 heterocomplexes. *J Biol Chem* **282**, 11795-11804 (2007).

65. Araki, T., *et al.* Expression, interaction, and proteolysis of death-associated protein kinase and p53 within vulnerable and resistant hippocampal subfields following seizures. *Hippocampus* **14**, 326-336 (2004).

66. Shamloo, M., *et al.* Death-associated protein kinase is activated by dephosphorylation in response to cerebral ischemia. *J Biol Chem* **280**, 42290-42299 (2005).

67. Velentza, A.V., Schumacher, A.M., Weiss, C., Egli, M. & Watterson, D.M. A protein kinase associated with apoptosis and tumor suppression: structure, activity, and discovery of peptide substrates. *J Biol Chem* **276**, 38956-38965 (2001).

68. Bialik, S., Berissi, H. & Kimchi, A. A high throughput proteomics screen identifies novel substrates of death-associated protein kinase. *Mol Cell Proteomics* **7**, 1089-1098 (2008).

69. Schumacher, A.M., Schavocky, J.P., Velentza, A.V., Mirzoeva, S. & Watterson, D.M. A calmodulin-regulated protein kinase linked to neuron survival is a substrate for the calmodulin-regulated death-associated protein kinase. *Biochemistry* **43**, 8116-8124 (2004).

70. Fraser, J.A. & Hupp, T.R. Chemical genetics approach to identify peptide ligands that selectively stimulate DAPK-1 kinase activity. *Biochemistry* **46**, 2655-2673 (2007).

71. Schumacher, A.M., Velentza, A.V., Watterson, D.M. & Dresios, J. Death-associated protein kinase phosphorylates mammalian ribosomal protein S6 and reduces protein synthesis. *Biochemistry* **45**, 13614-13621 (2006).

72. Tian, J.H., Das, S. & Sheng, Z.H. Ca2+-dependent phosphorylation of syntaxin-1A by the death-associated protein (DAP) kinase regulates its interaction with Munc18. *J Biol Chem* **278**, 26265-26274 (2003).

73. Houle, F., Poirier, A., Dumaresq, J. & Huot, J. DAP kinase mediates the phosphorylation of tropomyosin-1 downstream of the ERK pathway, which regulates the formation of stress fibers in response to oxidative stress. *J Cell Sci* **120**, 3666-3677 (2007).

74. Shani, G.*, et al.* Death-associated protein kinase phosphorylates ZIP kinase, forming a unique kinase hierarchy to activate its cell death functions. *Mol Cell Biol* **24**, 8611-8626 (2004).

75. Roux, P.P.*, et al.* RAS/ERK signaling promotes site-specific ribosomal protein S6 phosphorylation via RSK and stimulates cap-dependent translation. *J Biol Chem* **282**, 14056-14064 (2007).

76. Henshall, D.C.*, et al.* Expression of death-associated protein kinase and recruitment to the tumor necrosis factor signaling pathway following brief seizures. *J Neurochem* **86**, 1260-1270 (2003).

77. Chen, C.H.*, et al.* Bidirectional signals transduced by DAPK-ERK interaction promote the apoptotic effect of DAPK. *Embo J* **24**, 294-304 (2005).

78. Citri, A.*, et al.* Hsp90 recognizes a common surface on client kinases. *J Biol Chem* **281**, 14361-14369 (2006).

79. Wang, W.J.*, et al.* The tumor suppressor DAPK is reciprocally regulated by tyrosine kinase Src and phosphatase LAR. *Mol Cell* **27**, 701-716 (2007).

80. Eisenberg-Lerner, A. & Kimchi, A. DAP kinase regulates JNK signaling by binding and activating protein kinase D under oxidative stress. *Cell Death Differ* **14**, 1908-1915 (2007).

81. Llambi, F., *et al.* The dependence receptor UNC5H2 mediates apoptosis through DAP-kinase. *Embo J* **24**, 1192-1201 (2005).

82. Edinger, A.L. & Thompson, C.B. Death by design: apoptosis, necrosis and autophagy. *Curr Opin Cell Biol* **16**, 663-669 (2004).

83. Lockshin, R.A. & Zakeri, Z. Apoptosis, autophagy, and more. *Int J Biochem Cell Biol* **36**, 2405-2419 (2004).

84. Wyllie, A.H. Glucocorticoid-induced thymocyte apoptosis is associated with endogenous endonuclease activation. *Nature* **284**, 555-556 (1980).

85. Ohno, Y., *et al.* Simultaneous induction of apoptotic, autophagic, and necrosis-like cell death by monoclonal antibodies recognizing chicken transferrin receptor. *Biochem Biophys Res Commun* **367**, 775-781 (2008).

86. Thornberry, N.A. & Lazebnik, Y. Caspases: enemies within. *Science* **281**, 1312-1316 (1998).

87. Zamzami, N., *et al.* Mitochondrial control of nuclear apoptosis. *J Exp Med* **183**, 1533-1544 (1996).

88. Chai, J., *et al.* Structural and biochemical basis of apoptotic activation by Smac/DIABLO. *Nature* **406**, 855-862 (2000).

89. Li, L., *et al.* A small molecule Smac mimic potentiates TRAIL- and TNFalpha-mediated cell death. *Science* **305**, 1471-1474 (2004).

90. Balkwill, F. TNF-alpha in promotion and progression of cancer. *Cancer Metastasis Rev* **25**, 409-416 (2006).

91. Bradley, J.R. TNF-mediated inflammatory disease. *J Pathol* **214**, 149-160 (2008).

92. Varfolomeev, E.E. & Ashkenazi, A. Tumor necrosis factor: an apoptosis JuNKie? *Cell* **116**, 491-497 (2004).

93. Karin, M. & Lin, A. NF-kappaB at the crossroads of life and death. *Nat Immunol* **3**, 221-227 (2002).

94. Munshi, A., *et al.* TRAIL (APO-2L) induces apoptosis in human prostate cancer cells that is inhibitable by Bcl-2. *Oncogene* **20**, 3757-3765 (2001).

95. Sah, N.K., *et al.* Translation inhibitors sensitize prostate cancer cells to apoptosis induced by tumor necrosis factor-related apoptosis-inducing ligand (TRAIL) by activating c-Jun N-terminal kinase. *J Biol Chem* **278**, 20593-20602 (2003).

96. Kreuz, S., Siegmund, D., Scheurich, P. & Wajant, H. NF-kappaB inducers upregulate cFLIP, a cycloheximide-sensitive inhibitor of death receptor signaling. *Mol Cell Biol* **21**, 3964-3973 (2001).

97. Petersen, S.L., *et al.* Autocrine TNFalpha signaling renders human cancer cells susceptible to Smac-mimetic-induced apoptosis. *Cancer Cell* **12**, 445-456 (2007).

98. Guicciardi, M.E., *et al.* Cathepsin B contributes to TNF-alpha-mediated hepatocyte apoptosis by promoting mitochondrial release of cytochrome c. *J Clin Invest* **106**, 1127-1137 (2000).

99. Li, J.H. & Pober, J.S. The cathepsin B death pathway contributes to TNF plus IFN-gamma-mediated human endothelial injury. *J Immunol* **175**, 1858-1866 (2005).

100. Gewies, A. & Grimm, S. Cathepsin-B and cathepsin-L expression levels do not correlate with sensitivity of tumour cells to TNF-alpha-mediated apoptosis. *Br J Cancer* **89**, 1574-1580 (2003).

101. Levine, B. & Klionsky, D.J. Development by self-digestion: molecular mechanisms and biological functions of autophagy. *Dev Cell* **6**, 463-477 (2004).

102. Levine, B. Eating oneself and uninvited guests: autophagy-related pathways in cellular defense. *Cell* **120**, 159-162 (2005).

103. Klionsky, D.J.*, et al.* A unified nomenclature for yeast autophagy-related genes. *Dev Cell* **5**, 539-545 (2003).

104. Klionsky, D.J. Autophagy: from phenomenology to molecular understanding in less than a decade. *Nat Rev Mol Cell Biol* **8**, 931-937 (2007).

105. Maiuri, M.C., Zalckvar, E., Kimchi, A. & Kroemer, G. Self-eating and self-killing: crosstalk between autophagy and apoptosis. *Nat Rev Mol Cell Biol* **8**, 741-752 (2007).

106. Yin, X.M., Ding, W.X. & Gao, W. Autophagy in the liver. *Hepatology* **47**, 1773-1785 (2008).

107. Kabeya, Y.*, et al.* LC3, a mammalian homologue of yeast Apg8p, is localized in autophagosome membranes after processing. *Embo J* **19**, 5720-5728 (2000).

108. Yu, L.*, et al.* Regulation of an ATG7-beclin 1 program of autophagic cell death by caspase-8. *Science* **304**, 1500-1502 (2004).

109. Pyo, J.O.*, et al.* Essential roles of Atg5 and FADD in autophagic cell death: dissection of autophagic cell death into vacuole formation and cell death. *J Biol Chem* **280**, 20722-20729 (2005).

110. Shimizu, S., *et al.* Role of Bcl-2 family proteins in a non-apoptotic programmed cell death dependent on autophagy genes. *Nat Cell Biol* **6**, 1221-1228 (2004).

111. Pattingre, S., *et al.* Bcl-2 antiapoptotic proteins inhibit Beclin 1-dependent autophagy. *Cell* **122**, 927-939 (2005).

112. Kang, C., You, Y.J. & Avery, L. Dual roles of autophagy in the survival of Caenorhabditis elegans during starvation. *Genes Dev* **21**, 2161-2171 (2007).

113. Yue, Z., Jin, S., Yang, C., Levine, A.J. & Heintz, N. Beclin 1, an autophagy gene essential for early embryonic development, is a haploinsufficient tumor suppressor. *Proc Natl Acad Sci U S A* **100**, 15077-15082 (2003).

114. Espert, L., *et al.* Autophagy and CD4+ T lymphocyte destruction by HIV-1. *Autophagy* **3**, 32-34 (2007).

115. Djavaheri-Mergny, M., *et al.* NF-kappaB activation represses tumor necrosis factor-alpha-induced autophagy. *J Biol Chem* **281**, 30373-30382 (2006).

116. Crighton, D., *et al.* DRAM, a p53-induced modulator of autophagy, is critical for apoptosis. *Cell* **126**, 121-134 (2006).

117. Qu, X., *et al.* Autophagy gene-dependent clearance of apoptotic cells during embryonic development. *Cell* **128**, 931-946 (2007).

118. Ullman, E., *et al.* Autophagy promotes necrosis in apoptosis-deficient cells in response to ER stress. *Cell Death Differ* **15**, 422-425 (2008).

119. Samara, C., Syntichaki, P. & Tavernarakis, N. Autophagy is required for necrotic cell death in Caenorhabditis elegans. *Cell Death Differ* **15**, 105-112 (2008).

120. Zong, W.X. & Thompson, C.B. Necrotic death as a cell fate. *Genes Dev* **20**, 1-15 (2006).

121. Cohen, O., *et al.* DAP-kinase participates in TNF-alpha- and Fas-induced apoptosis and its function requires the death domain. *J Cell Biol* **146**, 141-148 (1999).

122. Pelled, D., *et al.* Death-associated protein (DAP) kinase plays a central role in ceramide-induced apoptosis in cultured hippocampal neurons. *J Biol Chem* **277**, 1957-1961 (2002).

123. Raveh, T., Droguett, G., Horwitz, M.S., DePinho, R.A. & Kimchi, A. DAP kinase activates a p19ARF/p53-mediated apoptotic checkpoint to suppress oncogenic transformation. *Nat Cell Biol* **3**, 1-7 (2001).

124. Schori, H., *et al.* Immune-related mechanisms participating in resistance and susceptibility to glutamate toxicity. *Eur J Neurosci* **16**, 557-564 (2002).

125. Inbal, B., Bialik, S., Sabanay, I., Shani, G. & Kimchi, A. DAP kinase and DRP-1 mediate membrane blebbing and the formation of autophagic vesicles during programmed cell death. *J Cell Biol* **157**, 455-468 (2002).

126. Jang, C.W., *et al.* TGF-beta induces apoptosis through Smad-mediated expression of DAP-kinase. *Nat Cell Biol* **4**, 51-58 (2002).

127. Wang, W.J., Kuo, J.C., Yao, C.C. & Chen, R.H. DAP-kinase induces apoptosis by suppressing integrin activity and disrupting matrix survival signals. *J Cell Biol* **159**, 169-179 (2002).

128. Yamamoto, M., Hioki, T., Ishii, T., Nakajima-Iijima, S. & Uchino, S. DAP kinase activity is critical for C(2)-ceramide-induced apoptosis in PC12 cells. *Eur J Biochem* **269**, 139-147 (2002).

129. Tang, X., *et al.* Hypermethylation of the death-associated protein kinase promoter attenuates the sensitivity to TRAIL-induced apoptosis in human non-small cell lung cancer cells. *Mol Cancer Res* **2**, 685-691 (2004).

130. Schumacher, A.M., Velentza, A.V., Watterson, D.M. & Wainwright, M.S. DAPK catalytic activity in the hippocampus increases during the recovery phase in an animal model of brain hypoxic-ischemic injury. *Biochim Biophys Acta* **1600**, 128-137 (2002).

131. Stevens, C.*, et al.* A germ line mutation in the death domain of DAPK-1 inactivates ERK-induced apoptosis. *J Biol Chem* **282**, 13791-13803 (2007).

132. Craig, A.L.*, et al.* The MDM2 ubiquitination signal in the DNA-binding domain of p53 forms a docking site for calcium calmodulin kinase superfamily members. *Mol Cell Biol* **27**, 3542-3555 (2007).

133. Charras, G. & Paluch, E. Blebs lead the way: how to migrate without lamellipodia. *Nat Rev Mol Cell Biol* **9**, 730-736 (2008).

134. Pollard, T.D. & Borisy, G.G. Cellular motility driven by assembly and disassembly of actin filaments. *Cell* **112**, 453-465 (2003).

135. Cunningham, C.C. Actin polymerization and intracellular solvent flow in cell surface blebbing. *J Cell Biol* **129**, 1589-1599 (1995).

136. Paluch, E., Piel, M., Prost, J., Bornens, M. & Sykes, C. Cortical actomyosin breakage triggers shape oscillations in cells and cell fragments. *Biophys J* **89**, 724-733 (2005).

137. Keller, H., Rentsch, P. & Hagmann, J. Differences in cortical actin structure and dynamics document that different types of blebs are formed by distinct mechanisms. *Exp Cell Res* **277**, 161-172 (2002).

138. Charras, G.T., Hu, C.K., Coughlin, M. & Mitchison, T.J. Reassembly of contractile actin cortex in cell blebs. *J Cell Biol* **175**, 477-490 (2006).

139. Fackler, O.T. & Grosse, R. Cell motility through plasma membrane blebbing. *J Cell Biol* **181**, 879-884 (2008).

140. Gadea, G., de Toledo, M., Anguille, C. & Roux, P. Loss of p53 promotes RhoA-ROCK-dependent cell migration and invasion in 3D matrices. *J Cell Biol* **178**, 23-30 (2007).

141. Tournaviti, S.*, et al.* SH4-domain-induced plasma membrane dynamization promotes bleb-associated cell motility. *J Cell Sci* **120**, 3820-3829 (2007).

142. Houle, F. & Huot, J. Dysregulation of the endothelial cellular response to oxidative stress in cancer. *Mol Carcinog* **45**, 362-367 (2006).

143. Houle, F.*, et al.* Extracellular signal-regulated kinase mediates phosphorylation of tropomyosin-1 to promote cytoskeleton remodeling in response to oxidative stress: impact on membrane blebbing. *Mol Biol Cell* **14**, 1418-1432 (2003).

144. Mills, J.C., Stone, N.L., Erhardt, J. & Pittman, R.N. Apoptotic membrane blebbing is regulated by myosin light chain phosphorylation. *J Cell Biol* **140**, 627-636 (1998).

145. Sebbagh, M.*, et al.* Caspase-3-mediated cleavage of ROCK I induces MLC phosphorylation and apoptotic membrane blebbing. *Nat Cell Biol* **3**, 346-352 (2001).

146. Mills, J.C., Stone, N.L. & Pittman, R.N. Extranuclear apoptosis. The role of the cytoplasm in the execution phase. *J Cell Biol* **146**, 703-708 (1999).

147. Totsukawa, G.*, et al.* Distinct roles of ROCK (Rho-kinase) and MLCK in spatial regulation of MLC phosphorylation for assembly of stress fibers and focal adhesions in 3T3 fibroblasts. *J Cell Biol* **150**, 797-806 (2000).

148. Blommaart, E.F., Krause, U., Schellens, J.P., Vreeling-Sindelarova, H. & Meijer, A.J. The phosphatidylinositol 3-kinase inhibitors wortmannin and LY294002 inhibit autophagy in isolated rat hepatocytes. *Eur J Biochem* **243**, 240-246 (1997).

149. Ito, S., Koshikawa, N., Mochizuki, S. & Takenaga, K. 3-Methyladenine suppresses cell migration and invasion of HT1080 fibrosarcoma cells through inhibiting phosphoinositide 3-kinases independently of autophagy inhibition. *Int J Oncol* **31**, 261-268 (2007).

150. Kuo, J.C., Wang, W.J., Yao, C.C., Wu, P.R. & Chen, R.H. The tumor suppressor DAPK inhibits cell motility by blocking the integrin-mediated polarity pathway. *J Cell Biol* **172**, 619-631 (2006).

151. Jin, Y., Blue, E.K. & Gallagher, P.J. Control of death-associated protein kinase (DAPK) activity by phosphorylation and proteasomal degradation. *J Biol Chem* **281**, 39033-39040 (2006).

152. Shang, T., Joseph, J., Hillard, C.J. & Kalyanaraman, B. Death-associated protein kinase as a sensor of mitochondrial membrane potential: role of lysosome in mitochondrial toxin-induced cell death. *J Biol Chem* **280**, 34644-34653 (2005).

153. Thomas, S.M., DeMarco, M., D'Arcangelo, G., Halegoua, S. & Brugge, J.S. Ras is essential for nerve growth factor- and phorbol ester-induced tyrosine phosphorylation of MAP kinases. *Cell* **68**, 1031-1040 (1992).

154. Wood, K.W., Sarnecki, C., Roberts, T.M. & Blenis, J. ras mediates nerve growth factor receptor modulation of three signal-transducing protein kinases: MAP kinase, Raf-1, and RSK. *Cell* **68**, 1041-1050 (1992).

155. Anjum, R., Roux, P.P., Ballif, B.A., Gygi, S.P. & Blenis, J. The tumor suppressor DAP kinase is a target of RSK-mediated survival signaling. *Curr Biol* **15**, 1762-1767 (2005).

156. McCubrey, J.A., *et al.* Roles of the Raf/MEK/ERK pathway in cell growth, malignant transformation and drug resistance. *Biochim Biophys Acta* **1773**, 1263-1284 (2007).

157. Martoriati, A., *et al.* dapk1, encoding an activator of a p19ARF-p53-mediated apoptotic checkpoint, is a transcription target of p53. *Oncogene* **24**, 1461-1466 (2005).

158. Gade, P., Roy, S.K., Li, H., Nallar, S.C. & Kalvakolanu, D.V. Critical role for transcription factor C/EBP-beta in regulating the expression of death-associated protein kinase 1. *Mol Cell Biol* **28**, 2528-2548 (2008).

159. Burrows, F., Zhang, H. & Kamal, A. Hsp90 activation and cell cycle regulation. *Cell Cycle* **3**, 1530-1536 (2004).

160. Christoph, F., *et al.* mRNA expression profiles of methylated APAF-1 and DAPK-1 tumor suppressor genes uncover clear cell renal cell carcinomas with aggressive phenotype. *The Journal of urology* **178**, 2655-2659 (2007).

161. van der Vaart, M. & Schaaf, M.J. Naturally occurring C-terminal splice variants of nuclear receptors. *Nuclear receptor signaling* **7**, e007 (2009).

162. Rozen, S. & Skaletsky, H. Primer3 on the WWW for general users and for biologist programmers. *Methods Mol Biol* **132**, 365-386 (2000).

163. Lapid., C. & Gao., Y. http://www.bioinformatics.org/primerx/index.htm. (2003).

164. Sanchez-Cespedes, M., *et al.* Gene promoter hypermethylation in tumors and serum of head and neck cancer patients. *Cancer Res* **60**, 892-895 (2000).

165. Kadlcikova, J., Holecek, M., Safranek, R., Tilser, I. & Kessler, B.M. Effects of proteasome inhibitors MG132, ZL3VS and AdaAhx3L3VS on protein metabolism in septic rats. *Int J Exp Pathol* **85**, 365-371 (2004).

166. Henshall, D.C., *et al.* Death-associated protein kinase expression in human temporal lobe epilepsy. *Ann Neurol* **55**, 485-494 (2004).

167. Ding, W.X. & Yin, X.M. Dissection of the multiple mechanisms of TNF-alpha-induced apoptosis in liver injury. *J Cell Mol Med* **8**, 445-454 (2004).

168. Werneburg, N.W., Guicciardi, M.E., Bronk, S.F. & Gores, G.J. Tumor necrosis factor-alpha-associated lysosomal permeabilization is cathepsin B dependent. *Am J Physiol Gastrointest Liver Physiol* **283**, G947-956 (2002).

169. Landon, L.A., Zou, J. & Deutscher, S.L. Is phage display technology on target for developing peptide-based cancer drugs? *Curr Drug Discov Technol* **1**, 113-132 (2004).

170. Chang, L., *et al.* The E3 ubiquitin ligase itch couples JNK activation to TNFalpha-induced cell death by inducing c-FLIP(L) turnover. *Cell* **124**, 601-613 (2006).

171. Turk, B., Turk, D. & Turk, V. Lysosomal cysteine proteases: more than scavengers. *Biochim Biophys Acta* **1477**, 98-111 (2000).

172. Gocheva, V., *et al.* Distinct roles for cysteine cathepsin genes in multistage tumorigenesis. *Genes Dev* **20**, 543-556 (2006).

173. Deiss, L.P., Galinka, H., Berissi, H., Cohen, O. & Kimchi, A. Cathepsin D protease mediates programmed cell death induced by interferon-gamma, Fas/APO-1 and TNF-alpha. *Embo J* **15**, 3861-3870 (1996).

174. Shohat, G., Spivak-Kroizman, T., Eisenstein, M. & Kimchi, A. The regulation of death-associated protein (DAP) kinase in apoptosis. *Eur Cytokine Netw* **13**, 398-400 (2002).

175. Fleischer, A., *et al.* Modulating apoptosis as a target for effective therapy. *Mol Immunol* **43**, 1065-1079 (2006).

176. Yoshimura, A. Signal transduction of inflammatory cytokines and tumor development. *Cancer Sci* **97**, 439-447 (2006).

177. Komarova, E.A., *et al.* p53 is a suppressor of inflammatory response in mice. *Faseb J* **19**, 1030-1032 (2005).

178. Li, J., Mahajan, A. & Tsai, M.D. Ankyrin repeat: a unique motif mediating protein-protein interactions. *Biochemistry* **45**, 15168-15178 (2006).

179. Smyth, D.R., Mrozkiewicz, M.K., McGrath, W.J., Listwan, P. & Kobe, B. Crystal structures of fusion proteins with large-affinity tags. *Protein Sci* **12**, 1313-1322 (2003).

180. Klose, J., *et al.* Hexa-histidin tag position influences disulfide structure but not binding behavior of in vitro folded N-terminal domain of rat corticotropin-releasing factor receptor type 2a. *Protein Sci* **13**, 2470-2475 (2004).

181. Hanazono, Y., Yu, J.M., Dunbar, C.E. & Emmons, R.V. Green fluorescent protein retroviral vectors: low titer and high recombination frequency suggest a selective disadvantage. *Hum Gene Ther* **8**, 1313-1319 (1997).

182. Anglesio, M.S., *et al.* Differential expression of a novel ankyrin containing E3 ubiquitin-protein ligase, Hace1, in sporadic Wilms' tumor versus normal kidney. *Hum Mol Genet* **13**, 2061-2074 (2004).

183. Ding, W.X., *et al.* Linking of autophagy to ubiquitin-proteasome system is important for the regulation of endoplasmic reticulum stress and cell viability. *Am J Pathol* **171**, 513-524 (2007).

184. Roshy, S., Sloane, B.F. & Moin, K. Pericellular cathepsin B and malignant progression. *Cancer Metastasis Rev* **22**, 271-286 (2003).

185. Schneider-Stock, R., *et al.* Close localization of DAP-kinase positive tumour-associated macrophages and apoptotic colorectal cancer cells. *J Pathol* **209**, 95-105 (2006).

186. Taha, T.A., *et al.* Tumor necrosis factor induces the loss of sphingosine kinase-1 by a cathepsin B-dependent mechanism. *J Biol Chem* **280**, 17196-17202 (2005).

187. Felbor, U., *et al.* Neuronal loss and brain atrophy in mice lacking cathepsins B and L. *Proc Natl Acad Sci U S A* **99**, 7883-7888 (2002).

188. Stevens, C., *et al.* Peptide combinatorial libraries identify TSC2 as a death-associated protein kinase (DAPK) death domain-binding protein and reveal a stimulatory role for DAPK in mTORC1 signaling. *J Biol Chem* **284**, 334-344 (2009).

189. Garcia, R., Franklin, R.A. & McCubrey, J.A. Cell death of MCF-7 human breast cancer cells induced by EGFR activation in the absence of other growth factors. *Cell Cycle* **5**, 1840-1846 (2006).

190. Lee, D.F., *et al.* IKK beta suppression of TSC1 links inflammation and tumor angiogenesis via the mTOR pathway. *Cell* **130**, 440-455 (2007).

191. Wang, L., Du, F. & Wang, X. TNF-alpha induces two distinct caspase-8 activation pathways. *Cell* **133**, 693-703 (2008).

Appendix I Published papers

Lin Y, Stevens C and Hupp T: Identification of a dominant negative functional domain on DAPK-1 that degrades DAPK-1 protein and stimulates TNFR-1-mediated apoptosis. J Biol Chem 282: 16792-802, 2007.

Lin Y, Stevens C, Hrstka R, Harrison B, Fourtouna A, Pathuri S, Vojtesek B and Hupp T: An alternative transcript from the death-associated protein kinase 1 locus encoding a small protein selectively mediates membrane blebbing. Febs J 275: 2574-84, 2008.

Lin Y, Stevens C, Harrison B, Pathuri S, Amin E and Hupp TR: The alternative splice variant of DAPK-1, s-DAPK-1, induces proteasome-independent DAPK-1 destabilization. Mol Cell Biochem 328: 101-7, 2009.